Quantum Database Architecture for the Quantum Data Scientist

A Theoretical Treatise on Lindblad Operators, EIT in Multi-Level Atomic Ensembles, and High-Fidelity Data Encoding

by

Ricard Santiago Raigada García

A dissertation submitted in partial fulfillment
of the requirements for the degree of
BSc
(Applied Data Science)

at the
Universitat Oberta de Catalunya
2024

The dissertation is approved by the following members:
PhD Jonatan Martín Rodríguez, Professor
M.Sc. Susana Acedo Nadal, Responsible Lecturer

Quantum Database Architecture for the Quantum Data Scientist: A Theoretical Treatise on Lindblad Operators, EIT in Multi-Level Atomic Ensembles, and High-Fidelity Data Encoding
© 2024
by Ricard Santiago Raigada García is licensed under Creative Commons Attribution-NonCommercial-NoDerivatives 4.0 International.

Quantum Database Architecture for the Quantum Data Scientist

A Theoretical Treatise on Lindblad Operators, EIT in Multi-Level Atomic Ensembles, and High-Fidelity Data Encoding

Ricard Santiago Raigada García

Keywords: Atomic structure, Quantum theory, Simulation models, Quantum database, Quantum algorithm

Abstract

Quantum memories are indispensable for driving secure quantum communication networks, as well as for solving challenges in large-scale data storage and processing. This thesis is based on quantum mechanics and quantum optics—particularly on Electromagnetically Induced Transparency (EIT) and the DLCZ protocol—, and addresses critical issues of Big Data management, ethical information handling, and data security in data science. However, providing high-fidelity storage, mitigating noisy channels, and designing efficient quantum algorithms for secure and ethical data handling remains an open challenge. This thesis presents an architecture for quantum databases that combines the physics of multi-level atomic ensembles with state-of-the-art quantum algorithms. The objective is to attain secure and ethical Big Data handling by means of quantum memory systems. A review is carried out through Lindblad operators and light-matter interactions, establishing a quantum database architecture capable of responding to the requirements of data science. Both in the Lambda scheme within an EIT-based quantum memory and the DLCZ protocol, the system achieves high-fidelity photon-atom coherence and secure storage. At the algorithmic level, the proposal leverages Hilbert subspaces as logical partitions —similar to sharding in classical databases—, enabling scalable data encoding and manipulation through unitary operations. These operations allow for the efficient and parallel retrieval of information, while maintaining coherence in noisy environments. The simulation results confirm the theoretical framework described and demonstrate the system's ability to establish an ethical treatment of Big Data while strengthening information security. This thesis thus novelly proposes the integration of quantum systems in data science, addressing privacy, ethics, and security issues at scale, offering a framework with practical applications of secure data governance.

Acknowledgements

I would like to express my gratitude to my thesis director, PhD Jonatan Martín Rodríguez, for accepting to direct my thesis, providing me with guidance and understanding throughout two semesters. His mentorship has been crucial for the successful completion of this work.

I would like to profoundly thank my undergraduate advisor, Xabier San Martín Aguirrezabal, for his steadfast support and heartening for my candidacy at CERN, which would not have been possible without his letter of recommendation, which is still active at the time of writing this thesis.

I extend my sincere appreciation to PhD Ángels Fitó Bertran, Rector of the University, for accepting a letter of recommendation from me in December 2024 to encourage the CERN selection process, as well as the Dean of the Computing, Multimedia, and Telecommunications Department for their collaboration in this endeavour.

I would like to thank Dr. William D. Oliver, Director of the MIT Center for Quantum Engineering, Associate Director of the MIT Research Laboratory of Electronics, and member of the National Quantum Initiative Advisory Committee for the videoconference discussion held on May 8, 2024. During this conversation, Dr. Oliver politely expressed his insights on the concept of a quantum database and assessed its feasibility. A conversation that I have had in the construction of this thesis.

I would also like to acknowledge the indirect contributions to this thesis, as they have been remarkable and influent professors that I have had in the creation of this work: Prof. Isaac Chuang, Prof. Peter Shor, Prof. Barton Zwiebach.

RICARD SANTIAGO RAIGADA GARCÍA
Barcelona, BCN, December 2024

Preface

Late to bed and early rising,
Ever luxury despising,
Ever training, never "sizing,"
I have suffered with the rest.
Yellow cheek and forehead ruddy,
Memory confused and muddy,
These are the effects of study
Of a subject so unblest.

10th November 1852, poem "A Vision."
James Clerk Maxwell[§]

After a certain high level of technical skill is achieved,
science and art tend to coalesce in esthetics, plasticity,
and form. The greatest scientists are artists
as well.

Albert Einstein[†], as quoted in The Ultimate Quotable Einstein. Recalled by Archibald Henderson, Durham Morning Herald, August 21, 1955. Einstein Archives 33-257

In the primordial silence, where even particles had no mass, an invisible, diffuse sea floods the void in space-time where each point is unique. A symmetrical sea that, as it began to cool, broke its perfect symmetry.

The perfection —the symmetry in the minimum state of the potential of the Higgs field— was broken. Apparent order became disorder, and mass was born. A wonderful manifestation of the excitation that allows the universe to exist in the way we know it.

In data science, the initial model is like a universe before the Higgs field. Potentially perfect and symmetrical, but without capturing the complexity of reality. As interactions occur and neurons learn specific details, spontaneous symmetry breaking emerges. Only at that precise moment, before the cold temperance of the data scientist, is the model of how the universe collapses into one of the infinite possibilities. The data scientist is to data what the Higgs field is to particles.

The breaking of symmetry—an apparent imperfection—from which the structures of the universe arise, giving birth to waves that carry information, known as data. Even more beautiful is knowing that Maxwell, who made it possible for us to discuss technological and information concepts today, saw symmetry in motion in electric and magnetic fields.

Beautiful, almost three years breaking the symmetry of data to reveal patterns and imagine what we would never imagine.

[§] Campbell and Garnett, 1882, p. 307
[†] Albert Einstein, 2011, p. 379.

I suppose that Einstein somehow reflected the same artistic connection that this work ultimately and perhaps in a hidden way, among so much technicality, tries to make us see that the breaking is not a failure, but a creative act. Only in it do we model chaos in patterns that find islands in the middle of the diffuse sea, envisage the beauty of the universe —the data.

It is not only understanding, it is the genesis of a new way of looking, it is beauty.

7th December 2024,
RICARD SANTIAGO RAIGADA GARCÍA

Contents

1 Introduction **1**
1.1 Social and business impact . . . 3

2 Objectives and Problems to be Solved **6**
2.1 Objectives and problems to be solved . . . 6
2.1.1 Objectives and key achievement indicators . . . 6

3 Methodology **8**

4 Definition of a Quantum Database **9**

5 Thesis Structure **13**

6 Quantum Memory Architecture **14**
6.1 Electromagnetically Induced Transparency . . . 14
6.1.1 Atomic Structure and Linewidth . . . 16
6.1.2 Stable States vs. Unstable . . . 24
6.1.3 Derivation of the light-atom interaction Hamiltonian . . . 26
6.1.4 Lindblad Equation . . . 28
6.1.5 Hamiltonian Interacting with Quantized Field . . . 31
6.1.6 Two-photon Resonance Condition . . . 33
6.1.7 Simple Dark State . . . 35
6.1.8 Mixing Angles . . . 35
6.1.9 General Dark State . . . 36
6.1.10 Mixing Angle Λ . . . 38
6.1.11 Hamiltonian with Spatial Dimension . . . 39
6.1.12 Light Field and Atomic Flip Operators . . . 39
6.1.13 Collective Operators and Process Dynamics . . . 40
6.1.14 Dark States of Polariton . . . 42
6.1.15 EIT Simulation . . . 43
6.2 Duan-Lukin-Cirac-Zoller Memories . . . 44
6.2.1 Atomic Assembly State . . . 44
6.2.2 Writing Process . . . 45
6.2.2.1 Entanglement Between Spin Wave and Writing Photon . . . 45
6.2.3 Reading Process . . . 46
6.2.3.1 Reading Efficiency . . . 46
6.3 Rydberg Blockade Mechanism . . . 46

7 Quantum Database Applications for a Data Scientist **48**
7.1 Introduction to Quantum Mechanics for the Data Scientist . . . 48
7.1.1 Linear Algebra . . . 48
7.1.1.1 The Hilbert Space . . . 49
7.1.1.2 Linear Operators and Matrices . . . 50
7.1.1.3 Operator Functions . . . 50
7.1.2 Postulates of Quantum Mechanics . . . 51
7.1.2.1 Axioms of Quantum Mechanics . . . 51
7.1.2.2 Distinguishing Quantum States . . . 51
7.1.2.3 Projective Measurements . . . 51
7.1.2.4 Positive Operator-Valued Measure . . . 52
7.1.2.5 Phase . . . 52
7.1.2.6 Composite Systems and Entanglement . . . 52
7.1.2.7 Universal Quantum Gates and Multi-Qubit Gates . . . 53
7.1.3 Density Operator . . . 53
7.1.4 The Schmidt Decomposition . . . 54
7.1.5 Purification . . . 54
7.1.6 The No-Cloning Theorem . . . 55
7.1.7 BB84 Protocol . . . 55
7.2 Entropy . . . 56
7.2.1 Quantum Entropy . . . 57
7.2.2 The Entropic Uncertainty Principle . . . 59
7.3 Challenges of Noise in Realistic Quantum Information Systems . . . 59
7.3.1 Foundations of Quantum Noise . . . 60
7.3.2 Practical Introduction to Quantum Key Distribution . . . 61
7.4 Benchmarking Techniques for Quantum Noise . . . 63
7.4.1 Benchmarking Quantum States . . . 63
7.4.2 Benchmarking Quantum Gates . . . 63
7.4.3 Quantum State Tomography . . . 64
7.5 Mitigating and Correcting Errors . . . 64
7.5.1 Correcting Codes . . . 64
7.5.2 Dynamical Error Suppression . . . 65
7.6 Practical Approach to Quantum Database for Data Scientists . . . 66
7.6.1 Encoding Databases with the Quantum Fourier Transform . . . 66
7.6.2 Role of Quantum Data Scientist . . . 68

8 Conclusion **69**

A Appendix of images **70**

B Tables **77**

C Proofs of Chapter 7 **79**

D Quantum Database Example Use **91**
D.1 Problem Description . . . 92
D.2 Implementation of the Quantum Database (qDB) . . . 93
D.3 Simulation . . . 94
D.4 Breve Overview of Grover's Search . . . 95
D.5 Breve Overview of Quantum Fourier Transformation . . . 96

E Fundamentals of Probability **98**
E.1 Basics . . . 98
E.1.1 Sample Space . . . 98
E.1.2 Probability of an event . . . 98
E.2 Random Variables . . . 99
E.2.1 Probability Function . . . 99
E.3 Cumulative Distribution Function (CDF) . . . 99
E.4 Expected Value . . . 99
E.4.1 Variance and Standard Deviation . . . 100
E.4.2 Covariance and Correlation . . . 100
E.5 Independent Events . . . 100
E.6 Common Probability Distributions . . . 100
E.7 Moment Generating Function . . . 100
E.8 Fourier Transform of the Wave Function . . . 101

F Formalisms of Quantum Mechanics **102**
F.1 Dirac notation . . . 102
F.2 Axioms of quantum mechanics . . . 102
F.2.1 States . . . 102
F.2.2 Observables . . . 103
F.2.3 Time Evolution . . . 103
F.2.4 Measurement . . . 103
F.3 Classical Mechanics vs. Quantum Mechanics . . . 103
F.4 Hermitian Operators . . . 104
F.5 Normalization of the Wave Function . . . 104
F.6 Orthonormality . . . 104
F.7 States in Superposition . . . 105
F.8 Commutators . . . 105
F.9 Angular Momentum . . . 105
F.10 Eigenfunctions and Eigenvalues . . . 107
F.11 Expected Value . . . 107

G Fundamentals of Quantum Computing **109**

H Fundamentals of Quantum Optics **112**

I Recommended Readings **116**

J Glossary **118**

List of Figures

A.1 Schema of a system with three levels of energy 70
A.2 **a)** Transition diagram of the hyperfine structure D_2 **b)** Transition diagram of the hyperfine structure D_1 (Steck, 2001) 71
A.3 Heisenberg uncertainty principle, illustrating the relationship between the uncertainties of position (Δx) and momentum (Δp). $\Delta x \Delta p = \frac{h}{4\pi}$ represents the quantum limit beyond which the uncertainty product is physically impossible (in quantum terms and not in classical physics). The colour gradient reflects different values of $\Delta x \Delta p - \frac{h}{4\pi}$. Own image generated with Python code. 72
A.4 Graph showing the real and imaginary parts of the first-order electrical susceptibility for the ON and OFF laser control states. Solid lines represent the ON state (Control ON). Dashed lines represent the OFF state (Control OFF). 73
A.5 Graph showing the imaginary part of the first order electrical susceptibility with the control laser in the active state (Control ON). 74
A.6 Schema illustrating the DLCZ memory with the Write and Read processes for the creation of collective atomic excitations in an atomic ensemble. 74
A.7 Toffoli matrix decomposition circuit into universal quantum gates. 75
A.8 Image (a) shows the density matrix of the pure state $|+\rangle$, uniform superposition on the states $|0\rangle$ and $|1\rangle$. Image (b) shows the representation on the Bloch sphere. Density matrix (c) shows the mixed state resulting from a probabilistic mixture (or superposition) of the states $|0\rangle$ and $|+\rangle$, with probability of 40 % and 60 % respectively. Representation (d) reflects the mixed state on the Bloch sphere. 75
A.9 Representation of polarizing filters. Note that if a photon is polarized on the diagonal basis, passing through a rectilinear polarizing filter, it is deflected to the left 50% of the time and 50% of the time to the right. 76
A.10 Quantum Circuit of the Quantum Database. 76

D.1 Probability distribution where the correct solution is department 3 with coded address 10, and 1000 shots. 94

H.1 Graphical representation of electromagnetic wave. 114

List of Tables

B.1 Values of K, $E_{F=x}$, E_{EQ} y E_{MD} for different values of F 77
B.2 Properties of a Complex Vector Space 77
B.3 Example of BB84 Protocol Transmission of 8 Bits 78
B.4 Department Pay Distribution 78

E.1 Axioms of Probability, (Wasserman, 2013) 99
E.2 Common Probability Distributions 101

F.1 Quantum numbers and their allowed values 106

G.1 Quantum Universal Gates 109
G.2 Quantum Gates and Matrix Representations 109
G.3 Non-exhaustive Circuit Equivalences Precomputed 111

Chapter 1

Introduction

Richard Feynman, winner of the Nobel Prize in Physics, said: "Nature isn't classical, dammit, and if you want to make a simulation of nature, you'd better make it quantum mechanical, and by golly it's a wonderful problem, because it doesn't look so easy." (Trabesinger, 2012). Feynman refers to the need to store information about individual particles that obey the rules of quantum mechanics that many physicists and chemists try to simulate. But the classical computer could not model the mechanics of many-body quantum systems.

In the 1970s, Paul Benioff theoretically proposed the possibility of building quantum computers, but it would be in 1982 when Feynman began to make this theory a reality (Ding & Chong, 2020b). Quantum computing works in subatomic nature to try to simulate systems with quantum behaviour from quantum behaviour itself (Wittek, 2014).

The excursus, which will follow bit by bit, will present more practical concepts until finishing with the context of quantum communication and quantum information. Where the concept of Quantum Key Distribution (QKD) will be presented. It is necessary for the reader to keep in mind that in these systems a quantum memory is necessary and indispensable. It is from this that the proposal for a quantum database arises. For a more precise approach to the proposal of this work, it will be advisable to complete it with the precise definitions of the objectives and problems to be solved section.

Many of today's technologies are based on applications of quantum mechanics. One promising area is quantum computing. Quantum computing has advantages over classical computing. Some features are the factorization of integers with an exponential speed (Wittek, 2014) or searching in unordered sets of data quadratically faster than in the classical one. Proved by Peter Shor (Peter

Shor, 1994; Shor, 1997).

Not only does it offer an advantage in certain types of algorithms but also with other characteristics such as taking advantage of superposition or quantum entanglement for distributed computing, space savings and speed (Ding & Chong, 2020a), among other aspects. Which means that in some currently demonstrated operations, quantum supremacy is achieved; a term coined by physicist John Preskill (Kaku, 2024).

Quantum computers have numerous applications with a high social and economic impact. In the context of data analytics and data science, JPMorgan Chase has partnered with IBM to analyse its data to make better financial risk predictions (Kaku, 2024). Many economic problems are based on optimization problems.

On the other hand, sciences that study nature, such as medicine, chemistry, or biology are highly benefited. Since a quantum computer has the possibility of accurately simulating the underlying nature of different phenomena as well as providing the computational muscle to carry it out. The main benefited fields could not be concluded without including the field of artificial intelligence (AI). With the advancement of AI systems, computational tasks are increasingly demanding considering that in our era, gold is data (Kaku, 2024), companies store mountains of data.

Some main direct applications are, for example, in solving problems such as solving the efficiency of fertilizer production (proposal for a second Green Revolution) (Kaku, 2024). One of the most important applications may be the contribution to quantum medicine, allowing us to discover exactly the root of the disease. So that drugs can be developed that address the issue in question. Currently, most drugs are validated through a process of trial and error that, using statistics, proves efficient regarding a disease. However, quantum simulation allows these diseases to be reproduced, allowing us to question why they happen. Why does Parkinson's occur?

It is being proven that the use of quantum computing compared to classical systems produces benefits. This leads to the question: why use quantum systems and store data in classical systems? A quantum state has characteristics that, due to quantum nature, make them stochastic and in numerous instances a deterministic state does not have a defined state. Therefore, storing information in a classical system involves collapsing quantum states into classical bits. This entails a loss of information and the impossibility of recovering information encoded in the quantum states, from the superposition states themselves to the information encoded in entropy or that encoded in different photonic properties.

1.1 Social and business impact

The general applications mentioned above do not constitute a definitive list, nor is it known how far they can go. This is in part due to ignorance of the limits in complexity theory that apply to quantum computers. It is known that they can solve problems in the BQP space and some PSPACE.

For instance, in polynomial space, the video game problem GO (nxn) (Hidary, 2019) can be considered. Definitely, it appears that there is no direct quantum algorithm that can solve it. However, it is known that this is a problem treated in Machine Learning (ML) and known as attacker-defender scenario in the reinforcement learning (RL) branch. However, one would think that if the ML field was to benefit and this is a PSPACE issue, perhaps a quantum computer would have something to say.

Certainly, the reader is not wrong, since in 2016 and 2017, a computer battles in the world GO competition (without any human understanding) and manages to solve all 57 Atari 2600 games with RL algorithms (Silver et al., 2016, 2017).

Kunczik (Kunczik, 2022) explores the use of RL with a quantum hybrid approach in the NISQ context. Demonstrating that connecting a quantum processing unit benefits the performance and improves the efficiency of the algorithm. This is because the problem type inherently has a massive state, with a lot of action space and possible rewards. Which makes it a complex computational problem.

RL algorithms are as important in previous problems as, for example, the theft of the Mona Lisa painting in 1911 or the airport bombing defence strategy (Brown et al., 2006). Attacker-defender scenarios are relevant and generate a positive impact in many disciplines. Especially where defence schemes need to be planned.

These are some social impacts, although at an algorithmic level. But are there more relevant impacts that will change the way we interact physically? Well, I don't know if the way we interact physically will change as Michio Kaku (Valencia, 2024) predicts with his 'Brainet', but it is clear that the internet is changing. Probably, it is due to the fact that it is digital and digital is slow (Valencia, 2024) or, also, to its insecurity in the face of post-quantum cryptography.

The quantum internet, the satellite-based QKD systems or simply the quantum satellite networks of quantum computing in wireless networks (Glisic & Lorenzo, 2022) are changing the current

5G revolution. There are many problems associated with the use of quantum computing with quantum sensors, and the simplest way is to implement the network through optical fibre. However, quantum computing does not behave like classical computing and photonic loss in fibre cannot be solved. Optically as simply as in the classic way through signal amplifiers. This is due to the fact of the no-cloning theorem. Although a way was discovered that through SWAPS entanglements the signal can be amplified.

Advances in quantum communication are notable because they have gone from using multiplexing to creating the QKD floodlight algorithm that allows secret key rates of gigabits per second without multiplexing, through the use of many photons per bit. Solving the loss of photon propagation in optical fibre and acting as an optical amplifier immune to passive eavesdropping.

Really, what social impact does it have? In the research of Zhang et al. (Zhang et al., 2018) it is possible to implement a secret key speed of 1.3 gigabits per second through a channel with an attenuation equivalent to 50 kilometres of optical fibre with the objective of implementing it on a metropolitan area scale. At the security level, it rises from a collective attack to a coherent attack. The protocol is immune to passive eavesdropping due to the comparison of the received light against an amplified spontaneous emission (ASE) reference performed in coherent detection. Being only susceptible to active attacks where a hacker could inject low-brightness light into the receiving terminal. Although the protocol itself implements channel monitoring using a spontaneous parametric converter to detect intrusions (Massachusetts Institute of Technology, 2024a).

This socially involves solving the security vulnerability of the RSA protocol of all encrypted state secrets, as well as banking transactions and, practically, any encrypted connection. Because Shor's algorithm can break classical encryption.

This thesis proposes the conceptualization of quantum database hardware for data analysts and data scientists, as well as an introduction and practical use of coding in a quantum database. The absence of a proposal that explores the real application of quantum computing in database systems and distributed computing environments has been detected.

Within the framework of data science, Big Data is addressed with Machine Learning (ML) tools. The area in the greatest degree where real Big Data is produced is the simulation of complex systems (Brunton & Kutz, 2022). Simulating the phenomenon of transport analysis can represent millions of degrees of freedom. Therefore, the incorporation of ML tools such as Proper orthogonal decomposition (POD), partial differential equation functional identification of nonlinear dynamics

(PDE-FIND) has been essential to perform simulations of flow dynamics in data-driven decision environments. This fact invites us to think that using Quantum ML in quantum computing will reduce complexity (Wittek, 2014) or, at least, allow the use of a larger data flow that is unaffordable in classical computing.

Chapter 2

Objectives and Problems to be Solved

2.1 Objectives and problems to be solved

In the context of data science, one of the main concerns that arise from the use of data is its privacy. There are many laws that try to regulate the use of customer data and, therefore, directly affect the data scientist.

Companies are concerned about data privacy from two perspectives, information security and ethics with their users. Therefore, in the practice of the data scientist, the administration, and management of the two previous issues must participate. The data scientist must integrate appropriate ethical issues into his or her work and ensure the integrity of the data, both in terms of veracity and cybersecurity issues.

Specifically, this work aims to propose an intermediate system between quantum sensors, a database, and a quantum computer to work on. Thus, solving: practical application of a quantum communication network and data security. Fundamental elements in data science: Big Data and its treatment, and data security. Creating a completely secure system that solves privacy and data eavesdropping problems.

2.1.1 Objectives and key achievement indicators

General objectives:

- Explore the feasibility of quantum databases through understanding the limitations and realities of quantum computing and existing hardware.
- Present the essential characteristics for a theoretical framework (quantum mechanics) for

quantum data management aimed at data scientists.

- Envision the future of quantum databases and quantum data governance, with the focus on data science and analytics in the quantum era.

Specific objectives:

- Discuss the current limitations and possibilities of quantum computing and existing hardware to understand feasibility.
- Discuss the hardware of quantum memories.
- Quality of the theoretical framework developed, through the understanding of existing requirements.
- Presentation of strategies and recommendations for quantum data management through the description of the use of a quantum database.
- Number of technical problems resolved compared to the total problems identified.

Chapter 3

Methodology

This thesis is supported by solid knowledge of the degree in relation to infrastructure and databases. As well as advanced programs such as the Quantum Computing Systems program at the University of Chicago (UChicago, 2024), the professional program in Quantum Realities at MIT with a score of 9.99 out of 10 (Massachusetts Institute of Technology, 2024a, 2024b) or the Atomic and Optical Physics 8.421x course at MIT.

The methodology of this thesis has been based on reading the state-of-the-art in the main techniques involved in the thesis, as well as in the field of quantum optics and quantum computing. The research readings have been completed with a large collection of books in the field. The work is eminently theoretical, so it has required a process of thinking and developing the framework of a quantum database.

Furthermore, a numerical simulation of Electromagnetically Induced Transparency (EIT) has also been performed, along with a simulation of the proposed algorithm for encoding the Quantum Database (qDB) on quantum software using Qiskit's QASM simulator.

Several visualizations of this thesis have been developed in Python. All the code developed in this thesis is written in Python and is available in a publicly accessible repository GitHub repository[§]. The repository is organized into projects using modular programming. Additionally, in cases where versioning may be complicated, a Conda environment is provided with all the necessary dependencies to ensure reproducibility of the thesis.

[§]Visit the link to access the main README file of the project.

Chapter 4

Definition of a Quantum Database

The objective of a storage system is to encode information temporarily or permanently. In quantum computing, one of the important issues is the coherence time of the system. In practical terms, how many quantum gates can be applied before the system becomes decoherent? For instance, suppose some information has been encoded into quantum states, the goal is to keep it alive for as long as possible. Quantum databases can be interpreted from the point of view of error correction and not so much as the mere fact of encoding information. In short, when a classic computer detects a corrupted part in a memory segment, skips that space or even has mechanisms to correct it such as a bit flipping.

The mission is to form error correction strategies to maintain information consistency. This is interesting because not only does it point out that the problem should be approached considering the objective of correcting errors, but it also uses information theory to explain some similar behaviours. That is why, based on this theory, the most fundamental idea on which to conceive the concept of a quantum database is proposed.

The transformation that occurred in the understanding of information in the paper A Mathematical Theory of Communication (Shannon, 1948) by Claude Shannon is well known. From that moment on, information came to be understood as a measurable quantity in a system (Stone, 2015). In fact, according to information theory (Lloyd, 2011), the universe could be understood as a large quantum computer. Ultimately, for example, the number of atoms that make up an apple is known; therefore, it is representable in terms of bits and, consequently, qubits. Therefore, the question of entropy, addressed from information theory, is a part of information encoded in a system that is unknown in principle.

Shannon, in his concern to describe the storage and transmission of information, proposed the metric known as Shannon entropy. He says that the entropy of a discrete random variable X with a probability distribution $p_X(x)$ is defined:

$$H(X) = -\sum_x p_X(x)\log(p_X(x)) \tag{4.1}$$

With a deeper and eminently probabilistic study, other properties such as conditional, joint entropy, mutual information, etc. are derived. It is easy to understand how entropy in a quantum system (from the perspective of information theory) does not have an exact translation. That is why the *von Neumann entropy* is used to measure the amount of information in a quantum system. It is crucial to understand that in the classical system entropy is mediated by the probability distribution of a random variable, however, in a quantum system the density operator function is used. This is due to the relationship with the Heisenberg uncertainty principle.

Also discarding the analysis of quantum properties that are derived from quantum entropy, it is important to highlight the Heisenberg uncertainty principle regarding the momentum and position of a particle. The more precise the measurement of one variable, the less known the other is. However, it is evident that measuring velocity and position does not indicate anything about the level of knowledge of the information contained in a quantum system, which is why the entropic uncertainty principle is used.

For practical purposes, the term memory is used interchangeably with database throughout this discussion. However, the term memory it is used in a more physical sense, referring to the storage medium, whereas the term database is referred as infrastructure system designed for data management. The existence of a quantum memory will be demonstrated. Let us assume the state of the systems A, B and the computational base:

$$\rho_{AB} \in \mathcal{B}(\mathcal{H}_A \otimes \mathcal{H}_B) \tag{4.2}$$

$$\left|\Phi^+\right\rangle_{AB} = \frac{1}{\sqrt{2}}(\left|+\right\rangle_A \left|+\right\rangle_B + \left|-\right\rangle_A \left|-\right\rangle_B) \tag{4.3}$$

Understanding the Bell state $|\Phi^+\rangle$ it is known that:

$$|+\rangle = \frac{1}{\sqrt{2}(|0\rangle + |1\rangle)}$$

$$|-\rangle = \frac{1}{\sqrt{2}(|0\rangle - |1\rangle)}$$

Substituting into the original expression and expanding it is obtained:

$$\left|\Phi^+\right\rangle_{AB} = \frac{1}{\sqrt{2}}(|0\rangle_A |0\rangle_B + |1\rangle_A |1\rangle_B)$$

If the system B measures in the operator σ_Z then it obtains the state $|0\rangle_B$, so the state A can only be in the state $|0\rangle_A$. Similarly, if system B measures $|1\rangle_B$, system A can only be at $|1\rangle_A$.

It is easily demonstrable by calculating the probability amplitude of the projection measurement B. For example, for $|0\rangle_B$:

$$(\mathbb{I}_A \otimes |0\rangle_B \langle 0|) \left|\Phi^+\right\rangle_{AB} = \frac{1}{\sqrt{2}}(|0\rangle_A + |0\rangle_B)$$

for $|1\rangle_B$:

$$(\mathbb{I}_A \otimes |1\rangle_B \langle 1|) \left|\Phi^+\right\rangle_{AB} = \frac{1}{\sqrt{2}}(|1\rangle_A + |1\rangle_B)$$

Finally, the square modulus of the amplitude ($\frac{1}{\sqrt{2}}$) is performed to obtain the probability:

$$\left|\frac{1}{\sqrt{2}}\right|^2 = \frac{1}{2}$$

This is because the wave function is expressed as a linear superposition: $P(x) = |\Psi(x,t)|^2$.

The demonstration of this quantum memory is based on the research of (Berta et al., 2009). It is proposed to use a measurement with a mean value operator (POVM). This is because the measurements that act on the space $\mathcal{H}$ are generalized to include both classical projective measurements, that is, orthogonal ones, and those that are not. In the context of evaluating the amount of information in a system, it is understood that it is carried out on a noisy channel, so including non-ideal projections is optimal.

The system A makes a measurement $\{M_A^x\}$ so it collapses by projecting itself into $|x\rangle_A \langle x|$. System B is intact, and the conditional probability for the state of system B is calculated based on

the measurement at A with result x.

$$\sigma_{XB} = \sum_x |x\rangle_A \langle x| \otimes \mathrm{Tr}_A((M_A^x \otimes \mathbb{I}_B)\rho_{AB}) \tag{4.4}$$

The uncertainty of the system B can be calculated according to (Berta et al., 2009) with the conditional entropy $H(X|B)_\sigma$. If a different measurement is made in system A, the sum of the individual uncertainties can be calculated. Additionally, the incompatibility of measurements in system B is measured as follows:

$$c = \underset{x,y}{max} || \sqrt{M_A^x} \sqrt{N_A^y} ||_\infty^2 \tag{4.5}$$

Therefore, it is concluded that if system A performs any of the previous POVM measurements, the uncertainty of system B is given by:

$$H(X|B)_\sigma + H(Y|B)_\delta \geq log\frac{1}{c} + H(A|B)_\rho \tag{4.6}$$

Being δ the state resulting from the second measurement ($\{N_A^y\}$) that can be obtained intuitively from the description of equation 4.

It has been demonstrated how a quantum state can be stored and recovered with a quantum entangled system the state of the other system without uncertainty as long as it is one of the Bell states. Subsequently, POVM measurements have been introduced and uncertainty quantification in projections that do not belong to one of the maximally entangled states. Among other things, the phase that the states have cannot be determined, so this is part of the uncertainty or information that is lost in non-maximally entangled quantum systems.

Chapter 5

Thesis Structure

The thesis is made up of two clearly differentiated parts. Chapter 6 is focused on a description in terms of the hardware architecture. While Chapter 7 is focused on the use of this hardware through an introductory review of quantum mechanics and a proposal for practical use on the quantum database focused on data scientists.

In Chapter 6, an introductory presentation of an EIT memory is made in terms of semiclassical physics. Where, bit by bit, the EIT quantum memory is introduced. Fundamental to understand, a more advanced type of memory known as Duan-Lukin-Cirac-Zoller (DLCZ) quantum memory.

After discovering the physical conceptualization of a quantum memory, in Chapter 7, a description of use is made at a high level, proposing a framework of use and exploration guidelines for data scientists. The reader will notice a change in quantum descriptions, going from talking about wave and motion equations to an approach from quantum computing to make it more accessible to data scientists. Replacing explanations in physical terms with a more abstract vision — through the representation of the qubit.

This thesis can be read in different directions depending on the level of specialization. For readers who are not familiar with quantum theory, it is suggested to start by reviewing the appendices, where one will find a lot of self-contained material that makes it possible to understand the rest of the work. Afterwards, the reader can start reading the first part of Chapter 7, and then start linearly from Chapter 6. For readers who are familiar with quantum theory, it is suggested to start directly with Chapter 6 and, if necessary, refresh some notions with the first part of Chapter 7.

Chapter 6

Quantum Memory Architecture

At this point, an understanding of the underlying hardware of a quantum memory will be made. It is important for the reader to understand that production has different interpretations depending on the level in which one works.

Regarding the hardware of the quantum memory, it will be explored from a standpoint mainly of semiclassical physics and later, it will move on to a quantum description.

On the other hand, in Chapter 7 a high-level quantum algorithm is explored, focusing on conjectures based on quantum mechanics rather than low-level hardware approximations.

This means that *per se* the descriptions made in the following chapter, the practical part, are not directly applicable to the descriptions of the suggested hardware. This is because this chapter deals with the physical device and the next deals with algorithms on an abstract level that must be converted to a hardware translation (in the proposed scheme) to be applicable.

For those interested in this field, it is recommended to read the article on optimization of quantum circuits on superconducting hardware (Raigada García, 2024a), although the same hardware as in this thesis is not presented, the steps to follow would still be important: qubit mapping, routing, and gate scheduling.

6.1 Electromagnetically Induced Transparency

The fundamental idea of Electromagnetically Induced Transparency (EIT) is to use a powerful laser capable of putting atoms in a coherent superposition state. A dark state is generated in the atoms, giving them the possibility of passing through material without being absorbed. Making an opaque

medium become transparent by modulating the refractive index of the medium, consequently, as will be seen later, lowering the speed of light in the medium.

Steve Harris discovered this effect in 1989 when he was working with autoionizing dark states (Harris, 1989). Later, he made the contribution of EIT carried out on a three-level Λ scheme (Boller et al., 1991).

The coupling laser must have a Rabi frequency capable of exceeding spontaneous emission rates, which allows creating a dark resonance. This gives rise to what is known as a transparency window through which a second laser can pass without being absorbed.

In general terms, an introductory version of the general operation of the EIT is presented, which is then seen in detail in a specific version in the following subsections.

To understand the operation of the Λ scheme depicted in Figure A.1, it is necessary to create the Hamiltonian of the interaction of light with the fundamental states of the system. Therefore, $H_{\text{int}} = -\mathbf{d} \cdot \mathbf{E}$ where the term $\mathbf{d}$ appears composed of the individual dipole moments resulting from the transitions from the ground states $|g\rangle$ and $|s\rangle$ to the excited state $|e\rangle$. $\mathbf{E}$ represents the electric field associated with the applied light beam.

In the Λ scheme, the probe beam couples the states $|g\rangle \leftrightarrow |e\rangle$, and the control beam couples the states $|s\rangle \leftrightarrow |e\rangle$. Since there is no coupling between $|g\rangle$ and $|s\rangle$, cross terms describing direct transitions like $|g\rangle \leftrightarrow |s\rangle$ are discarded. That is, leaving only the descriptions of transitions allowed by the electric dipoles between the ground states and the excited state.

Logically, to the Hamiltonian of interaction of light and ground states the Rabi frequencies $\Omega_i = \frac{-\langle g_i|\mathbf{d}_i \cdot \mathbf{E}_i|e\rangle}{\hbar}$ must be added. As previously mentioned, this is a semiclassical problem of light-matter interaction. The frequencies of the light fields are very high, which causes rapid oscillations in the equations of motion. It is common that in a stationary frame, a simplification of the equations is made by moving to a rotating frame. Since one is more interested in the slow evolution of the system. In this way, it depends solely on the detunings Δ_1 and Δ_2 where $\Delta_i = \omega_0 - \omega_{L,i}$.

$$\tilde{\Psi} = c_1(t)e^{-i\omega_{L,1}t}\,|g\rangle + c_2(t)e^{-i\omega_{L,2}t}\,|s\rangle + c_3(t)\,|e\rangle \tag{6.1}$$

The coefficients c_i correspond to the probability amplitudes of finding the system in the states, represented with the Dirac notation. $\omega_{L,1}$ refers to the frequency of the laser field that couples $|g\rangle \leftrightarrow |e\rangle$. Similarly, $\omega_{L,2}$ with $|s\rangle \leftrightarrow |e\rangle$.

The total Hamiltonian in the new basis is:

$$\tilde{H_0} + \tilde{H_{int}} = \frac{\hbar}{2} \begin{pmatrix} 0 & \Omega_g & \Omega_s \\ \Omega_g & 2\Delta_g & 0 \\ \Omega_s & 0 & 2\Delta_s \end{pmatrix} \tag{6.2}$$

6.1.1 Atomic Structure and Linewidth

Heavy alkali atoms are highly useful when laser-based methods are applied. They are easily cooled and trapped by laser light and "the elastic scattering cross-sections are large, facilitating evaporative cooling" (Anderson et al., 1995). Crucial in Bose-Einstein Condensation.

For this reason, in this thesis an isotope of the alkaline atom rubidium (^{87}Rb) has been chosen, which has one electron in its outermost shell and a principal quantum number of $n = 5$. The ground state and first excited state have the same quantum number, although with different orbital quantum numbers. Specifically, $l = 0$ for the ground state and $l = 1$ for the first excited state. The transitions between these states correspond to the D lines (Steck, 2001). In the literature, studies can be found that make comparisons with other alkaline metals, such as caesium (Cs). However, it is not the objective of this thesis to carry out a comparative study of the potential of alkalines for the construction of EIT quantum memories. Therefore, the use of the alkaline with the greatest demonstrated potential for use is assumed. To learn more about this subject, it is recommended to read the following research to discover the high potential of caesium and rubidium (Li et al., 2009; Manchaiah et al., 2022; Xue et al., 2021); for a more recent study where they are used simultaneously, consult (Holloway et al., 2016).

The energy scheme Λ is shown in Figure A.1. In the figure, it can be seen that there are three states: the two metastable states and the excited one. This is fundamental to the concept of quantum memories because a control beam is created that is coupled for the transition $|s\rangle \leftrightarrow |e\rangle$ and another probe beam that is coupled $|g\rangle \leftrightarrow |e\rangle$. This configuration is basic for the production of the EIT effect, on which this thesis is based, to store the data (information encoded in some photonic characteristics) and the control of the photon in the quantum memory.

Regarding the electronic configuration of ^{87}Rb, one must consider in which cases it is more convenient to use the D_1 or D_2 lines. The Figure A.2 shows the energy levels. The image is a composite of (Steck, 2001)'s experimental research. Very abstractly, when one is interested in stability and control, and simple atomic manipulation, D_1 is preferable. When radiation and

coupling strength, cooling power, or trapping capabilities are required, then the D_2 line is more suitable. This is useful for spectroscopy because of the greater variety of quantum states. Since it has more unfolding of the hyperfine layer.

The approximate limiting temperature for ^{87}Rb can be reached by Doppler cooling. In principle, it can be deduced from the reduced Plank constant ($\hbar$) and the Boltzmann constant (K_B). Then the natural line width (γ) for the D_2 transition $5S_{1/2} \rightarrow 5P_{3/2}$ is calculated with

$$T_D = \frac{\hbar\gamma}{2K_B} \tag{6.3}$$
$$T_D \approx 143\,\mu\text{K}$$

Where $\gamma = 2\pi \times$ 6 MHz.

The 6 MHz is obtained experimentally from the research of (Ye et al., 1996) who carried out an experimental study of the hyperfine structure of ^{87}Rb.

When spin-orbit coupling occurs, different energy levels are created, which are called fine structure. The equation that describes spin-orbit coupling is given by two variables: the angular momentum L and the electron spin S. Additionally, it incorporates the radial distance function $\xi(r)$.

$$H_{SO} = \xi(r) \cdot \mathbf{L} \cdot \mathbf{S} \tag{6.4}$$

The quantum numbers for ^{87}Rb are $L = 1(P)$ y $S = 1/2$. $J = 1/2$ for $5^2P_{1/2}$ and $J = 3/2$ for $5^2P_{3/2}$.

For $5^2P_{3/2}$ there are the levels $F = 3, 2, 1, 0$. In the figure A.2 you can see the MHz between each transition.

A quick derivation of the Dirac equation will now be carried out, which will deduct the degeneracy of the levels of the rubidium atom ^{87}Rb. The Dirac equation [§] is assumed in the following Hamiltonian form:

$$H = c\boldsymbol{\alpha} \cdot \mathbf{p} + \beta mc^2 \tag{6.5}$$

[§]The original formulation can be found in the *Proceedings of the Royal Society (London)*, and was published in February 1928. The original formula can be readily identified, as $\left[p_0 + \frac{e}{c}A_0 + \rho_1\left(\vec{\sigma}\cdot\left(\vec{p} + \frac{e}{c}\vec{A}\right)\right) + \rho_3 mc\right]\psi = 0$, (Eq. 14 Dirac & Fowler, 1928, p. 618). As well in the linear form as $(p_0 + \alpha_1 p_1 + \alpha_2 p_2 + \alpha_3 p_3 + \beta mc)\,\psi = 0$, (Eq. 4 Dirac & Fowler, 1928, p. 613)

$$i\hbar\frac{\partial\Psi}{\partial t} = H\Psi \tag{6.6}$$

An electromagnetic field was coupled to the above Dirac equation 6.6.

$$i\hbar\frac{\partial\Psi}{\partial t} = c\boldsymbol{\alpha}\cdot(\mathbf{p} - \frac{e}{c}\mathbf{A}) + V(r) \tag{6.7}$$

The potential $V(r)$ regards to the value of the electron charge plus a scalar potential. It can be obtained based on the deduction of the relation of the relativistic energy in the quadratic form. Solving for the energy E to obtain the hamiltonian $\sqrt{\mathbf{p}^2c^2 + m^2c^4}$, the final Dirac hamiltonian is deduced:

$$H = \frac{\mathbf{p}^2}{2m} + V(r) - \frac{\mathbf{p}^4}{8m^3c^2} + \frac{1}{2m^2c^2}\frac{1}{r}\frac{dV}{dr}\mathbf{S}\cdot\mathbf{L} + \text{Darwin correction} \tag{6.8}$$

Particularly, one is interested in the relativistic and spin-orbit correction of the unperturbed hamiltonian of the equation 6.8. Carry on the derivation based on the $\delta H_{\text{SO correction}} = \frac{1}{2m^2c^2}\frac{1}{r}\frac{dV}{dr}\mathbf{S}\cdot\mathbf{L}$, the fine structure is obtained in terms of the E_{n,l,j,m_j}. This form actually groups spin-orbit, Darwin [§] and relativistic corrections. Expressed in terms of n, j:

$$E_{n,j} = \frac{mc^2a^2}{2n^2}\left[1 + \frac{\alpha^2}{n^2}\left(\frac{n}{j+\frac{1}{2}} - \frac{3}{4}\right)\right] \tag{6.9}$$

A more complex theory is required because rubidium ^{87}Rb is a multielectron atom due to the electron-electron interaction and a non-coulomb potential. The outermost electron moves in a potential similar to that of a hydrogen-like atom. Precisely for that reason, a Quantum Defect Theory (QDT) must be used. For this purpose, the Rydberg constant for the hydrogen (R_H) it is related to the deviation of the energy levels similarly to hydrogen due to the shielding effect of the internal electrons —resulting in a less effective nuclear charge than the real nuclear charge of the

[§] In the paper of Dirac and Fowler, 1928, Dirac mentions the work of Charles Galton Darwin—*The Electron as a Vector Wave*, Proc. Roy. Soc. A, vol. 116, p. 227 (1927). In that work, he discusses the quantum theory of the electron as a vector wave (Charles Galton, 1927). He contributed to the development of relativistic quantum mechanics and electron spin. C. G. Darwin visited Bohr, as well as Dr. Klein. Known for several important contributions, Klein in particular—as well as Gordon—influenced the derivation of the Dirac equation. In 1909, C. G. Darwin belonged to Trinity College. His coach was Herman. He is the son of George H. Darwin, who also attended Trinity College in 1868 and was coached by Routh. G. H. Darwin is the son of the famous naturalist Charles R. Darwin. C. G. and G. H. Darwin attended the most brilliant centre of training in mathematical physics in Europe -Cambridge University. Information regarding the list of successful coaching students (year, wrangler, collage, coach) can be found in the Appendix *A* of the book Warwick, 2003, pp. 512–523. The genealogy presented is an elaboration of the author of this thesis that complements the list of successful students in the referenced book.

nucleus.

$$E_{n,l,j} = -\frac{R_H}{(n-\delta_{n,l})^2} \tag{6.10}$$

The fine structure splitting due to the coupling of the spin-orbit corresponds to $\Delta E_{FS} = \xi_{n,l} \langle \mathbf{L} \cdot \mathbf{S} \rangle$. The first term is related to the spin-orbit coupling constant $\xi_{n,l}$. The second term $\langle \mathbf{L} \cdot \mathbf{S} \rangle$ is related to the expected value of the spin-orbit operator. Concretely, for a given l:

$$\langle \mathbf{L} \cdot \mathbf{S} \rangle = \frac{1}{2} \left[j(j+1) - l(l+1) - s(s+1) \right] \tag{6.11}$$

The electron spin is represented by s. The only values can take are $\pm\frac{1}{2}$. The coupling spin-orbit hamiltonian is transformed into:

$$H_{SO} = \frac{1}{2m^2c^2} \frac{1}{r} \frac{dV}{dr} \mathbf{L} \cdot \mathbf{S} \tag{6.12}$$

Where $V(r)$ is the central effective potential of the valence electron. The coupling spin-orbit constant $\xi_{n,l}$, it is computed in the following manner:

$$\xi_{n,l} = \frac{1}{2m^2c^2} \left\langle \frac{1}{r} \frac{dV}{dr} \right\rangle \tag{6.13}$$

Therefore, it is obtained:

$$E_{FS} = \xi_{n,l} \langle \mathbf{L} \cdot \mathbf{S} \rangle = \frac{\xi_{n,l}}{2} \left[j(j+1) - l(l+1) - s(s+1) \right] \tag{6.14}$$

The dipolar magnetic interaction constant A, magnetic angular momentum I, and the electron magnetic moment J are related to the dipolar magnetic interaction Hamiltonian.

$$H_{MD} = A \mathbf{I} \cdot \mathbf{J} \tag{6.15}$$

The total angular momentum is the sum $F = I + J$ of the magnetic angular momentum and the electron magnetic moment. One can deduce the following: $F^2 = (I+J)^2 = I^2 + 2\,\mathbf{I} \cdot \mathbf{J} + J^2$, $\mathbf{I} \cdot \mathbf{J} = \frac{1}{2}(F^2 - I^2 - J^2)$. As will be seen, $I \cdot J$ will be important to compute the expected value in the states $|F, m_F\rangle$.

The expected value of the magnetic dipolar interaction Hamiltonian 6.15 it can be calculated

as:

$$\langle F, m_F | H_{MD} | F, m_F \rangle \;=\; A \, \langle F, m_F | \mathbf{I} \cdot \mathbf{J} | F, m_F \rangle, \tag{6.16}$$

$$\begin{aligned}
\langle \mathbf{I} \cdot \mathbf{J} \rangle &= \frac{1}{2}(\langle F^2 \rangle - \langle I^2 \rangle - \langle J^2 \rangle) \\
\langle F^2 \rangle &= F(F+1)\hbar^2, \quad \langle I^2 \rangle = I(I+1)\hbar^2, \quad \langle J^2 \rangle = J(J+1)\hbar^2, \\
\langle \mathbf{I} \cdot \mathbf{J} \rangle &= \frac{1}{2}(F(F+1) - I(I+1) - J(J+1)) \\
K &= F(F+1) - I(I+1) - J(J+1)
\end{aligned} \tag{6.17}$$

For simplicity, it is assumed the variable K. The reduced Plank's constant $\hbar$ it is considered absorbed in the A term since not affects to the energy difference, and it is common in all terms. In this way, the following is obtained:

$$E_{MD} = \frac{A}{2} K \tag{6.18}$$

Following this, the Hamiltonian for the electric quadrupolar interaction, where B represents the electric quadrupolar constant, is obtained from:

$$\begin{aligned}
H_{EQ} &= B \, \frac{\left[3(\mathbf{I} \cdot \mathbf{J})^2 + \frac{3}{2}(\mathbf{I} \cdot \mathbf{J}) \;-\; I(I+1)\, J(J+1) \right]}{I(I-1)\, J(2J-1)}, \\
\langle \mathbf{I} \cdot \mathbf{J} \rangle &= \frac{1}{2} \, K \, (\hbar^2), \quad \langle (\mathbf{I} \cdot \mathbf{J})^2 \rangle = \left(\frac{K}{2} \right)^2 (\hbar^4), \\
N &= \left(\frac{3K^2}{4} + \frac{3K}{4} - I(I+1)\, J(J+1) \right) \hbar^4, \quad D = I(I-1)\, J(2J-1).
\end{aligned} \tag{6.19}$$

The interested reader seeking a rigorous resolution should verify it through the quadratic potential of the operator using the property $\langle F^4 \rangle = [F(F+1)\hbar^2]^2$ and the expansion of $(\mathbf{I} \cdot \mathbf{J})^2 = I_i J_i I_j J_j$. For simplicity, it is acceptable to express it in terms of K: $\langle (\mathbf{I} \cdot \mathbf{J})^2 \rangle = \left(\frac{K}{2} \right)^2$.

$$H_{HFS} = H_{MD} + H_{EQ} = \frac{A}{2} K + B \frac{N}{D} \tag{6.20}$$

The constant A is the magnetic dipole interaction and the constant B is the electric quadrupole interaction constant. $A = 84.85$MHz, $B = 12.52$MHz. The constants come from experimental research at (Brown University, 2010). Summary of calculations to obtain the line width in $5^2P_{3/2}$ as shown in Table B.1.

It has critical implications in the development of a quantum database. In figure A.1, the fundamental levels and the excited level could be seen. The diagram of the separations of the energy levels configure the proposed scheme.

It is convenient to describe some other implications that should be considered. Some of those, especially the ones that implies an electric or electromagnetic field, have a relevant importance since can alter the hamiltonian of the system producing a degeneracy. In that case, one would be interested in perform computation related to perturbation theory. For that purpose, it is recommended to read the article (Raigada García, 2024d), is a detailed analysis of the anharmonic oscillator with its Hamiltonian is presented and the ground state energy corrections up to the second order in the parameter λ are studied. Moreover, the article (Raigada García, 2024c), that examines the application of the first-order time-independent perturbation theory to a $\frac{1}{2}$-spin particle.

One can observe a term g_F in the diagram A.1 which is related to the hyperfine Landé factor. Landé factor g describes the relation of the total magnetic moment and the total angular momentum of a particle. In the presence of an external magnetic field $\mathbf{B}$, the atomic levels split due to the well-known Zeeman effect. It can be expressed as:

$$\begin{aligned} \boldsymbol{\mu_l} &= \frac{-e}{2\,m\,c}\,\mathbf{L}, \\ \boldsymbol{\mu_s} &= \frac{-e}{2\,m\,c}\,\mathbf{S}, \\ H_{\text{Zeeman}} &= -(\boldsymbol{\mu_l} + \boldsymbol{\mu_s}) \cdot \mathbf{B}, \\ H_{\text{Zeeman}} &= \frac{e}{2\,m\,c}\left(L_z + 2\,S_z\right) B. \end{aligned} \tag{6.21}$$

Consider that $\mathbf{B} = B_{\hat{z}}$ aligns on the z-axis and the factor two comes from the gyromagnetic factor of the electron spin. A more experimented reader should note that in terms of perturbative theory, the Hamiltonian can be constructed based on weak and strong effects.

One must consider the relative strength of the external magnetic field B compared to an internal field, B_{int} which is related to the atom's own internal interaction. For instance, the spin-orbit coupling. In the case of an external magnetic field is much weaker than the internal magnetic field $B \ll B_{\text{int}}$, it is known as the weak Zeeman effect:

$$H = H^{(0)} + \delta H_{FS} + \delta H_{\text{Zeeman}} \tag{6.22}$$

Since B is small, it is convenient to treat it as a small perturbation term δH_{Zeeman}. For that

reason, the first two terms can be combined into a single Hamiltonian:

$$H = \tilde{H}^{(0)} + \delta H_{\text{Zeeman}} \tag{6.23}$$

Similarly, the strong Zeeman effect is produced when an external magnetic field is much stronger than the internal magnetic field $B \gg B_{\text{int}}$. Since B is large, the Zeeman term is dominant and one, it is conditioned to treat the fine structure as a small perturbation.

$$\begin{aligned} H &= H^{(0)} + \delta H_{\text{Zeeman}} + \delta H_{FS} \\ H &= \tilde{H}^{(0)} + \delta H_{FS} \end{aligned} \tag{6.24}$$

Intuitively, one can consider that having a weak Zeeman effect is a better case because theoretically, one knows the unperturbed Hamiltonian and the fine structure. Instead, in the strong Zeeman, the correction sought is within the Hamiltonian $\tilde{H}^{(0)}$. Seams that one is not in a good place. But, in fact, is much easier to solve than the weak Zeeman effect. In the weak case, the Zeeman effect introduces a small correction in a degenerated system. That produces a mix of states due to the spin-orbit coupling. Carefully, one has to determine when the Zeeman term affects the quantum perturbed states in the fine structure. Note that the perturbed matrix it is not diagonal in the base of the coupled states $|n, l, j, m_j\rangle$. Finding the corrected eigenvalues and eigenstates is therefore a challenge, since linear combinations of states can occur.

On the contrary, in the case of the strong Zeeman effect, the Zeeman term δH_{Zeeman} is not known, however, the eigenstates of the Hamiltonian without corrections $H^{(0)}$ in the decoupled basis $|n, l, m_l, m_s\rangle$ are eigenstates of the Zeeman term when the magnetic field is strong. It is because it is diagonal in the basis of δH_{Zeeman}. In which L_z and S_z acts directly on m_l and m_s.

Consider the electron magnetic moment:

$$\mu_J = -g_J \mu_B \frac{\mathbf{J}}{\hbar}, \quad \text{where } \mu_B \text{ is Borh's magneton} \tag{6.25}$$

The energy correction due to the Zeeman effect with fine structure is:

$$
\begin{aligned}
\Delta E_{\text{Zeeman}} &= \langle F, m_F | H_{\text{Zeeman}} | F, m_F \rangle \\
H_{\text{Zeeman}} &= g_J \mu_B \frac{\mathbf{F} \cdot \mathbf{B}}{\hbar} \\
g_J &= g_L \frac{F(F+1) + L(L+1) - S(S+1)}{2J(J+1)} + g_S \frac{F(F+1) - L(L+1) + S(S+1)}{2J(J+1)} \\
g_F &= g_J \frac{F(F+1) + J(J+1) - I(I+1)}{2F(F+1)}
\end{aligned}
\tag{6.26}
$$

Then the energy correction became:

$$
\begin{aligned}
\Delta E_{\text{Zeeman}} &= -g_F \mu_B B \frac{m_F}{\hbar} \\
\Delta E_{\text{Zeeman}} &= g_F \mu_B B m_F
\end{aligned}
\tag{6.27}
$$

It is convenient to omit the negative term because one is interested in the shift of energy. Numerically solving for rubidium ^{87}Rb, consider the computed terms $g_F = 2/3$,$g_J = 4/3$, $\mu_B = 9.274 \times 10^{-24} J/T$, and the equation 6.27. Separating by energy per unit magnetic field and converting to frequencies in units of h, one obtains the same value as the diagram A.2:

$$
\begin{aligned}
\Delta_\nu &= \frac{E_{\text{Zeeman}}}{h} = \frac{g_F \mu_B}{h} B m_F \\
\frac{\Delta_\nu}{B} &\approx 9.33 \times 10^5 \text{Hz/Gauss} = 0.933 \text{MHz/Gauss}
\end{aligned}
\tag{6.28}
$$

Line D_1 corresponds to the transition of $5^2P_{1/2} \leftrightarrow 5^2S_{1/2}$, line D_2 corresponds to the transition of $5^2P_{3/2} \leftrightarrow 5^2S_{1/2}$. In the figure A.2, one can see that the wavelength at D_1 is $\approx$ 794.978nm and at D_2 it is $\approx$ 780.241 nm.

The wavelength determines the interaction of light with the ^{87}Rb atom. Particularly, visible wavelengths favour the use of standardized techniques in quantum optics such as lasers and precise detectors in this wavelength range. The photon-atom interaction is important because the efficiency of quantum memory depends on it.

Each transition has different transition probabilities and line widths. Therefore, the level with greater degeneration is usually preferred because it has a higher absorption coefficient. The total angular momentum of each state has been previously described in detail. To determine the number of degenerate states or, in other words, the number of different states that share that energy, (Tipler, 2000), proceed as follows:

$$5^2P_{1/2}(J = 1/2) = 2J + 1 = 2 \text{ degenerate states}$$

$$5^2P_{3/2}(J = 3/2) = 2J + 1 = 4 \text{ degenerate states}$$

A more significant number of degenerate states implies more final states in the metastable state transition, thus increasing the total absorption probability. In practical terms, the D_2 line has more degenerate states that can be pathways for the transition from the ground state, which implies a greater absorption capacity. The photonic absorption allows the photon to be stored in the atomic structure of ^{87}Rb.

The ability to maintain consistency for each of the two lines should be considered. However, this is a complex issue to discuss because, in addition, probabilistic Raman scattering is used, and it has been proven that depending on the sending angle, a greater probability of photonic loss occurs. The decay rate γ_{obs} is influenced by the diffusion of the atomic coherence pattern (Chrapkiewicz et al., 2014). That is out of the scope of this thesis.

Synthesizing, if simplicity is sought in the states and less sensitivity to external perturbations, derived, for instance, from processes where the atoms are not needed at a high level of excitation and in addition, less spin-orbit coupling is needed, then the line D_1 is preferable. For cases where a high absorption coefficient, radiation capacity, coupling or the construction of traps is required, then the D_2 line is preferred.

A higher absorption coefficient, radiation capacity, strong coupling, and the possibility to build traps are desired, the D_2 line is the preferred choice. The selection of this line width is further supported by several factors. First, the D_2 line has stronger electric dipole transitions, thus improving the absorption probability. Second, one is interested in a coherent control of quantum states, so a higher value of J implies a more complex Zeeman splitting with the presence of magnetic fields, which favours the manipulation of atomic states. Finally, the wavelength is available in commercial diode lasers and efficient detectors in that range. This type of laser is often used in quantum optics and quantum communication, so they offer a reliable standard.

6.1.2 Stable States vs. Unstable

Quantum systems are exposed to a loss of information, in physical terms, entropy increases. Therefore, a system that stores certain information over time loses this information until it becomes an

intractable system. This process of information loss is called decoherence. It is crucial that a quantum system preserves quantum coherence.

This section explains coherence in terms of the quantum system described, and in Chapter 7 it can be seen that it also applies to algorithmic descriptions in quantum computing. It is recommended that the reader consult an explanatory article on a Google Quantum AI research published in August 2024 (Raigada García, 2024b) (see also the original paper Acharya et al., 2024), where they managed to demonstrate a quantum memory system that reduces quantum error rates. Demonstrating the possibility of building fault-tolerant quantum computers. The reader must understand that when Google talks about quantum memory, it refers to maintaining coherence on a circuit to which quantum gates are applied, that is, it is worked with, with the aim of maximizing the lifetime. While this thesis is concerned with temporarily storing the state of a quantum system, to later recover a coherent quantum state on which to operate.

The reader can deduce that this is a critical fact in the production of a functional quantum computer within a quantum communications network. Google Quantum AI through error correction can maintain coherence in a system, while the proposed approach complements the use of the quantum computer in several ways.

Firstly, being able to store a quantum state of a system to which operations are being applied to preserve the state while calculations are being performed on other qubits. This is a strategy to increase the durability of a quantum system with which it is being operated. Aligned with the objectives of Google's research.

Secondly, offering the possibility of storing a quantum system in a quantum database to later recover it coherently without collapsing it to a classical state. This may have applications in quantum communication systems, for example, in secure communication, quantum satellite sensors, or in general, sensors that work in quantum format, but that until now, could only be collapsed to classical states and operated with them. This would be the case of LiDAR sensors.

In these systems, stable states are essential for the preservation of quantum coherence. Particularly, the dark state generated in the three-level Λ system. The coherent superposition of the base states has been explained previously. It has been concluded that there is a minimization of spontaneous transitions, which reduces the chances of decoherence.

On the other hand, atoms that are in the excited state $|e\rangle$ tend to decay towards fundamental states, since spontaneous emissions of photons occur. This is problematic because the photons

emitted in the decay of the $|e\rangle$ state are photons that are out of phase regarding the coherent field, so they contribute noise to the system. Spontaneous decay will be treated in the Lindblad equation 6.1.4 section, an equation that describes how an open quantum system interacts with its environment and loses coherence. This type of state with high decoherence is known as an unstable state.

6.1.3 Derivation of the light-atom interaction Hamiltonian

The concept of EIT has been described previously from a semiclassical and simple perspective. From now on, the EIT version of quantum memory will be derived.

To begin, it is important to recall that the system under consideration is a three-level Λ system: two metastable and one unstable; which interact with an electromagnetic field. Separated by an energy corresponding to the frequency of the atomic transition ω_0.

The Hamiltonian of an atom without interaction is expressed as:

$$\mathrm{H}_{\mathrm{atom}} = \frac{\hbar\omega_0}{2}\begin{pmatrix} 1 & 0 \\ 0 & -1 \end{pmatrix} \tag{6.29}$$

Where the square matrix of dimension 2×2 corresponds to the Pauli matrix Z defined by Wolfgang Pauli, which represents the operator corresponding to the two-level system. Henceforth, this matrix will be referred to as σ_z. For an introduction to Pauli matrices, it is recommended to consult the Pauli's publication from May 1927, "Zur Quantenmechanik des magnetischen Elektrons" (Pauli, 1927).

The Hamiltonian of the electromagnetic field is classically described by the electric field associated with an electromagnetic wave.

$$\mathbf{E}(t) = \mathbf{E}_0\, e^{i\omega t} + \mathrm{h.c.} \tag{6.30}$$

Where $\mathbf{E}$ corresponds to the amplitude of the electric field and ω to the frequency of the wave.

To calculate the interaction Hamiltonian, the interaction between the electromagnetic field and the atom must be evaluated. Considering the electric dipole coupling between atom and field. The dipole interaction operator can be found as:

$$
\begin{aligned}
H_{int} &= -\left(\left\langle e\middle|\sum_{i,j}\langle i|\hat{\mathbf{d}}|j\rangle\ |i\rangle\,\langle j|\middle|g\right\rangle\cdot\begin{pmatrix}0 & 1\\ 0 & 0\end{pmatrix} + \left\langle g\middle|\sum_{i,j}\langle i|\hat{\mathbf{d}}|j\rangle\ |i\rangle\,\langle j|\middle|g\right\rangle\right)\cdot\begin{pmatrix}0 & 0\\ 1 & 0\end{pmatrix}\Bigg)\cdot\mathbf{E}(t)\\
&= -\Big[\langle e|\hat{\mathbf{d}}|g\rangle\cdot\sigma_{eg} + \langle g|\hat{\mathbf{d}}|e\rangle\cdot\sigma_{ge}\Big]\cdot\mathbf{E}(t)\\
&= -\Big[\mathbf{d_{eg}}\cdot\sigma_{eg} + \mathbf{d_{ge}}\cdot\sigma_{ge}\Big]\cdot\mathbf{E}(t),
\end{aligned}
$$

$$
H_{int} = -\mathbf{d}\cdot\mathbf{E}(t) \tag{6.31}
$$

$\mathbf{d}$ is the electric dipole moment operator of the atom. As seen in the deduction, d_{xy} corresponds to the transition dipole moments. The excitation operator is σ_{xy} and the relaxation operator σ_{xy}. Applying the rotation framework as described, from here on out called the rotating wave approximation (RWA), one get:

$$
H_{\text{int}} = -\frac{\hbar}{2}\Big[\Omega_p(t)\,\hat{\sigma}_{eg}\,e^{i\Delta_p t} + \Omega_c(t)\,\hat{\sigma}_{es}\,e^{i\Delta_c t} + \text{h.c.}\Big] \tag{6.32}
$$

The Rabi frequencies of the probe beam and the control beam are calculated and substituted into the equation 6.32:

$$
\Omega_p(t) = \frac{\mathbf{d}_{ge}\cdot\mathbf{E}_p(t)}{\hbar} \quad , \quad \Omega_c(t) = \frac{\mathbf{d}_{se}\cdot\mathbf{E}_c(t)}{\hbar} \quad , \quad \hbar = \frac{h}{2\pi}
$$

$\Omega_p(t)$ corresponds to the coupling $\langle g| \leftrightarrow |e\rangle$, similarly $\Omega_c(t)$ corresponds to the coupling $\langle s| \leftrightarrow |e\rangle$. The detunings are calculated as:

$$
\Delta_p = \omega_p - \omega_{eg} \quad , \quad \Delta_c = \omega_c - \omega_{es}
$$

The control Hamiltonian is calculated as:

$$
H_{\text{control}} = -\hbar\,\Omega_c(t)\,\hat{\sigma}_{es}\,e^{i\omega_c t} + \text{h.c.}
$$

which under the RWA is:

$$H_{\text{control}} = -\frac{\hbar}{2}\Big(\Omega_c(t)\,\hat{\sigma}_{es}\,e^{i\Delta_c t} + \text{h.c.}\Big) \tag{6.33}$$

The same is done with the probe Hamiltonian:

$$H_{\text{probe}} = -\hbar\,\Omega_p(t)\,\hat{\sigma}_{eg}\,e^{i\omega_p t} + \text{h.c.}$$

$$H_{\text{probe}} = -\frac{\hbar}{2}\Big(\Omega_p(t)\,\hat{\sigma}_{eg}\,e^{i\Delta_p t} + \text{h.c.}\Big) \tag{6.34}$$

Finally, the complete Hamiltonian results from joining the control and probe Hamiltonian: $H_{\text{total}} = H_{\text{control}} + H_{\text{probe}}$:

$$H_{\text{total}} = -\frac{\hbar}{2}\Big[\Omega_p(t)\,\hat{\sigma}_{eg}\,e^{i\Delta_p t} + \Omega_c(t)\,\hat{\sigma}_{es}\,e^{i\Delta_c t} + \text{h.c.}\Big] \tag{6.35}$$

6.1.4 Lindblad Equation

Up to this point, a series of conditions have been prepared that result in an open quantum system. At this time, one is interested in understanding how the quantum system interacts with its environment. Especially, to understand decoherence and dissipation. Aspects that have been discussed previously.

The way to understand the evolution of a quantum system is through the Schrödinger equation. However, in this thesis one is interested in adding dissipative effects, so an extension of the Schrödinger equation known as the Lindblad equation will be used.

The Lindblad equation allows modelling the non-unitary evolution of the density matrix associated with a quantum state under certain conditions that perturb the state, such as the processes of decoherence, spontaneous emission and relaxation. To construct the description of the time evolution of the density matrix, the process begins by considering the description of the coherent evolution of the density matrix under the conditions imposed on the interaction Hamiltonian in the Equation 6.35. The concept of a commutator is used to accomplish this.

$$[H_{int},\,\rho] = H_{int}\rho - \rho H_{int}$$

$$\frac{-i}{\hbar}[H_{int},\, \rho]$$

The subsequent step involves including the dissipation terms into the Lindblad equation, which will affect the light-atom interaction Hamiltonian. It could well be considered that spontaneous radiation exists in any state. While this is acceptable, it does not fully reflect the real behaviour. Let us recall that in Section 6.1.1 the advantages of the ground and excited states were explained. The reader will understand that the only state that has significant spontaneous emission and is therefore the one that is likely to lead the system to an incoherent state is the excited state. For this reason, in the description of dissipation, it is convenient to only include the terms that refer to spontaneous radiation regarding the excited state $|e\rangle$: Γ_{eg}, Γ_{es}. This simplifies the model, while including stable states lacks a strong foundation, since they are inherently stable.

$$\frac{dp}{dt} = \frac{-i}{\hbar}[H_{int},\, \rho] + \sum_{i,j} \Gamma_{ij} \left(\sigma_{ij} \rho \sigma_{ji}^{\dagger} - \frac{1}{2} \left\{ \sigma_{ji}^{\dagger} \sigma_{ij}, \rho \right\} \right) \tag{6.36}$$

Equation 6.36 is derived from the general form of the Lindblad equation to adapt it to the proposed scheme. Transitions appear between the states represented by projection operators, with decoherence rates $\Gamma_{i,j}$. Since one is working RWA, the system is represented as follows:

$$\begin{aligned}
\rho_{es} &= \frac{i\,\Omega_c\, e^{i\Delta_p t}}{(\Gamma_{eg} + \Gamma_{es} + \Gamma_{ss}) + 2i\,\Delta_c} \rho_{gs} \\
\rho_{gs} &= -\frac{i\,\Omega_c\, e^{i\Delta_c t}}{(\Gamma_{ss}) + 2i\,(\Delta_c - \Delta_p)} \rho_{ge} \\
\rho_{eg} &= \frac{i\,\Omega_p e^{i\Delta_p t}}{(\Gamma_{eg} + \Gamma_{es} + \Gamma_{ee}) + 2i\,\Delta_p} + \frac{i\,\Omega_c\, e^{i\Delta_c t}}{(\Gamma_{eg} + \Gamma_{es} + \Gamma_{ee}) + 2i\,\Delta_p} \rho_{sg}
\end{aligned} \tag{6.37}$$

ρ_{es} describes the coherence between $|e\rangle$ and $|s\rangle$. As can be seen, it is recovered the Rabi frequency of the control field, the decoherence rate and the detuning Δ_c of the transition $|s\rangle \leftrightarrow |e\rangle$. ρ_{gs} describes the superposition between the states $|g\rangle$ and $|s\rangle$ and expresses the relative detuning between the control and test fields. ρ_{eg} describes the coherence between $|e\rangle$ and $|g\rangle$. The first fraction is the coherence induced by the probe beam, and the second fraction represents the coupling of the control beam.

With the non-diagonal components of the equation 6.37 one can understand the evolution of the system; however, one still does not know anything about the transparency of the medium. In other words, the focus will be on understanding refraction and velocity. To begin by stating that

a particle with momentum, p, can be associated with a plane or matter wave. By utilizing the wavelength of de Broglie, it is obtained:

$$\lambda = \frac{h}{p}, \quad p = |p|, \quad p = \frac{h}{\lambda} = \frac{h}{2\pi}, \quad \frac{2\pi}{\lambda} = \hbar k \quad k \equiv \frac{2\pi}{\lambda}$$

$f(x - \omega t)$ is a wave packet of the general form with $\omega(k)$ as the frequency associated with wave number k. It is well-known that the wave function can be expressed as a superposition of plane waves:

$$\Psi(x,t) = \int dk \Phi(k) e^{i(kx - \omega t)} \tag{6.38}$$

Where Φ is a function centred around a particular value of k_0. To see the speed of propagation of the wave packet, the principle of stationary phase is used. The phase of the integral is given by $\varphi(k) = kx - \omega(k)t$. Since one is interested in seeing where the phase varies slowly, one must evaluate the values of k close to that point. To achieve this, the derivative of $\varphi(k)$ with respect to k must be zero. Therefore:

$$\frac{\partial \varphi}{\partial k} = x - t \quad \frac{\partial \omega}{\partial k} = 0$$

From the above relationship, it follows that the wave packet moves with a group velocity:

$$v_g = \frac{dx}{dt} = \frac{d\omega}{dk} \tag{6.39}$$

This is related to the dispersion of the medium, the refractive index depends on the frequency of the light ω. It is known that the refractive index n is related to the electrical susceptibility of the medium $\chi^{(1)}$ (Fleischhauer et al., 2005, p. 2). Since n varies with frequency, the consequence is that the group velocity will also vary. Therefore, returning to the relationship between the wave number k and the frequency ω, it can be written as:

$$\begin{aligned} n &= \sqrt{1 + \mathrm{Re}[\chi^{(1)}]} \\ v_g &= \frac{c}{n + \omega \frac{\partial n}{\partial \omega}} \end{aligned} \tag{6.40}$$

$\frac{\partial n}{\partial \omega}$ is the dispersion of the refractive index as a function of frequency. Note that in practice, it

refers to the probe beam (ω_p) in the medium.

At this point, the reader may wonder why one is measuring the photon's velocity group instead of directly measuring the photon's velocity. Recall that this is a quantum system, so it is not possible to simultaneously measure the position and momentum accurately for both terms. This is described by Heisenberg's uncertainty principle, which states:

$$\Delta x \Delta p \geq \frac{\hbar}{2} \tag{6.41}$$

The principle arises from the commutation between quantum operators. Given two Hermitian operators A and B, the commutator $[A, B]$ does not vanish. Defining the uncertainties as ΔA and ΔB:

$$(\Delta A)^2 = \langle \Psi | A^2 | \Psi \rangle - \langle \Psi | A | \Psi \rangle^2$$

Similarly, for B, it can be rewritten as:

$$\Delta A \, \Delta B \;\geq\; \frac{1}{2} \left| \langle \Psi | [A, B] | \Psi \rangle \right|$$

Regarding momentum and position, the switched operators obey: $[\hat{x}, \hat{p}] = i\hbar$ so the relation generates the inequality 6.41. Refer to Figure A.3 for a visual representation.

Particles that have mass have their speed expressed through the momentum $v = \frac{p}{m}$. However, photons do not have mass, so it depends on the refractive index of the medium. The measurement of the speed of a photon is limited by the uncertainty in the momentum. Therefore, the phase velocity of a wave is not measured, but rather the group velocity, therefore, of the wave packet. If one wanted to reduce the uncertainty between the two measurements to a minimum, one should minimize the value of the product $\Delta A \Delta B$ so that it results in $\frac{\hbar}{2}$. This would indicate that the quantum state is in a coherent state with minimal uncertainty.

6.1.5 Hamiltonian Interacting with Quantized Field

An electromagnetic field can be considered as a quantum harmonic oscillator. In the subsequent deductions, the mode of the field will be described by the ladder operators (a, $a^\dagger$). Keep in mind that these operators satisfy the commutation relation $[a, a^\dagger] = \hat{a}\hat{a}^\dagger - \hat{a}^\dagger\hat{a} = 1$.

Let the atom size is much smaller than the wavelength of the field, and it is propagated in

one direction and polarization. That assumption is known as the dipole approximation. The quantized electric field in the volume quantized is expressed as follows. For a similar quantization of electromagnetic field, refer to Puri, 2001, pp. 119–123 and Vahala, 2004, p. 376:

$$\hat{E}(r,t) = i \sum_{k,\lambda} \sqrt{\frac{\hbar\omega_k}{2\epsilon_0 V}} \Big(\hat{a}_{k,\lambda}\, \mathbf{e}_{k,\lambda}\, e^{i(\mathbf{k}\cdot\mathbf{r}-\omega_k t)} \; - \; \hat{a}^{\dagger}_{k,\lambda}\, \mathbf{e}^{*}_{k,\lambda}\, e^{-i(\mathbf{k}\cdot\mathbf{r}-\omega_k t)} \Big) \tag{6.42}$$

The equation has two important parts, the creation, and annihilation operators (a, $a^{\dagger}$) multiplied by the polarization vector ($\mathbf{e}_{k,\lambda}$) with determined phase. Included in the phases is the angular frequency ($\omega = c|\mathbf{k}|$) mode $\mathbf{k}$. Furthermore, V is the quantization volume (Scully & Zubairy, 1997).

The original model was proposed by Jaynes and Cummings in the paper title *Comparison of quantum and semiclassical radiation theories with application to the beam maser* (Jaynes & Cummings, 1962). Later, you will find this type of model referred to in the literature as the Jaynes-Cummings model. It contains the theoretical framework for the quantization of a field used in this thesis. It is a complex text, but it investigates topics related to the study of this thesis, which will not be addressed specifically, such as Einstein's coefficients A[§] and B[†].

The interaction Hamiltonian can be constructed considering that the distribution charge of the atom it is sufficiently smaller to make the electric field roughly constant. Expressing the dipole moment of the atom as $\hat{\mathbf{d}}$, the interaction Hamiltonian can be described as (Puri, 2001):

$$\hat{H}_{\text{int}} = -\hat{\mathbf{d}} \cdot \hat{E}(r,t) \tag{6.43}$$

Recall that the atom lives in a three level configuration (Λ-Schema). Therefore:

$$\hat{\mathbf{d}} = \mathbf{d}_{ge}\, \hat{\sigma}_{eg} + \mathbf{d}_{es}\, \hat{\sigma}_{se} + \text{h.c.} \tag{6.44}$$

[§]It represents the transition probability per unit time of spontaneous emission of a photon by an atom in an excited state, that is, an electron in the upper level will drop to the lower level (Fox, 2006, pp. 48–51). The radioactive lifetime therefore arises from $\tau = \frac{1}{A_{1\leftarrow 2}}$ where the coefficient A expresses the transition from level 2 to level 1.

[†]It represents the probability of absorption, that is, the atom transitions from the low-energy level to the excited state by absorbing the required energy from a photon (Fox, 2006, pp. 48–51).

The above expansion involves the atomic estates described as:

$$\begin{aligned}
\mathbf{d}_{ge} &= \langle g|\hat{\mathbf{d}}|e\rangle, \\
\mathbf{d}_{es} &= \langle e|\hat{\mathbf{d}}|s\rangle, \\
\hat{\sigma}_{\alpha\beta} &= |\alpha\rangle\,\langle\beta|\,.
\end{aligned} \tag{6.45}$$

When the atomic transition frequency is much greater than the Rabi frequency ($\omega_0 \gg \Omega$), it is convenient to ignore the faster oscillations. Consequently, the complex phase ($e^{\pm i(\mathbf{k}\cdot\mathbf{r}-\omega_k t)}$) and counter-rotation terms ($e^{\pm i(\mathbf{k}\cdot\mathbf{r}+\omega_k t)}$) vanish. Re-expressing the Equation 6.43 over the RWA:

$$\hat{H}_{\text{int}} = -\hbar \sum_{i=1}^{N} \Big(g\,\hat{a}\,\hat{\sigma}_{eg}^{(i)}\, e^{i\mathbf{k}_p\cdot\mathbf{r}_i} \;-\; \Omega_c(t)\, e^{-i\omega_c t}\,\hat{\sigma}_{es}^{(i)} \Big) + \text{h.c.} \tag{6.46}$$

Take into account that the vacuum Rabi frequency of the transition $|g\rangle \leftrightarrow |e\rangle$ it is contained in the term g as:

$$g = \frac{\mathbf{d}_{ge}\cdot\mathbf{e}_p}{\hbar}\sqrt{\frac{\hbar\omega_p}{2\epsilon_0 V}}$$

Note that $\mathbf{e}_p$ is the unitary polarization vector of the electromagnetic field.

The total Hamiltonian of the system can be expressed in terms of the perturbed Hamiltonian ($\hat{H}_0$) and unperturbed Hamiltonian (H). Over this purpose, $\hat{H}_0$ can be expressed including the energies of the atomic estates plus the energies of the electromagnetic field contained in the Equation 6.46.

$$\begin{aligned}
\hat{H}_{\text{total}} &= \hat{H}_0 + \hat{H}_{\text{int}}, \\
\hat{H}_0 &= \sum_{i=1}^{N} \Big(\hbar\omega_g\,\hat{\sigma}_{gg}^{(i)} + \hbar\omega_e\,\hat{\sigma}_{ee}^{(i)} + \hbar\omega_s\,\hat{\sigma}_{ss}^{(i)} \Big) + \hbar\omega_p\,\hat{a}^\dagger\hat{a}, \\
\hat{H}_{\text{total}} &= \sum_{i=1}^{N} \Big(\hbar\omega_g\,\hat{\sigma}_{gg}^{(i)} + \hbar\omega_e\,\hat{\sigma}_{ee}^{(i)} + \hbar\omega_s\,\hat{\sigma}_{ss}^{(i)} \Big) + \hbar\omega_p\,\hat{a}^\dagger\hat{a} \\
&\quad - \hbar \sum_{i=1}^{N} \Big(g\,\hat{a}\,\hat{\sigma}_{eg}^{(i)}\, e^{i\mathbf{k}_p\cdot\mathbf{r}_i} \;-\; \Omega_c(t)\, e^{-i\omega_c t}\,\hat{\sigma}_{es}^{(i)} \Big) + \text{h.c.}
\end{aligned} \tag{6.47}$$

6.1.6 Two-photon Resonance Condition

The detuning of a photon is described by $\Delta = \omega_p - \omega_{eg}$, and the detuning of the two photons is described by the relation $\delta = (\omega_p - \omega_c) - (\omega_s - \omega_g)$. The two-photon resonance condition

is produced when the detuning between the beam laser and the atomic transitions satisfy the relationship $\omega_p - \omega_c = \omega_s - \omega_g$. The difference between the frequency lasers and the difference of energy in the $|g\rangle$ y $|s\rangle$ match, and therefore $\delta = 0$. This implies that a coherent transition between states $|g\rangle \leftrightarrow |s\rangle$ can occur via state $|e\rangle$.

The total Hamiltonian interaction under the RWA (Equation 6.47) can be expressed in the base $\{|g\rangle, |e\rangle, |s\rangle\}$ in matrix form.

$$\hat{H}_{\text{total}} = \begin{pmatrix} \hbar\omega_g & -\frac{\hbar g}{2}e^{-ik_p\cdot r} & 0 \\ -\frac{\hbar g}{2}e^{-ik_p\cdot r} & \hbar\omega_e & -\frac{\hbar\Omega_c(t)}{2}e^{-i\omega_c t} \\ 0 & -\frac{\hbar\Omega_c(t)}{2}e^{-i\omega_c t} & \hbar\omega_s \end{pmatrix} \tag{6.48}$$

The above matrix can be simplified by a change of basis $|\Psi\rangle \rightarrow |\Psi'\rangle = e^{i\omega_p t}\hat{a}\hat{a}^\dagger |\Psi\rangle$. In this way, the time phases associated with the laser fields are eliminated. In the new basis, the following stationary matrix is obtained, where $\Delta = \omega_e - \omega_g - \omega_p$ is the one-photon mismatch:

$$\hat{H}_{\text{total}} = \begin{pmatrix} 0 & -\frac{\hbar g}{2} & 0 \\ -\frac{\hbar g}{2} & \Delta & -\frac{\hbar\Omega_c}{2} \\ 0 & -\frac{\hbar\Omega_c}{2} & \Delta \end{pmatrix} \tag{6.49}$$

At the base of the states $|g\rangle$, $|s\rangle$, $|e\rangle$ a wave function is proposed:

$$|\Psi\rangle = c_g |g\rangle + c_e |e\rangle + c_s |s\rangle \tag{6.50}$$

The wave function can be expressed in terms of the time-independent Schrödinger equation: $H|\Psi\rangle = E|\Psi\rangle$. Assuming the two-photon resonance condition, $\delta = 0$, one is ready to solve to obtain the eigenstates and eigenvalues.

$$\begin{cases} -\frac{\hbar g}{2}c_e = Ec_g \\ -\frac{\hbar g}{2}c_g + \Delta c_e - \frac{\hbar\Omega_c}{2}c_s = Ec_e \\ -\frac{\hbar\Omega_c}{2}c_e + \Delta c_s = Ec_s \end{cases} \tag{6.51}$$

Given the resonance condition, $\Delta = 0$ is imposed, simplifying the system of equations to:

$$\begin{cases} -\frac{\hbar g}{2} c_e = E c_g \\ -\frac{\hbar g}{2} c_g - \frac{\hbar \Omega_c}{2} c_s = E c_e \\ -\frac{\hbar \Omega_c}{2} c_e = E c_s \end{cases} \tag{6.52}$$

6.1.7 Simple Dark State

One needs to find a non-trivial solution $(c_g, c_e, c_s \neq 0)$ to the Equation System 6.52. Consequently, it involves solving: $\det\left(\hat{H}_{\text{total}} - E\hat{I}\right) = 0$.

$$\det \begin{pmatrix} -E & -\frac{\hbar g}{2} & 0 \\ -\frac{\hbar g}{2} & -E & -\frac{\hbar \Omega_c}{2} \\ 0 & -\frac{\hbar \Omega_c}{2} & -E \end{pmatrix} = 0 \tag{6.53}$$

The eigenvalues are:

$$E_0 = 0, \quad E_\pm = \pm \frac{\hbar}{2} \sqrt{\Omega_c^2 + g^2}. \tag{6.54}$$

The above eigenvalues correspond to the dark state $\left|\Psi^0, E_0 = 0\right\rangle$ and the luminous states $\left|\Phi^\pm, E_\pm = \pm\frac{\hbar}{2}\sqrt{\Omega_c^2 + g^2}\right\rangle$. Solving the Equation System 6.52 for $E_0 = 0$ and consequently for $c_e = 0$, $c_g = \Omega_c$, $c_s = -g$; normalising one gets:

$$\left|\Psi^0\right\rangle = \frac{\Omega_c \left|g\right\rangle - g \left|s\right\rangle}{\sqrt{\Omega_c^2 + g^2}} \tag{6.55}$$

The state $\left|\Psi^0\right\rangle$ has no absorption and emission of photons from the probe field due to there is no interaction with $|e\rangle$. Besides, is a coherent superposition of $|g\rangle, |s\rangle$.

It is important to note that resolving for $|\Phi^\pm\rangle$ the result is a combination of the basis states and the adjustments corresponds to the Rabi frequencies and the energies. Since exists interaction with the state $|e\rangle$, there is the possibility to experiment a radioactive decay that emits a photon contributing to the objective (EIT effect).

6.1.8 Mixing Angles

To understand how Rabi frequencies and detuning affect states, the mixing angles θ and ϕ will be used, which describe the composition of the eigenstates as a function of the basis states. The angle

θ is defined as the ratio of the Rabi frequency of the probe field to the control field $\tan\theta = \frac{\Omega_p}{\Omega_c}$.

Regarding the state $\left|\Psi^0\right\rangle$ the proportion of action can be defined using the angle θ:

$$\left|\Psi^0\right\rangle = \cos\theta\,|g\rangle - \sin\theta\,|s\rangle \tag{6.56}$$

The above equation is sometimes called as dark state (Lambropoulos & Petrosyan, 2007, p. 114). By normalizing, the proportion relations are obtained:

$$\cos\theta = \frac{\Omega_c}{\sqrt{\Omega_p^2 + \Omega_c^2}}, \quad \sin\theta = \frac{\Omega_p}{\sqrt{\Omega_p^2 + \Omega_c^2}} \tag{6.57}$$

The angle ϕ is obtained by diagonalizing the subspace in which $|e\rangle$ is involved with the combination of the other two states: stable and metastable. Therefore, this process arises from the light state $|\Phi^{\pm}\rangle$.

$$\tan 2\phi = \frac{\sqrt{\Omega_p^2 + \Omega_c^2}}{\Delta} \tag{6.58}$$

6.1.9 General Dark State

Based on the mixing angles, the simple dark state can be re-expresed as:

$$\left|\Psi^0, 1\right\rangle = \cos\theta(t)\,|G,1\rangle - \sin\theta(t)\,|S,0\rangle \tag{6.59}$$

The above equation expresses the situation where all photons are in $|g\rangle$ and one photon is in the probe field as $|G,1\rangle = |g_1, g_2, \cdots, g_N; 1 \text{ probe}\rangle$ as a base collective state. Additionally, express a collective state of excited atoms in the estate $|S\rangle$ and no photon in the probe field as $|S,0\rangle = \frac{1}{\sqrt{N}}\sum_{i=1}^{N} e^{i\mathbf{k}_p\cdot\mathbf{r}_i}\,|g_1, g_2, \cdots, g_N; 0 \text{ probe}\rangle$. The collective excited state is a symmetrical superposition of the estates. Note that the above equation considers the evolution of the dark state, incorporating the time factor.

Consider the case where $\Omega_p \ll \Omega_c \Rightarrow \theta \approx 0$ thus $\left|\Psi^0\right\rangle \approx |g\rangle$. This means that the transition between $|g\rangle \leftrightarrow |e\rangle$ it is unlikely. Particularly, coherence is achieved. Now, consider the opposite situation where $\Omega_p \gg \Omega_c \Rightarrow \theta \to \infty$. Considering $\theta \approx \frac{\pi}{2}$ then $\left|\Psi^0\right\rangle \approx -|s\rangle$. In this case, the majority of the atoms is in the metastable state $|s\rangle$. Due to this fact, the transition between $|s\rangle \leftrightarrow |e\rangle$ is probably.

Based on the entire previous derivation, the states are re-expressed in a clearer way, considering the inclusion of the mixing angles that allow describing the model adjustments in terms of the control and probe fields as well as the mixing between ground and excited states.

$$\begin{aligned} \left|\Phi^{\pm}\right\rangle &= \sin\theta\sin\phi\,|g\rangle + \cos\phi\,|e\rangle + \cos\theta\sin\phi\,|s\rangle \\ \left|\Psi^{0}\right\rangle &= \cos\theta\,|g\rangle - \sin\theta\,|s\rangle \end{aligned} \tag{6.60}$$

The simple dark state can be generalized based on the collective states. The k atom in the symmetric collective state $|S\rangle$ can be expressed as:

$$\left|S^{k}\right\rangle = \frac{1}{\sqrt{\binom{N}{k}}} \sum_{\{j_1,\ldots,j_k\}} e^{i(\mathbf{k}_p\mathbf{r}_{j_1}+\cdots+\mathbf{k}_p\mathbf{r}_{j_k})}\,|g_1,\ldots,s_{j_1},\ldots,s_{j_k},\ldots,g_N\rangle \tag{6.61}$$

Considering the base collective state with $n-k$ photons in the probe field

$$|G, n-k\rangle = |g_1, g_2, \cdots, g_N; (n-k)_{\text{probe}}\rangle \tag{6.62}$$

Hence, the combined state it is written as $\left|S^k, n-k\right\rangle = \left|S^k\right\rangle \otimes |(n-k)_{\text{probe}}\rangle$ —superposition of states weighted by coefficients.

The coefficients are related to the probability amplitudes associated with each transition, depending on the mixing angle θ. A combinatorial factor is needed to distribute k excitations among n trials. Therefore, the general dark state can be constructed using the ladder operator $\hat{a}^\dagger$ of creation for the probe field photon and in the collective creation operator $\hat{S}^\dagger$ for the atomic excitations:

$$(\cos\theta\hat{a}^\dagger - \sin\theta\hat{S}^\dagger)^n\,|G,0\rangle \tag{6.63}$$

where $\hat{S}^\dagger = \frac{1}{\sqrt{N}}\sum_{j=1}^{N} e^{i\mathbf{k}_p\mathbf{r}_j}\hat{\sigma}_{sg}^{(j)}$, and expanding the operator using the binomial theorem:

$$\begin{aligned} \left(\cos\theta\,\hat{a}^\dagger - \sin\theta\,\hat{S}^\dagger\right)^n |G,0\rangle &= \sum_{k=0}^{n}\binom{n}{k}\left(-\sin\theta\right)^k\left(\cos\theta\right)^{n-k}(\hat{S}^\dagger)^k(\hat{a}^\dagger)^{n-k}\,|G,0\rangle \\ &= \sum_{k=0}^{n}\sqrt{\frac{n!}{k!(n-k)!}}\left(-\sin\theta\right)^k\left(\cos\theta\right)^{n-k}\left|S^k, n-k\right\rangle. \end{aligned} \tag{6.64}$$

$$C_k = \sqrt{\frac{n!}{k!(n-k)!}}\left(-\sin\theta\right)^k\left(\cos\theta\right)^{n-k}. \tag{6.65}$$

The superposition of the excitation is considered, where it can be in the amplitude, $-\sin\theta$, as an atomic state or as a photon state in the probe field with amplitude $\cos\theta$. Recall the use of square root, as it is probability amplitudes rather than probabilities. The Equation 6.65 largely follows the original and reference paper in the field by Fleischhauer and Lukin title *Quantum memory for photons: Dark-state polaritons* (Fleischhauer & Lukin, 2002). Therefore, the general dark state formulation is:

$$\left|\Psi^0, n\right\rangle = \sum_{k=0}^{n} C_k \left|S^k,\, n-k\right\rangle \tag{6.66}$$

6.1.10 Mixing Angle Λ

Previously, the θ mixing angles have been explored, now they will be applied under a three-level system in Λ configuration. In this way, it will be understood how the θ mixing angle is affected by the Rabi frequencies and the number of atoms in the system. As seen, this involves the description of the superposition of atomic states in the dark state.

Formerly, it has been shown that the angle θ is defined as the ratio of the Rabi frequency of the probe field to the control field $\tan\theta = \frac{\Omega_p}{\Omega_c}$. Now the vacuum Rabi frequency relative to the number of atoms in the medium and the Rabi frequency in the control field will describe the mixing angle $\tan\theta(t) = \frac{g\sqrt{N}}{\Omega(t)}$ (Fleischhauer et al., 2005, p. 13).

The denominator arises from the consideration of the quantized probe field interacting with N atoms. Due to the collective coherence, the effective Rabi frequency between field and atom is amplified. Again, consider that the square root is needed, since one is working with amplitudes. Remember that the time evolution of the dark state (Equation 6.59), is described by the effective Hamiltonian in the rotating frame and discarding the excitation in state $|e\rangle$:

$$\hat{H} = -\hbar\big(g\sqrt{N}\,\hat{\mathcal{E}}\,\hat{S}^\dagger \;+\; \Omega(t)\,\hat{S}^\dagger\hat{S}\big) + \text{h.c.} \tag{6.67}$$

$\hat{\mathcal{E}}$ is the normalized electric field operator, and $\hat{S}^\dagger$ is the collective spin excitation creation operator. Note the important relations: $\tan\theta(t) \ll 1 \Rightarrow \theta(t) \approx 0$, and $\tan\theta(t) \gg 1 \Rightarrow \theta(t) \approx \frac{\pi}{2}$.

6.1.11 Hamiltonian with Spatial Dimension

For a realistic understanding of the kinetic evolution of photons and the interaction with atoms, it is necessary to introduce the spatial dependence of the Hamiltonian. Let us assume that the wave propagation is in the z-direction. Note that it is usually chosen by convention, but it has practical reasons, since it simplifies the equations such as Maxwell's and allows describing the wave propagation by separating the variations in transverse space (x, y) from the variation in z.

It is purposed to add the z-direction dependence in the same deduction discussed in the Equations 6.43, 6.46, 6.47. Start by adding a dimension to the quantized electric field:

$$\hat{E}^{(+)}(z,t) = \mathcal{E}_0\, \hat{a}(z)\, e^{i(k_p z - \omega_p t)}. \tag{6.68}$$

Now, the interaction Hamiltonian for an atom in z_j position is described by the dipolar momentum operator of an atom j:

$$\hat{H}_{\text{int}} = -\sum_{j=1}^{N} \big(\hat{\mathbf{d}}_j \cdot \hat{E}^{(+)}(z,t) \big). \tag{6.69}$$

The expansion of the dipolar momentum operator is $\hat{\mathbf{d}}_j = d_{eg}\, \hat{\sigma}^j_{ge} + d_{es}\, \hat{\sigma}^j_{se} + \text{h.c.}$. Based on that expansion, it is constructed the Hamiltonian of interaction under the RWA exactly as did it in Equation 6.46:

$$\hat{H}_{\text{int}} = -\hbar \sum_{j=1}^{N} \Big(g\, \hat{a}(z_j)\, e^{i(k_p z_j - \omega_p t)}\, \hat{\sigma}^j_{ge} \;+\; \Omega_c\, e^{i(k_c z_j - \omega_c t)}\, \hat{\sigma}^j_{se} \Big) + \text{h.c.} \tag{6.70}$$

The Equation 6.70 allows constructing the new total Hamiltonian exactly as did it in Equation 6.47. Note that the spacial phase e^{ikz} in the Equation 6.70 captures the wave propagation. The probe field propagates in one direction ($+z$) with k_p as wave number, and the control field propagates bidirectional ($\pm z$) with k_c as wave number [§].

6.1.12 Light Field and Atomic Flip Operators

The electric field is described by the slow envelope operator because it oscillates comparatively slowly compared to the fast oscillations of the complex phase.

[§] Recall the Equation 6.1.4: $k \equiv \frac{2\pi}{\lambda}$

$$\hat{E}^{(+)}(z,t) = \mathcal{E}_0\,\hat{\mathcal{E}}(z,t)\,e^{\,i(k_p z-\omega_p t)} \tag{6.71}$$

One is using the atomic flip with spatial and temporal dependency, where $\tilde{\sigma}^j_{\mu\nu}(t)$ is the slow envelop operator and $e^{i(k_p z_j-\omega_p t)}$ is the fast oscillations representing the electromagnetic wave propagating in z-direction with velocity c.

$$\hat{\sigma}^j_{\mu\nu} = \tilde{\sigma}^j_{\mu\nu}(t)\,e^{\,i(k_p z_j-\omega_p t)} \tag{6.72}$$

The spatial dependence is represented by the term $e^{ik_p z}$ and shows the behaviour of the wave along the z-axis. The temporal dependence is represented by the term $e^{-\omega_p t}$ and corresponds to the temporal oscillation of the wave. Including each of these phases in the atomic operator implies the tuning of absorption and emission regarding the optic field. Due to this fact, $e^{ik_p z_j}$ ensures the correct, coherent contribution to the collective process. Consequently, $e^{-\omega_p t}$ tune the atomic dynamic to the optical field.

The slow envelope approximation assumes much slower oscillations of spatial and temporal variations than complex phase oscillations (Sazonov, 2017). Thus, it allows simplifying the equations of motion [§].

6.1.13 Collective Operators and Process Dynamics

The collective operators allow to characterize the dynamics of the system through the description of the atoms in the medium and their interaction with the light field. Based on this assumption, is why one can finally construct the motion equations to explain the spatial-time evolution of the system. Based on these premises, the collective operators are presented: collective operator of quantized light field $\mathcal{E}(z,t)$, collective polarization $\hat{P}(z,t)$ and collective spin wave $\hat{S}(z,t)$.

$$\hat{\mathcal{E}}(z,t) = \frac{1}{\sqrt{N}}\sum_{j=1}^{N}\hat{E}^{(+)}(z,t), \tag{6.73}$$

$$\hat{P}(z,t) = \frac{1}{N}\sum_{j=1}^{N}\hat{\sigma}^j_{ge}\,e^{-\,ik_p z_j}, \tag{6.74}$$

[§]Note that these descriptions are essential to describe the coherent excitations of the atomic medium that carry quantum information (spin wave).

$$\hat{S}(z,t) = \frac{1}{N}\sum_{j=1}^{N} \hat{\sigma}_{gs}^{j}\, e^{-\,ik_p z_j} \tag{6.75}$$

Note that the Equation 6.73 regards the electric field in the z-position, the Equation 6.74 regards the collective coherence between $|g\rangle$ and $|e\rangle$ states of the atoms, and the Equation 6.75 explains the coherent excitation of the $|g\rangle$ and $|s\rangle$ states in the atomic medium —wave spin.

Following the original paper title *Dark-State Polaritons in Electromagnetically Induced Transparency* (Fleischhauer & Lukin, 2000) the equations of motion are derived.

The equation for the quantized light field follows the Maxwell equation in a polarized field:

$$\Big(\frac{\partial}{\partial t} + c\,\frac{\partial}{\partial z}\Big)\,\hat{\mathcal{E}}(z,t) = i\,\omega_p\,\hat{P}(z,t) \tag{6.76}$$

Considering the coupling regarding the atoms and $\omega_p = c\,k_p$, $g = d_{eg}\,\mathcal{E}_0/\hbar$, the equation for the quantized light field is the subsequent, where c is the velocity of light in the vacuum and L is the length of the atomic medium:

$$Bigl(\frac{\partial}{\partial t} + c\,\frac{\partial}{\partial z}\Big)\,\hat{\mathcal{E}}(z,t) = i\,g\,\sqrt{N}\,\hat{P}(z,t)\,\frac{L}{N} \tag{6.77}$$

The equation for the collective polarization is derived from the Heisenberg picture of the Langevin equations (see Fleischhauer & Lukin, 2000) (also see Likharev, 2024, pp. 305–307). The general form takes the form of the following equation minus the dissipation and the sum of the fluctuations of the environment. Each discipline (quantum optics, dissipative quantum systems, etc.) slightly adapts the formulation and the inclusion of terms:

$$\frac{\partial}{\partial t}\hat{O} = \frac{i}{\hbar}\Big[\hat{H},\,\hat{O}\Big] \tag{6.78}$$

The equation for the collective polarization is the subsequent, where γ is the decoherence rate of $|e\rangle$, Δ is the detuning of a photon, and $\hat{F}_P$ is the polarization-associated noise operator:

$$\frac{\partial}{\partial t}\,\hat{P}(z,t) = -\big(\gamma + i\,\Delta\big)\,\hat{P}(z,t) + i\,g\,\sqrt{N}\,\hat{\mathcal{E}}(z,t) + i\,\Omega(t)\,\hat{S}(z,t) + \sqrt{2\,\gamma}\,\hat{F}_P(z,t) \tag{6.79}$$

The same way is derived the spin wave motion equation. Based on the same idea:

$$\frac{\partial}{\partial t}\,\hat{S}(z,t) = \frac{i}{\hbar}\left[\hat{H},\,\hat{S}(z,t)\right] \;-\; \gamma_s\,\hat{S}(z,t) \;+\; \hat{F}_S(z,t) \tag{6.80}$$

The equation for the collective spin wave is the subsequent, where γ is the decoherence rate of $|s\rangle$, and $\hat{F}_S$ is the noise operator associated with the spin wave:

$$\frac{\partial}{\partial t}\,\hat{S}(z,t) = -\gamma_s\,\hat{S}(z,t) \;+\; i\,\Omega^*(t)\,\hat{P}(z,t) \;+\; \sqrt{2\,\gamma_s}\,\hat{F}_S(z,t) \tag{6.81}$$

6.1.14 Dark States of Polariton

A polariton is a bosonic quasiparticle (Fleischhauer & Lukin, 2000) created by the coherent superposition of atomic wave spin and photons. It is essential for transferring and storing quantum information. For a quantum database, it is important because there are two critical processes: photon storage and photon recovery. Decrementing $\Omega(t)$ the dark polariton transfers the quantum information from the light field to the wave spin or atomic structure (matter). These process is the photon storage. To make possible the recovery of the photons, it is necessary to increment $\Omega(t)$ to transfer the quantum information from the atom to the light field. Note that the modulation of $\Omega(t)$ is referred to as being through θ. In addition, the cancellation of components in $|e\rangle$, there is no spontaneous emission and therefore there is no loss of information; thus the quantum database would safely store the information encoded in one of the characteristics of the photons.

The n excitation of the dark state polariton is (Fleischhauer & Lukin, 2000, 2002; Lukin et al., 2000):

$$\left|\Psi^0, n_k\right\rangle = \frac{1}{\sqrt{n!}}\left(\hat{\Psi}_k^\dagger\right)^n |G\rangle\,, \tag{6.82}$$

Since all atoms are in the basis of the system and there are no photons in the field, the number of polaritons or excitations is represented by n. $\hat{\Psi}_k^\dagger$ is the dark polariton creation operator with wavenumber k. It is defined as a linear combination of the photon creation operator $\hat{\mathcal{E}}_k^\dagger$ in mode k and the wave spin excitation creation operator $\hat{S}_k^\dagger$ in mode k via mixing angles.

$$\hat{\Psi}_k^\dagger = \cos\theta\;\hat{\mathcal{E}}_k^\dagger \;-\; \sin\theta\;\hat{S}_k^\dagger. \tag{6.83}$$

6.1.15 EIT Simulation

Up to now, a three-level system in Λ configuration with interaction with a probe and control field has been described. The couplings of the Rabi frequencies with the ground, metastable and excited states have been described. Solving the equations of the previous section to find analytically a unique solution is an intractable problem.

The description of the system is a complex problem that addresses a set of coupled partial differential equations (PDEs), known in the literature as Maxwell-Bloch equations and used in nonlinear optics (Saksida, 2005), (also see. S. Malinovsky & R. Berman, 2011, pp. 120–135). The equations describing the behaviour of bosonic quasiparticles include the propagation of the electromagnetic field and the time evolution of the coherences of the atomic populations. The variables of the equations are interdependent and highly coupled both in time and space, which makes the PDEs nonlinear. The dependence comes from multiple parameters such as the Rabi frequencies, the detuning and the decay rate. The resulting PDEs, assuming they could be solved analytically, would not have a closed solution space. On the other hand, the Hamiltonian of the system, when including decoherence, makes it non-Hermitian, so it is not orthogonal.

For this reason, it is more appropriate to propose a numerical simulation based on the Lindblad equation (Equation 6.36) that describes the time evolution of the density matrix ρ of the system. In the simulation, the first order electrical susceptibility $\chi^{(1)}$ obtained from the coherence ρ_{ge} has been calculated. The probe field introduces a perturbation and ρ_{ge} shows the response to it. The real part of $\chi^{(1)}$ represents the dispersion, while the imaginary part represents the absorption.

In the visualizations, the steady states are calculated for values of Δ_p and ρ_{ge} is represented to graph the evolution of the system, both when the control is off; therefore, it is in an absorptive state, and when the control is on, and therefore, the medium is transparent in resonance. The parameters chosen in the tests arise indicatively from experiments previously presented, as Steck, 2001. It has been guaranteed that the parameters chosen in this thesis offer a viable configuration based on all the characteristics and requirements presented in the previous sections. Requirements like $\Delta_p \approx 0$ such that $\Omega_p \ll \Omega_c$. For this purpose, the cost function has been defined:

$$\text{cost}(\Omega_p, \Omega_c, \Delta) = \langle e|\rho_{ss}(\Omega_p, \Omega_c, \Delta)|e\rangle \ + \ P(\Delta) \tag{6.84}$$

Function that minimizes the population in the excited state $|e\rangle$— $\langle e|\rho_{ss}|e\rangle$. And applies a

penalty $P(\Delta)$ if $\Delta_{\min} \leq \Delta \leq \Delta_{\max}$ or if Δ exceeds 1000—because there are no longer dynamic effects of interest. The simulation uses the `steadystate` function in QuTIP, the L-BFGS-B[§†] method has been used to find the steady state of the Lindblad equation and for parameter optimization. This method is a restricted quasi-Newton optimization algorithm, available at `scipy.optimize.minimize`[‡]. This method is suitable because it allows the use of bound constraints, and is suitable for complex functions or those with many parameters. The calculation is based on using finite differences of the gradient from an approximation to the Hessian matrix.

The graphs where the results can be seen can be found in the appendix. The graph A.4, shows the real and imaginary parts of $\chi^{(1)}$ both with the control on and with the control off. It can be seen that when the control is on, the desired transparency window is created where the atomic medium becomes transparent. It can be seen in the orange curve around 0 on the x-axis. To better appreciate the results, a second graph is provided showing only the transparency window, refer to the Figure A.5.

6.2 Duan-Lukin-Cirac-Zoller Memories

DLCZ quantum memories were proposed by Lu-Ming Duan et al. (Duan et al., 2001) as a scheme for storage and retrieval of photonic quantum states in an atomic medium. DLCZ uses the Λ scheme with all atoms prepared in the ground state. Detection of a photon in a particular spatial mode projects the atomic cloud into an excited collective spin-wave state. Thus, information is stored in the atomic collective coherence. Recovery of the original quantum state is done by re-impacting the readout laser to convert the spin-wave into a photon again. Refer to the Figure A.6 to understand the updated Λ scheme with the spontaneous Raman emission writing process and the readout process.

6.2.1 Atomic Assembly State

In Equation 6.61, the symmetric collective state $\left|S^k\right\rangle$ for k photons is derived. Now, one is only interested in a single photon detected after the writing process. Therefore, in Equation 6.61 one must replace it by $k = 1$. The write bean induces spontaneous Raman scattering —key in the

[§]The original paper was published in 1997, and titled as *Algorithm 778: L-BFGS-B: Fortran Subroutines for Large-Scale Bound-Constrained Optimization.*

[†]The main *purpose of algorithm L-BFGS-B is to minimize a nonlinear function of n variables* (Zhu & Byrd, 1997, p. 1).

[‡]Although the function is executed in Python, the calculation optimization is done in Fortran.

process (Sangouard et al., 2009, p. 3). An atom absorbs a photon from the write beam and emits a photon in another direction, which transitions to $|s\rangle$. It is a probabilistic entanglement generation (Hammerer et al., 2010, p. 28), due to this fact, is an unlikely probabilistic process given the weak field regime. The spontaneous emission of $|e\rangle \rightarrow |s\rangle$ with the emission of a photon is described as:

$$|\Psi\rangle = |G\rangle\,|0\rangle \;+\; \sqrt{p}\sum_{i=1}^{N} e^{\,i\,(\mathbf{k}_\omega - \mathbf{k}_{\omega o})\cdot\mathbf{r}_i}\,|g_1,\cdots,s_i,\cdots,g_N\rangle\,|1\rangle \tag{6.85}$$

The amplitude $\sqrt{p}$ has been represented as the probability of emitting a photon that excites an atom in $|s\rangle$. Furthermore, $|0\rangle$ and $|1\rangle$ are the number of photons in the write-output mode. The phase corresponds to the wave vectors of the writing modes that depend on the atomic positions and the phase relationship between the incident field and the emitted photon. Upon detection of a photon, $|1\rangle$ the wave function collapses and the atomic system is projected into the collective state with a single excitation. Then the previous amplitude is absorbed in the detection condition, since the probability is centred in the superposition. Given the detection, the system will already be in the collective state.

Note that the reader does this similarly to the EIT, where a probe and control field are applied to produce a coherent excitation in a dark subspace. In contrast, in the DLCZ, the detection of the photon is what creates the spatial distribution of the spin-wave —similar to the excited collective state in EIT.

6.2.2 Writing Process

As it has been intuited in the previous section, writing is the process by which the atomic cloud is illuminated with a weak writing beam that induces a spontaneous Raman scattering of the atoms in the $|g\rangle$ state. The detection of the photon marks the success by creating a coherent superposition of equal amplitudes and phases determined as a function of the wave vector of the detected light. The writing process interaction Hamiltonian can be described in the same way as did it previously in other sections: $H_{\text{write}} \approx \hbar\, g_\omega \sum_{i=1}^{N} \hat{\sigma}_{eg}^{(i)}\,\hat{a}_\omega \;+\; \text{h.c.}$

6.2.2.1 Entanglement Between Spin Wave and Writing Photon

The entanglement between the spin wave and the writing photon arises because the state before detection is not separable because knowing the result of a photon measurement collapses the atomic

part into a non-trivial state: $|\Psi\rangle \neq |X\rangle_{\text{atom}} \otimes |Y\rangle_{\text{write output}}$

6.2.3 Reading Process

To recover the quantum information stored in the spin wave, the read beam is coupled between $|s\rangle \leftrightarrow |e\rangle$. Analogously, in the writing process, one obtains: $H_{\text{read}} \approx \hbar\, g_r \sum_{i=1}^{N} \hat{\sigma}_{es}^{(i)}\, \hat{a}_r \; + \; \text{h.c.}$ Where $\hat{a}_r$ is the read beam mode (control beam of EIT). When the beam hits the state $|S_k\rangle$ it stimulates the coherent emission of a photon in the conjugate direction, returning the atomic system to the ground state $|G\rangle$.

6.2.3.1 Reading Efficiency

The efficiency of the reading η_r is based on the temporal evaluation under the reading beam. Therefore, it depends on the atomic optical density. In an ideal environment, a high value is sought since it minimizes the losses. The storage time of a quantum state affects the decoherence, so the system can be completely corrupted. From the optical perspective, if there is high optical density, low Doppler broadening and controlled or reduced decoherence; the efficiency would be very high. However, there are no real vacuum environments, currently replicable and that do not introduce elements that distort, for example, the decoherence. The probability of success is expressed as a function of the length of the medium L and of $\chi^{(1)}$ of the transition. Again, numerical calculations require integrating the Maxwell-Bloch equations in $\eta_r \approx \exp\Big(-\operatorname{Im}\big[\chi^{(1)}(\Delta_p = 0)\big]\, L\Big)$.

6.3 Rydberg Blockade Mechanism

Rydberg blockade allows to better tune the dynamics of DLCZ memories as the atoms acquire strong dipolar interactions that limit the number of simultaneous collective excitations in a given volume or blocking radius. In this way, the generation of multiple simultaneous photons can be controlled. However, this required addition increases the complexity of the Hamiltonian by adding more nonlinear and inter-atom inter-distance dependent terms. Therefore, it is not feasible to solve it analytically. Basically, the dynamics is that given an atom excited in the Rydberg state $|s'\rangle$, its nearest neighbour remains in an energetically unfavourable state for an energetic transition. Thus, the Rydberg blockade mechanism increases the fidelity by driving the DLCZ memory into multi-pair entanglement.

The most relevant physical considerations are to note that the direct dipole-dipole interaction that scales approximately as $1/R^3$ where $R = |\mathbf{r}_i - \mathbf{r}_j|$ is the distance between two atoms is not correct, since most combinations of Rydberg states are not directly resonantly coupled. The coupling arises from a virtual mixing with other energetically close atomic levels. Therefore, the effective potential is obtained from the second order perturbation theory (Griffiths & Schroeter, 2019, pp. 279–285). Considering the non-resonant dipole-dipole interaction $\hat{V}_{dd}$ between $|s's'\rangle$ and with the possibility of virtually connecting $|\alpha\rangle$, the energy correction of the perturbative Hamiltonian $\hat{V}$ is obtained:

$$E^{(2)} = \sum_{\alpha \neq \psi_0} \frac{\left|\langle \alpha | \hat{V} | \psi_0 \rangle\right|^2}{E_{\psi_0} - E_\alpha} \tag{6.86}$$

However, the second-order correction actually leads to the effective van der Waals potential — assuming sufficient interatom distance. The potential gives rise to $V_{vdW}(R) = \frac{C_6}{R_6}$. In the literature it is easy to find the coefficient C_6 since the interactions between Rydberg atoms change from the $1/R^3$ to $1/R^6$ regime. It is not an arbitrary result, but rather a standard for Rydberg states leading to a non-resonant van der Waals interaction with R^{-6} scaling.

The experimental feasibility of Rydberg blockade can be calculated by Fermi's golden rule. With this rule, one can calculate the transition rates induced by a perturbation. For illustration, to obtain the radiative decay rate of the Rydberg state $\Gamma \sim \frac{2\pi}{\hbar}|V_{fi}|^2\rho(E)$, (Zwiebach, 2022, pp. 911–919). The density of states matrix is represented by $\rho(E)$. Finally, knowing the decay rate Γ to a lower energy state, the lifetime $\tau = 1/\Gamma$ can be obtained.

Chapter 7

Quantum Database Applications for a Data Scientist

7.1 Introduction to Quantum Mechanics for the Data Scientist

7.1.1 Linear Algebra

Definition 7.1.1.1 A *vector* $|\psi\rangle$ is an element of a vector space $\mathcal{V}$ over the field $\mathbb{C}$. In a finite dimension, any $|\psi\rangle$ belonging to the finite basis can be represented as $|\psi\rangle = \sum_{i=1}^{n} \psi_i |e_i\rangle, \quad \psi_i \in \mathbb{C}$. A vector is characterized by its magnitude $\|\vec{\psi}\|$ and direction. A vector has the properties of addition $(+)$, scalar multiplication $(\cdot)$, dot product $(\cdot)$, and magnitude $(\|\cdot\|)$. Refer to Proof of the Definition 7.1.1.1.

Definition 7.1.1.2 A set of linearly independent $|\psi\rangle$ that spans the space is called a *basis*. The number of elements in the basis is the *dimension* of $\mathcal{V}$. A set of vectors $\{|\psi_i\rangle\}$ is linearly independent if $\sum_i c_i |\psi_i\rangle = 0 \implies c_i = 0 \forall i$. Refer to Proof of the Definition 7.1.1.1.

Definition 7.1.1.3 A *complex vector space* $\mathcal{V}$ is a set $|\psi\rangle$ over $\mathbb{C}$ defined by the operations $(\mathcal{V}, +, \cdot)$. For $(+)$: $\vec{u}, \vec{v} \in V \implies \vec{u} + \vec{v} \in V$ and, for $(\cdot)$: $c \in \mathbb{C}, \vec{v} \in V \implies c \cdot \vec{v} \in V$. Satisfying the properties of a complex vector space, as summarized in Table B.2, with the following axioms $(\forall \vec{u}, \vec{v}, \vec{w} \in V$ and $a, b \in \mathbb{C})$.

Definition 7.1.1.3 A *linear transformation* $A : \mathcal{V} \to \mathcal{V}$ satisfy $A(\alpha|\psi\rangle + \beta|\phi\rangle) = \alpha A|\psi\rangle + \beta A|\phi\rangle \quad \forall \alpha, \beta \in \mathbb{C}$.

7.1.1.1 The Hilbert Space

Definition 7.1.1.1.1 The *norm* of a $|\psi\rangle$ in $\mathcal{V}$ regarding the inner product $\langle\cdot|\cdot\rangle$ is defined as $\|\psi\rangle\| = \sqrt{\langle\psi|\psi\rangle}$. Refer to Proof of the Definition 7.1.1.1.1.

Definition 7.1.1.1.2 The *unit vector* corresponds to $\| \, |\psi\rangle \, \| = 1$ when $|\psi\rangle \in \mathcal{V}$. Refer to Proof of the Definition 7.1.1.1.2.

Definition 7.1.1.1.3 It is said that a unit vector in a two-dimensional complex vector space isomorphic to $\mathbb{C}^2$ is a *quantum bit* or *qubit*. Refer to Proof of the Definition 7.1.1.1.3.

Definition 7.1.1.1.4 Let $|\phi\rangle$, $|\psi\rangle$ two vectors in $\mathcal{H}$ are *orthogonal* if $\langle\phi|\psi\rangle = 0$. A $|\psi\rangle$ is *normalized* if $\langle\psi|\psi\rangle = 1$. Normalized states are called *pure states*. Refer to Proof of the Definition 7.1.1.1.4.

Definition 7.1.1.1.5 The *Cauchy–Schwarz inequality* established for any $|\phi\rangle, |\psi\rangle \in \mathcal{H}$: $|\langle\phi|\psi\rangle| \leq \|\phi\| \cdot \|\psi\|$. Refer to Proof of the Definition 7.1.1.1.5.

Definition 7.1.1.1.6 An *inner product space* $(\mathcal{H}, \langle\cdot|\cdot\rangle)$ is a complex vector space $\mathcal{H}$ with sesquilinear, and complete inner product $\langle\cdot|\cdot\rangle : \mathcal{H} \times \mathcal{H} \to \mathbb{C}$. Satisfying linearity in the second argument, conjugate symmetry $\langle\phi|\psi\rangle = \overline{\langle\psi|\phi\rangle}$, and positive definiteness $\langle\psi|\psi\rangle \geq 0$ and $\langle\psi|\psi\rangle = 0 \Leftrightarrow |\psi\rangle = 0$. Refer to Proof of the Definition 7.1.1.1.6.

Definition 7.1.1.1.7 A set $\{|e_i\rangle\}$ forms a complete *orthonormal basis* if $\sum_i |e_i\rangle \langle e_i| = I$. Refer to Proof of the Definition 7.1.1.1.7.

Definition 7.1.1.1.8 A *Hilbert space* $\mathcal{H}$ is a complete inner product space. Completeness ensures convergence of Cauchy sequences. A quantum state is a representation of a unit vector in $\mathcal{H}$. Refer to Proof of the Definition 7.1.1.1.8.

Remark 7.1.1.1.1 Appling the above definitions, a *qubit* is usually expressed as $|\psi\rangle = \alpha\,|0\rangle + \beta\,|1\rangle$. Using the complex amplitude of the vectors, the norm is computed as $|\,|\alpha\rangle\,|^2 + |\,|\beta\rangle\,|^2 = 1$. The states $|0\rangle$ and $|1\rangle$ corresponds to the orthonormal computational basis state $\{|0\rangle\,, |1\rangle\}$. Refer to Proof of Remark 7.1.1.1.1.

Definition 7.1.1.1.9 Let two Hilbert spaces $\mathcal{H}_A$ and $\mathcal{H}_B$, the *tensor product* $\mathcal{H}_A \otimes \mathcal{H}_B$ describes composite systems; $|\psi\rangle \in \mathcal{H}_A, \quad |\phi\rangle \in \mathcal{H}_B, \quad |\psi\rangle \otimes |\phi\rangle \in \mathcal{H}_A \otimes \mathcal{H}_B$. Refer to Proof of the Definition 7.1.1.1.9.

7.1.1.2 Linear Operators and Matrices

Definition 7.1.1.2.1 Assume $A : \mathcal{H} \to \mathcal{H}$ as a linear operator, if $AA^\dagger = A^\dagger A$, then A is *normal*. Refer to Proof of the Definition 7.1.1.2.1.

Definition 7.1.1.2.2 For an operator A, the *adjoint* $A^\dagger$ satisfies $\langle\phi|A\psi\rangle = \langle A^\dagger\phi|\psi\rangle$. An operator H is *Hermitian* or self-adjoint if $H = H^\dagger$. Hermitian operators have real eigenvalues. Refer to Proof of the Definition 7.1.1.2.2.

Theorem 7.1.1.2.1 Any *Hermitian operator* H on a finite-dimensional $\mathcal{H}$ space can be written as $H = \sum_i \lambda_i |e_i\rangle \langle e_i|$. The λ_i are real eigenvalues and $|e_i\rangle$ are eigenvectors of the orthonormal basis. Refer to Proof of the Theorem 7.1.1.2.1.

Definition 7.1.1.2.3 Let $H|e_i\rangle = \lambda_i |e_i\rangle$, then λ_i is *eigenvalue* and $|e_i\rangle$ its *eigenvector*. For a Hamiltonian H, eigenvalues are the *eigenenergies* of the system. Refer to Proof of the Definition 7.1.1.2.3.

Definition 7.1.1.2.4 A matrix U with entries in $\mathbb{C}$ or $U : \mathcal{H} \to \mathcal{H}$, is *unitary* if $U^\dagger U = I$. Similarly, is unitary if $UU^\dagger = I$, then U is normal. Refer to Proof of the Definition 7.1.1.2.4.

Definition 7.1.1.2.5 For an operator A, the *trace* can be calculated as $\mathrm{Tr}(A) = \sum_i \langle e_i|A|e_i\rangle$. Refer to Proof of the Definition 7.1.1.2.5.

Definition 7.1.1.2.6 The *commutator* establishes $[A, B] = AB - BA$ and the *anticommutator* establishes $\{A, B\} = AB + BA$. Refer to Proof of the Definition 7.1.1.2.6.

Definition 7.1.1.2.7 Let a rank-2 tensor T^{ij} is *antisymmetric* if $T^{ij} = -T^{ji}$. Refer to Proof of the Definition 7.1.1.2.7.

Definition 7.1.1.2.8 The *Pauli matrices* $\sigma_x, \sigma_y, \sigma_z$ act on $\mathbb{C}^2$, and form a basis for, a single-qubit Hermitian operators:

$$\sigma_x = \begin{pmatrix} 0 & 1 \\ 1 & 0 \end{pmatrix}, \quad \sigma_y = \begin{pmatrix} 0 & -i \\ i & 0 \end{pmatrix}, \quad \sigma_z = \begin{pmatrix} 1 & 0 \\ 0 & -1 \end{pmatrix}$$

Refer to Proof of the Definition 7.1.1.2.8.

7.1.1.3 Operator Functions

Definition 7.1.1.3.1 Let a diagonalizable operator H and analytic function f exponentials $e^{-iHt/\hbar}$ define *unitary evolutions*; $f(H) = \sum_i f(\lambda_i) |e_i\rangle \langle e_i|$. Refer to Proof of the Definition 7.1.1.3.1.

Remark 7.1.1.3.1 Let $A : \mathcal{H} \to \mathcal{H}$ is normal if and only if A is *diagonalizable*. Is Hermitian

then, A is normal, and diagonalizable. The well-known *Theorem of Spectral Decomposition* explains these properties.

7.1.2 Postulates of Quantum Mechanics

7.1.2.1 Axioms of Quantum Mechanics

For a further explanation of the axioms of quantum mechanics, refer to Appendix F.2.

Postulate 7.1.2.1.1 A *quantum state* can be represented by a $|\psi\rangle$ or a density operator ρ, where $\rho = \sum_j p_j |\psi_j\rangle \langle\psi_j|, \quad p_j \geq 0, \quad \sum_j p_j = 1$. Refer to Proof of Postulate 7.1.2.1.1.

Postulate 7.1.2.1.2 The results of a *measurement* collapse the wave function, resulting in eigenvalues. The probability of obtaining λ_i is $\mathrm{Tr}(P_i\rho)$, with $P_i = |e_i\rangle \langle e_i|$. Refer to Proof of Postulate 7.1.2.1.2.

Postulate 7.1.2.1.3 In absence of decoherence, the *evolution* is unitary:

$$\rho(t) = U(T)\rho(0)U^\dagger(t), \quad U(t) = e^{-iHt/\hbar}$$

Refer to Proof of Postulate 7.1.2.1.3.

7.1.2.2 Distinguishing Quantum States

Postulate 7.1.2.2.1 Two quantum states ρ and σ are *distinguishable* if there exists a set of measurement operators that yields outcomes allowing one to infer which state was prepared. The full distinguishable can only be achieved if $\rho\sigma = 0$, and thus, are orthogonal subspaces. Refer to Proof of Postulate 7.1.2.2.1.

Theorem 7.1.2.2.1 The *Helstrom Bound Theorem* establishes that giving two quantum states ρ_0 and ρ_1 with prior probabilities p_0 and p_1, the minimum error probability in distinguishing them optimally is given by $P = \frac{1}{2}(1 - \|p_0\rho_0 - p_1\rho_1\|_1)$, where $\|A\| = \mathrm{Tr}\sqrt{A^\dagger A}$. Refer to Proof of the Theorem 7.1.2.2.1.

7.1.2.3 Projective Measurements

Definition 7.1.2.3.1 A *projective measurement* is described by an observable set of projection operators $\{P_i\}$ such that $P_iP_j = \delta_{ij}P_i$, and $\sum_i P_i = I$ —special case of measurement strategies associated with Hermitian observables. The probability of obtaining an outcome when measuring

a state is the computed by the trace. The post-measurement state is $\rho_i = \frac{P_i \rho P_i}{p(i)}$. Refer to Proof of the Definition 7.1.2.3.1.

7.1.2.4 Positive Operator-Valued Measure

Definition 7.1.2.4 A *Positive Operator-Valued Measure* (POVM) is a set of positive semi-definite operators $\{E_i\}$ that sum to the identity. POVMs do not need to be associated with the spectral decomposition of an observable like projective measurements. The probability of the outcome i for state ρ is $p(i) = \mathrm{Tr}(E_i \rho)$. Refer to Proof of the Definition 7.1.2.4.

Remark 7.1.2.4 POVMs allow describing generalized measurements like non-projective measurements.

7.1.2.5 Phase

Definition 7.1.2.5.1 A *global phase* factor $e^{i\theta}$ applied to a state $|\psi\rangle$ does not change any physical prediction. Instead, a *relative phase* between the components of a superposition affects the interference terms and therefore has physical consequences. Refer to Proof of the Definition 7.1.2.5.1.

Definition 7.1.2.5.2 Let a *unitary operator* $U = e^{-iHt/\hbar}$, the phase factors of the Hamiltonian comes from eigenvalues. The difference in the energies λ_i produces *relative phase* in the time evolution. Refer to Proof of the Definition 7.1.2.5.2.

7.1.2.6 Composite Systems and Entanglement

Definition 7.1.2.6.1 Two subsystems A, B, the joint state is in the $\mathcal{H}_A \otimes \mathcal{H}_B$ space. A state is *entangled* if it cannot be written as a simple tensor product. Refer to Proof of the Definition 7.1.2.6.1.

Definition 7.1.2.6.2 An *ensemble* $\{p_j, |\psi_j\rangle\}$ is a mixed state $\rho = \sum_j p_j |\psi_j\rangle \langle\psi_j|$. Refer to Proof of the Definition 7.1.2.6.2.

Definition 7.1.2.6.3 A *quantum channel* $\mathcal{E}$ is a *completely positive trace-preserving* (CPTP) map $\mathcal{E}(\rho) = \sum_k E_k \rho E_k^\dagger, \quad \sum_k E_k^\dagger E_k = I$, where $\{E_k\}$ are the Kraus operators. Note $\mathrm{Tr}(\mathcal{E}(\rho)) = 1 \quad \forall \rho$. These channels allow modelling noise, decoherence and general evolution beyond unitary dynamics, as will be seen later. Refer to Proof of the Definition 7.1.2.6.3.

7.1.2.7 Universal Quantum Gates and Multi-Qubit Gates

Definition 7.1.2.7.1 A set of *gates* is universal if any unitary on n qubits can be equivalently written in a finite sequence of these gates. A standard universal set includes $\{H, T, \text{CNOT}\}$. To consult the matrix of these gates, refer to G.1. Every multi-qubit gate can be built from single-qubit gates and controlled operations. For illustrate, consider the three qubit Toffoli Gate [§] that can be constructed base on universal gates. To consult the decomposition, see the graph A.7 located in the appendix.

7.1.3 Density Operator

Definition 7.1.3.1 Let a Hilbert space $\mathcal{H}$ a *density operator* ρ is a positive semi-definite operator ($\rho \geq 0$) with $\text{Tr}(\rho) = 1$. A density operator can be written as, $\rho = \sum_j p_j \left|\psi_j\right\rangle \left\langle\psi_j\right|$, where $\left|\psi_j\right\rangle$ are the state vectors and $p_j \geq 0, \quad \sum_j p_j = 1$. A *pure state* corresponds to the $\text{Tr}(\rho^2) = 1$, and *mixed states* satisfy $\text{Tr}(\rho^2) < 1$.

Remark 7.1.3.1 It is crucial for the reader to refer to Figure A.8. The reader will find a representation of a pure state and a mixed state, as well as a helpful visualization of the density matrix. As a complement to the visualizations, the deductions that should be carried out from the definitions presented above are presented below as a form of proof.

Pure state The *density matrix* is Hermitian since it is equal to its transposed conjugate:

$$\rho = \begin{bmatrix} 0.5 & 0.5 \\ 0.5 & 0.5 \end{bmatrix}, \quad \rho^\dagger = \rho$$

Complies with the property $\text{Tr}(\rho^2) = 1$:

$$\rho^2 = \begin{bmatrix} 0.5 & 0.5 \\ 0.5 & 0.5 \end{bmatrix} \cdot \begin{bmatrix} 0.5 & 0.5 \\ 0.5 & 0.5 \end{bmatrix} = \begin{bmatrix} 0.5 & 0.5 \\ 0.5 & 0.5 \end{bmatrix}$$

$$\text{Tr}(\rho^2) = 0.5 + 0.5 = 1$$

The density matrix corresponds to the well-known superposition state $|+\rangle$ of the states $|0\rangle$ and $|1\rangle$. In quantum computing, it is called Hadamard $|\psi\rangle = \frac{1}{\sqrt{2}}(|0\rangle + |1\rangle)$. The eigenvalues of ρ are $[1, 0]$.

[§] Refer to Matrix G.2

Mixed State The density matrix is Hermitian:

$$\rho = \begin{bmatrix} 0.8 & 0.2 \\ 0.2 & 0.2 \end{bmatrix}, \quad \rho^\dagger = \rho$$

A mixed state is characterized by $\mathrm{Tr}(\rho^2) < 1$:

$$\rho^2 = \begin{bmatrix} 0.8 & 0.2 \\ 0.2 & 0.2 \end{bmatrix} \cdot \begin{bmatrix} 0.8 & 0.2 \\ 0.2 & 0.2 \end{bmatrix} = \begin{bmatrix} 0.68 & 0.2 \\ 0.2 & 0.08 \end{bmatrix}$$

$$\mathrm{Tr}(\rho^2) = 0.68 + 0.08 = 0.76 < 1$$

The density matrix is a mixed state of the state $|0\rangle$ with probability 0.6 and $|+\rangle$ with probability 0.4. Easily verifiable from the reconstruction of the density matrix $\rho = 0.6\,|0\rangle\langle 0| + 0.4\,|+\rangle\langle +|$. The eigenvalues of ρ are $\lambda_1 = \frac{5+\sqrt{13}}{10}, \quad \lambda_2 = \frac{5-\sqrt{13}}{10}$.

Interpreted geometrically, the pure state lives on the surface of the sphere, while a mixed state is found in the inner part of the Bloch sphere.

7.1.4 The Schmidt Decomposition

Definition 7.1.4.1 For any pure bipartite state $|\psi\rangle \in \mathcal{H}_A \otimes \mathcal{H}_B$, there exists orthonormal bases $|u_i\rangle$ of $\mathcal{H}_A$ and $|v_i\rangle$ of $\mathcal{H}_B$ such $|\psi\rangle = \sum_i \sqrt{\lambda_i}\,|u_i\rangle \otimes |v_i\rangle$, with Schmidt coefficients $\lambda_i \geq 0$, and $\sum_i \lambda_i = 1$. Refer to Proof of the Definition 7.1.4.1.

Theorem 7.1.4.1 The *uniqueness of the Schmidt decomposition* says that it is unique, unless there are degeneracies in the coefficients. The Schmidt rank corresponds to the number of non-zero λ_i, a measure of entanglement.

7.1.5 Purification

Definition 7.1.5.1 A *purification* of a mixed state ρ on $\mathcal{H}_A$ is a pure state $|\Psi\rangle \in \mathcal{H}_A \otimes \mathcal{H}_B$ for some auxiliary space $\mathcal{H}_B$ such as $\mathrm{Tr}_B(|\Psi\rangle\langle\Psi|) = \rho$. Refer to Proof of the Definition 7.1.5.1.

Lemma 7.1.5.1 By performing a spectral decomposition and choosing $|\Psi\rangle = \sum_i \sqrt{p_i}\,|e_i\rangle \otimes |f_i\rangle$ with $\{|f_i\rangle\}$ on $\mathcal{H}_B$, any mixed state ρ can construct a purification.

Proof 7.1.5.1 Using the same studied case in Remark 7.1.3.1 consider the next proof of lemma. Let the mixed state ρ on $\mathcal{H}_A$. The spectral decomposition is $\rho = \lambda_1\,|v_1\rangle\langle v_1| + \lambda_2\,|v_2\rangle\langle v_2|$. Recall

the precomputed values of the eigenvalues of ρ. The eigenvectors are $|v_1\rangle = \begin{bmatrix} 0.9571 & 0.2898 \end{bmatrix}^\top$, $|v_2\rangle = \begin{bmatrix} -0.2898 & 0.9571 \end{bmatrix}^\top$. Let $\{|f_1\rangle, |f_2\rangle\}$ an orthonormal basis of the auxiliary $\mathcal{H}_B$. To construct the purification $|\Psi\rangle \in \mathcal{H}_A \otimes \mathcal{H}_B$, define $|\Psi\rangle = \sqrt{\lambda_1}\,|v_1\rangle \otimes |f_1\rangle + \sqrt{\lambda_2}\,|v_2\rangle \otimes |f_2\rangle$. Computing $|\Psi\rangle\langle\Psi| = \lambda_1 |v_1\rangle\langle v_1| \otimes |f_1\rangle\langle f_1| + \lambda_2 |v_2\rangle\langle v_2| \otimes |f_2\rangle\langle f_2|$. The partial trace over $\mathcal{H}_B$ eliminate $|f_1\rangle\langle f_1|$ and $|f_2\rangle\langle f_2|$, thus $\mathrm{Tr}_B(|\Psi\rangle\langle\Psi|) = \lambda_1 |v_1\rangle\langle v_1| + \lambda_2 |v_2\rangle\langle v_2|$. Computing yields $\mathrm{Tr}_B(|\Psi\rangle\langle\Psi|) \equiv \rho = \begin{bmatrix} 0.8 & 0.2 \\ 0.2 & 0.2 \end{bmatrix}$. In short, $|\Psi\rangle = \frac{5+\sqrt{13}}{10}|v_1\rangle \otimes |f_1\rangle + \frac{5-\sqrt{13}}{10}|v_2\rangle \otimes |f_2\rangle$.

7.1.6 The No-Cloning Theorem

Definition 7.1.6.1 There is no unitary operation $U : \mathcal{H} \otimes \mathcal{H}_a \to \mathcal{H} \otimes \mathcal{H}_a$ such as $U(|\psi\rangle|e\rangle) = |\psi\rangle, \quad U(|\phi\rangle|e\rangle) = |\phi\rangle|\phi\rangle \quad |\psi\rangle, |\phi\rangle$. Refer to Proof of the Definition 7.1.6.1.

Remark 7.1.6.1 No unitary operation can take two arbitrary unknown states $|\psi\rangle, |\phi\rangle$ on $\mathcal{H}$, and produce a copy with perfect fidelity.

Proof 7.1.6.1 If there exists a unitary operation U, the inner product would be preserved, resulting in a contradiction unless $|\psi\rangle = |\phi\rangle$ or they are orthogonal.

7.1.7 BB84 Protocol

In 1984, Bennett and Brassard proposed the first quantum key distribution (QKD) protocol —BB84 protocol[§]. The protocol uses two-level encryption of quantum system for transmission of bits between two parties sharing a key and is secured by quantum mechanics. For this, four quantum states used, which are prepared and measured in two conjugate bases —the computational $\{|0\rangle, |1\rangle\}$ and the diagonal $\{|+\rangle, |-\rangle\}$. Maintaining the previous chapter, a polarization-based photonic notation[†] will be used to explain the protocol. Moreover, the interested reader will better understand the approach by reading the original publication at the bottom of the page.

Using the nomenclature common in the QKD field and in Bennett's paper, Alice chooses a random sequence of bits and a basis. The basis Z produces states $|0\rangle, |1\rangle$, and the basis X produces the states $|+\rangle, |-\rangle$. Each bit is quantum-encoded. All bits received by Bob are randomly evaluated in one of the bases. Alice and Bob then publicly discuss the basis used, and not the

[§]Paper presented at International Conference on Computers, Systems & Signal Processing Bangalore, India Dec 9-12, 1984 Vol 1, (Bennett & Brassard, 2014)

[†]$|0\rangle \equiv \leftrightarrow$ horizontal polarization, $|1\rangle \equiv \updownarrow$ vertical polarization, $|+\rangle \equiv \nearrow\!\!\!\!\swarrow$ right diagonal polarization, $|-\rangle \equiv \nwarrow\!\!\!\!\searrow$ left diagonal polarization.

result. Results where the evaluation is in another basis are discarded. Results that are randomly evaluated on the same basis form the shared quantum key.

To illustrate the working of the protocol, one follows the same procedure as in the original paper —be sure to see Table B.3 for the complete example. Consider an 8-bit transmission. Alice randomly chooses a base and the sending bit, while Bob performs the measurement with his chosen base. Once all the bits have been measured, the measurement is publicly discussed.

Note that if Alice chooses base Z the shipment is $\{0 : \updownarrow, 1 : \leftrightarrow\}$, if she chooses base X the shipment is $\{+ : \nearrow\!\!\!\swarrow, - : \nwarrow\!\!\!\searrow\}$. If Bob measures on base Z and the transmission was on the same base, he will know with certainty the state of the computational base. Similarly, if he measures on base X when the transmission was on the same base, then he will know for sure the specific result of the diagonal basis. For the rest of the possibilities, he will only know the result with equiprobability.

This protocol ensures the secure transmission of bits without the possibility of an eavesdropper cloning the quantum state[§] or observing it because this would collapse the measurements, offering an indistinguishable altered result.

7.2 Entropy

Definition 7.2.1 The measure of uncertainty in a classical system is measured with the *Shannon entropy*, which establishes that for a discrete probability distribution $\{p_i\}$ with $\sum_i p_i = 1$ is $H(\{p_i\}) = -\sum_i p_i \log p_i$. Refer to Proof of the Definition 7.2.1.

Definition 7.2.2 Let p and $1-p$ be a binary distribution, the *binary entropy function* is measured as $H_2(p) = -p\log p - (1-p)\log(1-p)$. Refer to Proof of the Definition 7.2.2.

Definition 7.2.3 Given a probability distribution $p = \{p_i\}$ and $q = \{q_i\}$, the *classical relative entropy* or *Kullback–Leibler Divergence* (Kullback & Leibler, 1951) is measured as $D(p\|q) = \sum_i p_i \log \frac{p_i}{q_i}$. Refer to Proof of the Definition 7.2.3.

Definition 7.2.4 The *conditional entropy* of a joint probability $p(x, y)$ is a measure of the uncertainty of a distribution Y given another X distribution; $H(Y|X) = \sum_x p(x)H(p(y|x))$. Refer to Proof of the Definition 7.2.4. Refer to Shannon, 1948.

Definition 7.2.5 To know the amount of information shared by two joint probabilities $p(x, y)$ —*mutual information*; it is quantified as $I(X : Y) = H(X) + H(Y) - H(X, Y)$. Refer to Proof of the Definition 7.2.5. Refer to Shannon, 1948.

[§]No-Cloning Theorem 7.1.6

Definition 7.2.6 The *joint entropy* for a joint distribution $p(x, y)$ is defined as $H(X, Y) = -\sum_{x,y} p(x, y) \log p(x, y)$. Refer to Shannon, 1948.

Definition 7.2.7 The *data processing inequality* states that $X \to Y \to Z$ form a Markov chain, then $I(X\colon Z) \leq I(X\colon Y)$. Refer to Proof of the Definition 7.2.7. Refer to Shannon, 1948.

Remark 7.2.1 Through Shannon entropy, the minimum number of bits necessary to encode a random variable without loss is established —*Shannon's coding theorem* or *data compression*. Refer to Shannon, 1948.

7.2.1 Quantum Entropy

In this section, no proofs or demonstrations will be provided due to the high complexity, specialization and extension of these. It is outside the scope and objective of this thesis for an introduction to a framework for quantum data science. However, reference is made to texts where the reader can find a specialized extension, most of which include proofs.

Definition 7.2.1.1 The *von Neumann entropy* or quantum entropy sets that, for a density operator ρ in Hilbert space $\mathcal{H}$, can be measured as $S(\rho) = -\mathrm{Tr}(\rho \log \rho)$. In the case where $\rho = \sum_i \lambda_i |e_i\rangle \langle e_i|$ is a spectral decomposition, then: $S(\rho) = \sum_i -\lambda_i \log \lambda_i$. Refer to Wehrl, 1978.

Properties 7.2.1.1 $S(\rho) = 0$ if and only if ρ is a pure state; von Neumann entropy is concave in ρ; for an ensemble $\{p_j, \rho_j\}$, then $S\left(\sum_j p_j \rho_j\right) \geq \sum_j p_j S(\rho_j)$.

Definition 7.2.1.2 The *quantum relative entropy* sets that for two density operators ρ and σ, $D(\rho\|\sigma) = \mathrm{Tr}(\rho(\log \rho - \log \sigma))$. Refer to the work of Kullback and Leibler, 1951, also see Umegaki, 1962.

Theorem 7.2.1.1 The *Klein's inequality* sets that for two density operators ρ and σ, $D(\rho\|\sigma) = \mathrm{Tr}(\rho \log \rho - \rho \log \sigma) \geq 0$.

Corollary 7.2.1.1 The *Fannes' inequality* sets for $\|\rho - \sigma\|_1 \leq \epsilon$, where $\|\cdot\|_1$ is the trace norm, then $|S(\rho) - S(\sigma)| \leq \epsilon \log(d) + h_2(\epsilon)$, where d is the $\dim(\mathcal{H}$ and $h_2(\epsilon)$ is the binary entropy. Refer to Fannes, 1973.

Theorem 7.2.1.2 The *strong subadditivity* sets for a tripartite state ρ_{ABC}, $S(\rho_{AB}) + S(\rho_{BC}) \geq S(\rho_{ABC}) + S(\rho_B)$. The von Neumann entropy ensures a form of monotonicity under partial trace (Lindblad, 1975). There is a network of publications leading up to the proof of the theorem. The final phase is referenced so that the reader can find the proof of the theorem. Refer in an orderly manner to Lieb, 1973; Lieb and Ruskai, 1973, 2002.

Theorem 7.2.1.3 The *Holevo Bound* sets the limit of information accessible in any measurement of a quantum state. For an ensemble $\{p_j, \rho_j\}$, and a classical random variable X encoding j, $\chi(\{p_j, \rho_j\}) = S\left(\sum_j p_j \rho_j\right) - \sum_j p_j S(\rho_j)$. Consider M as the measurement outcome, then, for any POVM $\{E_m\}$, $I(X\colon M) \leq \chi(\{p_j, \rho_j\})$. Refer to James P, 1964, and for a direct proof refer to Holevo, 1973. For a complex approach proof, see Schumacher et al., 1996; Yuen and Ozawa, 1993.

Definition 7.2.1.3 Given probability distributions $\{p_i\}$ and $\{q_i\}$ arranged in non-increasing order, $\mathcal{P}$ majorizes $\mathcal{Q}$, $\mathcal{P} \succ \mathcal{Q}$, if $\sum_{i=1}^{k} p_i \geq \sum_{i=1}^{k} q_i \quad \forall k$, all elements are equal. Intuitively, $\mathcal{P}$ is more dispersed, so majorization induces partial ordering on sets of probability distributions.

Remark 7.2.1.1 Respect to Shannon entropy, if $\mathcal{P} \succ \mathcal{Q}$ then, $H(p) \leq H(q)$. Intuitively, the first distribution has less or equal entropy than the second. Similarly for a von Neumann entropy, if the spectrum of ρ majorize the spectrum of the state σ, then $S(\rho) \leq S(\sigma)$.

Definition 7.2.1.4 The von Neumann entropy $S(\rho)$ is Schur-concave. This property leads to the above remark intuition —$S(\rho) \leq S(\sigma)$. Hence, it ensures the idea of misinformation of quantum states, if $\mathcal{P} \succ \mathcal{Q}$, then $\mathcal{P}$ has greater quantum entropy.

The *quantum channel capacity* is the maximum asymptotic rate at which a noisy quantum channel can faithfully transmit quantum information.

Definition 7.2.1.5 The *Holevo–Schumacher–Westmoreland* states that for a quantum channel $\mathcal{E}$, and an ensemble, the maximum classical information that can be accessed is limited by the Holevo number χ, and the classical capacity $C(\mathcal{E})$ is given by the limit $C(\mathcal{E}) = \lim_{n\to\infty} \frac{1}{n}\chi(\{p_j, \rho_j^{\otimes n}\})$. Refer to Alexander Semenovich, 1979; Fuchs, 1997; Hausladen et al., 1996; Holevo, 1998; King and Ruskai, 1999; Schumacher and Westmoreland, 1997.

Theorem 7.2.1.3 A quantum channel CPTP $\mathcal{E}\colon \mathcal{L}(\mathcal{H}_A) \to \mathcal{L}(\mathcal{H}_B)$ can be isometrically dilated $\mathcal{E}(\rho) = \mathrm{Tr}_E(U\rho U^\dagger)$ for an ancilla space E, and a unitary operator U acting in a bigger space $\mathcal{H}_A \otimes \mathcal{H}_E$, where Tr_E is the partial trace over the ancilla space E. The theorem is called *Stinespring dilatation theorem.*

Remark 7.2.1.2 Any quantum channel can be treated as a unitary operation over a larger space where the ancillary space E resides, followed by a partial trace over E. That is, a quantum system can be modelled as part of a larger global unitary evolution.

Definition 7.2.1.5 The *Choi-Jamiołkowski isomorphism* establishes for a quantum channel $\mathcal{E}$ a correspondence between quantum channels and positive operators in a larger tensor space starting from the Choi operator $\Omega_{\mathcal{E}}$, defined as $\Omega_{\mathcal{E}} = (\mathcal{E} \otimes I)(|\Omega\rangle\langle\Omega|)$, where $|\Omega\rangle = \sum_i |i\rangle_A |i\rangle_{A'}$ is

a maximally entangled vector between two spaces $\mathcal{H}_A$. For the Choi-Jamiołkowski isomorphism, refer to Jiang et al., 2013; Salgado et al., 2004 also see this important article Haapasalo, 2021

Remark 7.2.1.3 $\Omega_{\mathcal{E}}$ encodes the quantum information over a quantum channel $\mathcal{E}$. The $\Omega_{\mathcal{E}}$ operator allows representing a quantum channel as a CPTP in the $\mathcal{H}_A \otimes \mathcal{H}_B$. It is a very helpful tool to map a quantum channel in a bigger tensorial space to work easily in quantum information.

Approaching the quantum information in a more physical context, a mention of the *Bekenstein's Entropy Bound* is required. For a more complete explanation, refer to Preskill, 2022, p. 20.

Definition 7.2.1.6 Bekenstein, motivated by quantum gravity, proposed entropy (coarse-grained entropy interpretation in Bekenstein, 1981)in quantum field theory. The entropy S of a system with energy E and a linear region size R is bounded by $S \leq 2\pi ER/\hbar c$. For the original paper, refer to Bekenstein, 1981.

7.2.2 The Entropic Uncertainty Principle

Definition 7.2.2.1 Let observables A and B, measured on a state ρ, and probability distributions of outcomes as $p(a)$ and $p(b)$, respectively. The *entropic uncertainty relation* states that $H(p(a)) + H(p(b)) \geq \alpha$, where the constant α depends on the overlap of eigenbases of the two observables. Refer to Deutsch, 1983; Kraus, 1987.

Theorem 7.2.2.1 The *Maassen–Uffink Entropic Uncertainty* theorem says that one cannot simultaneously have arbitrarily low uncertainty in two non-commutable observables. The theorem establishes two orthonormal bases $\{|a_i\rangle\}$, $\{|b_j\rangle\}$, $H(p(a)) + H(p(b)) \geq \log \frac{1}{2}$, where $c = \underset{i,j}{max}|\langle a_i|b_j\rangle|^2$. Refer to Maassen and Uffink, 1988.

7.3 Challenges of Noise in Realistic Quantum Information Systems

Several noise sources affect a quantum system in terms of fidelity and coherent. A description of the final system can be modelled using quantum channels —$\rho \mapsto \mathcal{E}(\rho)$. There are two types of noise: systematic noise and stochastic noise.

Systematic noise is a deterministic error that can be corrected by improving systems, such as better calibration. For instance, the correct rotation when applying a gate to a quantum computing system.

Stochastic noise, on the other hand, arises from random fluctuations in the environment and can be characterized by temporal correlation functions and power spectral densities. For example, effects caused by incomplete vacuum, thermal noise, or effects from an external fluctuating magnetic field.

7.3.1 Foundations of Quantum Noise

Recall the Definition 7.1.2.6.3 for the following quantum noise models:

Definition 7.3.1.1 The random errors that lead a state ρ to be a mixture of the maximally mixed state I/d with error probability p are described by the *depolarizing quantum channel* as $\mathcal{E}(\rho) = (1-\rho)\rho + \frac{p}{d}I$ (Chuang & Nielsen, 1996).

Definition 7.3.1.2 The energy loss is modelled by the *amplitude damping quantum channel* as $\mathcal{E}(\rho) = A_0\rho A_0^\dagger + A_1\rho A_1^\dagger$, where:

$$A_0 = \begin{pmatrix} 1 & 0 \\ 0 & \sqrt{1-p} \end{pmatrix}, \quad A_1 = \begin{pmatrix} 0 & \sqrt{p} \\ 0 & 0 \end{pmatrix}$$

Definition 7.3.1.3 The loss of coherence in superpositions is described by the *phase shift channel*[§]:

$$\mathcal{E}(\rho) = (1-p)\rho + pZ\rho Z$$

Definition 7.3.1.4 The *autocorrelation function* (Legendre, 1993) $\phi_x(\tau)$ for a fluctuating parameter $x(t)$ is:

$$\phi_x(\tau) = \lim_{T\to\infty} \frac{1}{T} \int_{-T/2}^{T/2} x(t)x(t+\tau)dt$$

Theorem 7.3.1.1 For second-order stationary processes, the power spectral density $S_x(\omega)$ is related to the autocorrelation and is known as the *Wiener-Khinchine* theorem (Wiener, 1930):

$$s_x(\omega) = \int_{-\infty}^{\infty} \phi_x(\tau)e^{-i\omega\tau}d\tau$$

Definition 7.3.1.5 A quantum state can be represented in the Bloch sphere (Bloch, 1946) using $\rho = \frac{1}{2}(I + \mathbf{r}\cdot\sigma)$, where $\mathbf{r} = (\mathbf{r}_x, \mathbf{r}_y, \mathbf{r}_z) \in \mathbb{R}$ is the Bloch vector with $|\mathbf{r}| \leq 1$, and σ are the Pauli matrices.

[§] $Z \equiv \sigma_z$, in quantum computation is preferred the gate notation

Remark 7.3.1.1 The pure state is described by $|\mathbf{r}| = 1$, the mixed state is described by $|\mathbf{r}| \leq 1$, and the maximally mixed state is described by $\mathbf{r} = 0, \rho = I/2$.

Proposition 7.3.1.1 Any element $\rho_{ij} \in \rho$ of a qubit can be expressed as:

$$\rho = \begin{pmatrix} \frac{1+r_z}{2} & \frac{r_x - ir_y}{2} \\ \frac{r_x + ir_y}{2} & \frac{1-r_z}{2} \end{pmatrix}$$

Remark 7.3.1.2 Note that the depolarization channel contracts the sphere towards the origin, the dephasing channel deforms the sphere into an oblate shperoid along the z-axis, and the amplitude dampling channel contracts the sphere towards the north pole.

7.3.2 Practical Introduction to Quantum Key Distribution

An optical system that emits individual photons ideally generates Fock states $|\psi\rangle = |n\rangle\,, \quad n = 1$, where $|n\rangle$ is a state with n photons in a quantum mode. A single photon source emits states like: $\rho = (1-p)\,|0\rangle\,\langle 0| + p\,|n\rangle\,\langle n|$, where $n = 1$ for ideal sources. The probability of multiple emission is $p \approx 1$. However, in practice, emission sources such as lasers emit coherent states (Poisson) following: $|\psi\rangle = e^{-\langle n}/2\rangle \sum_{n=0}^{\infty} \frac{\langle n\rangle^{n/2}}{\sqrt{n!}}\,|n\rangle$, where $\langle n\rangle$ is the average number of photons per pulse. The practical problem arises from the multiple emission $n > 1$ of coherent states, where a Photon-Number Splitting (PNS) attack vulnerability occurs.

Definition 7.3.2.1 *Eavesdropping* is a passive attack where an attacker measures transmitted states without directly interfering.

Definition 7.3.2.2 In a *PNS attack* (Lütkenhaus & Jahma, 2002), the eavesdropper measures the number of photons in a pulse, retains one, and forwards the rest.

Remark 7.3.2.1 A PNS attack is similar to the Man-in-the-Middle (MitM), where an attacker intercepts a bit string and retransmits it to the legitimate recipient without raising suspicion among legitimate agents.

Proposition 7.3.2.1 The use of a *Fock state* minimizes the errors related to the emission of multiple photons, and minimizes the risk of a PNS attack.

Proposition 7.3.2.2 The use of *Decoy state* (Lo et al., 2004) between two agents enables a PNS attack to be detected due to the variation in pulse intensity. For illustrate, the QKD Floodlight protocol implements the Decoy states that allow detecting discrepancies in the probability distribution.

The transmission of a photon for quantum communications is a hard process. Consider that in an idyllic vacuum, if you emit a photon with a laser, it could only get from the start to the end point as long as they are at the same height and there is no physical impediment in between. Hence, without further considerations, emitting a photon with a laser could not be done over distances of much more than a few meters due to buildings and terrestrial topology. The use of fibre is preferred —or a groundbreaking line of research that explores satellite quantum communication.

The transmission of a photon through a fibre channel decreases exponentially as the distance z increases. The intensity $I(z)$ of an optical beam transmitted in fibre is measured:

$$I(z) = I_0 e^{-\alpha z}, \quad \alpha = \frac{-10}{L} \log_{10}\left(\frac{I(L)}{I(0)}\right)$$

where $\alpha = \frac{\text{dB}}{\text{Km}}$ is the attenuation coefficient. The probability of detecting P_d a single photon over a fibre channel considering the detector efficiency is:

$$P_d = \eta_t e^{-\alpha L}$$

Recall that this cannot be solved as in classical optical fibre by cloning the bits and multiplexing the signal, since, according to the no-cloning theorem (Wootters & Zurek, 1982), this cannot be done on quantum states. So one of the ways to extend the transmission of a photon is by using repeaters and quantum memories.

Quantum errors produced in transmission are calculated from the proportion of erroneous bits detected and the total number of bits transmitted. Defining the quantum bit error rate as QBER, the maximum information acquired by an eavesdropper E is bounded by the binary entropy H:

$$I(E\colon A) \leq H(\text{QBER})$$

Theoretical analysis in the security literature on BB84-type QKD protocols indicates that a QBER $> 11\%$ indicates intrusion since it exceeds the error correction and privacy enhancement limit. While a QBER $\leq 7\%$ guarantees data security.

7.4 Benchmarking Techniques for Quantum Noise

7.4.1 Benchmarking Quantum States

Definition 7.4.1.1 *Fidelity* is a measure of similarity between an ideal quantum state $|\phi\rangle$ and an experimental state ρ, and is described as:

$$F(\rho, |\phi\rangle) = \sqrt{\langle\phi|\rho|\phi\rangle}$$

Fidelity is reduced to $F(|\psi\rangle, |\phi\rangle) = |\langle\psi|\phi\rangle|$ for two pure states. Refer to Jozsa, 1994.

Proposition 7.4.1.1 The *properties of the fidelity* says that for $F = 1$ if and only if $\rho = |\phi\rangle\langle\phi|$ since ρ is a positive operator with unitary trace. By the trace of ρ is defined $F \leq 1$. Finally, derived from the linearity of the trace operator if $\rho = \sum_i p_i |\psi_i\rangle\langle\psi_i|$, then $F(\rho, |\phi\rangle) = \sum_i p_i |\langle\psi_i|\phi\rangle|^2$.

Definition 7.4.1.2 A *quantum state tomography* reconstructs ρ from measurements in different bases:

$$\langle\sigma_m\rangle = \hat{m} \cdot \vec{r}, \quad \hat{m} \in \{x, y, z\}$$

The experimental estimates in N copies of the state are:

$$\langle\sigma_m\rangle_E = \frac{N\uparrow - N\downarrow}{N}$$

7.4.2 Benchmarking Quantum Gates

Definition 7.4.2.1 The *fidelity of a gate* F_g measures the closeness between an experimental process $\mathcal{E}$ and an ideal quantum operator U:

$$F_g = \int d\psi F(\mathcal{E}(|\psi\rangle\langle\psi|), U|\psi\rangle\langle\psi|U^\dagger)$$

where $d\psi$ is a uniform measurement over the pure state space.

Theorem 7.4.2.1 The entanglement fidelity in a d-dimensional system is related to the *average fidelity of a gate*:

$$F_g = \frac{dF_e + 1}{d + 1}$$

Definition 7.4.2.2 A better benchmarking technique is the *randomized benchmarking* technique (Knill et al., 2007), which applies random sequences of Clifford group gates followed by their inverse.

Thus, the average fidelity is calculated by the exponential decay rate $F(n) = Ap^n + B$, where the probability of success is $p = 1 - \epsilon$, being ϵ the average error rate per gate, and n is the length of the sequence.

7.4.3 Quantum State Tomography

Definition 7.4.3.1 For a *multi-qubit tomography*, the density ρ for n-qubit is $\rho = \frac{1}{2^n} \sum_{i_1,\cdots,i_n} c_{i_1},\cdots,i_n \sigma_{i_1} \otimes \cdots \otimes \sigma_{i_n}$ where $\sigma_{i_k} \in \{I,\, \sigma_x,\, \sigma_y,\, \sigma_z\}$. The total number of measurements is equivalent to $4^n - 1$.

Definition 7.4.3.2 The *quantum process tomography* for a process $\mathcal{E}$, the operator χ is reconstructed using E_i base operators as $\mathcal{E}(\rho) = \sum_{ij} \chi_{ij}\, E_i\, \rho\, E_j^\dagger$. The degrees of freedom in χ are $4^{2n} - 4^n$, χ is semi-definite positive and trace preserving.

7.5 Mitigating and Correcting Errors

7.5.1 Correcting Codes

Definition 7.5.1.1 Depending on the code architecture and physical interactions there is a *fault tolerance threshold* ϵ_{th} that if it is less than the physical error rate p of the gates, the quantum system can scale arbitrarily large through error correction techniques without passing the acceptable logical error threshold. Fault tolerance implies that a failure in one component does not propagate into multiple uncontrollable failures.

Theorem 7.5.1.1 A set of universal quantum gates is implemented in a fault-tolerant manner if $p < \epsilon_{\text{th}}$. Refer to Aharonov and Ben-Or, 1999.

Definition 7.5.1.2 A *surface code* (Kitaev, 1997) is a topological code that organizes physical qubits into a 2D or 3D lattice and applies local parity checks—bit-flip and phase-flip—so that it can detect and correct errors. Using ancilla or measurement qubits that measure local stabilizers associated with regions such as platelets, hypervolumes, locations with probability of error are identified and corrected using matching algorithms. The topology prevents global error propagation and provides a typical tolerance threshold $\sim 10^{-3}$.

Definition 7.5.1.3 A quantum gate that operates qubit-by-qubit between two coded blocks without mixing qubits within a block is called a *transverse quantum gate* (Gottesman, 1997a). It prevents a physical error from propagating to multiple logical qubits.

Definition 7.5.1.4 Let G_n ($\{I,\, X,\, Y,\, Z\}$) a Pauli group in n qubits with phases $\{\pm 1,\, \pm i\}$. An

Abelian subgroup $S \subseteq G_n$, where S is a stabilizer, and $-I \notin S, \quad gg' = g'g, \quad \forall g, g' \in S$, defines a *stabilizer code* $\mathcal{C}$. Refer to Gottesman, 1997b.

Definition 7.5.1.5 All the fixed $|\psi\rangle$ for all operators of S are known as the *coded space* V_S:

$$|\psi\rangle \in V_S \iff g|\psi\rangle = |\psi\rangle, \quad \forall g \in S.$$

The $\mathcal{C}$ is described as $[n, k]$ if $\dim(V_S) = 2^k$, where n corresponds to the physical qubit number, and k are the logical qubits.

Definition 7.5.1.6 Let $\mathcal{C}$ be a generator stabilizer $\{g_1, \cdots, g_r\}$, the projections associated with each generator g_j (Ding & Chong, 2020b, p. 146) define a *syndrome* of a state $|\psi\rangle$ or of a density ρ, in general.

$$\text{Syndrome}(|\psi\rangle) = \lambda_r, \quad g_j\,|\psi\rangle = \lambda_j\,|\psi\rangle\,, \quad \lambda_j \in \{\pm 1,\, \pm i\}$$

Every g_j is measured by an ancilla qubit giving an ± 1 outcome. The outcome vector constitutes the syndrome.

Example 7.5.1.1 Let $E = X_i$ as the bit-flip error over the qubit i., then, a generator $g_j \in S$ such that $\{g_j,\, X_i\} = 0$ anticommutator, so $g_j\, E\,|\psi\rangle \neq E\, g_j\,|\psi\rangle$. The syndrome of $|\psi\rangle$ implies an opposite sign in the g_j measurement, detecting the error in the position i.

7.5.2 Dynamical Error Suppression

Definition 7.5.2.1 The application of θ-rotation pulses around the phases to cancel coherent calibration errors is known as a *π-pulse sequence*. Refer to Viola and Lloyd, 1998.

Definition 7.5.2.2 $\hat{U}_{\text{real}}(\epsilon)$ is the net operation with error and is fulfilled $\left.\frac{\partial \hat{U}_{\text{real}}(\epsilon)}{\partial \epsilon}\right|_{\epsilon=0} = 0$, then the pulse sequence suppresses the *first order errors* since the error parameter lacks linear terms, reducing the effective error suffered by the qubit. Refer to Biercuk et al., 2010.

Definition 7.5.2.3 A qubit that is dephased by quasi-static noise characterized by a spectral density $S(\omega)$; applying a sequence of inverse π-pulses at specific times refocuses the phase evolution and changes the effective decoherence rate. Considering a sign function $y(t), \quad \{\pm 1\}$, the phase acquired by the qubit from the inversion produced by the π-pulses is $phi(t) = \int_0^t y(t')\delta\omega(t')dt'$, where $\delta\omega(t')$ is the fluctuation of the phase shift term. Let $Y(\omega)$ be the Fourier transform of $y(t)$.

The decoherence due to noise is calculated on a and the filter function:

$$\Gamma = \int_0^\infty \frac{d\omega}{2\pi} S(\omega)|Y(\omega)|^2$$

Which implies that coherence is $\propto e^{-\Gamma}$. The factor $|Y(\omega)|^2$ acts as a filter that shifts the noise spectrum towards frequencies that minimize the dephasing rate and $s(\omega)$. Spin echo, CPMG, XY-8 are examples of π-pulses that generate various $Y(\omega)$. Refer to Biercuk et al., 2010.

7.6 Practical Approach to Quantum Database for Data Scientists

7.6.1 Encoding Databases with the Quantum Fourier Transform

Consider a 2^n-dimensional $\mathcal{H}_A$ space associated to address register and a 2^m-dimensional $\mathcal{H}_D$ space associated to data register. The computational bases in $\mathcal{H}_A$ is denoted by $|x\rangle$, and $|0\rangle^{\otimes m}$ a reference in $\mathcal{H}_D$.

Definition 7.6.1.1 Let $D = \{D_x | x \in \{0, 1, \cdots, 2^n - 1\}\}$ a classical or quantum data set, where D_x is represented as a state $|D_x\rangle \in \mathcal{H}_D$. A unitary operator $U_{\text{qDB}} \colon \mathcal{H}_A \otimes \mathcal{H}_D \to \mathcal{H}_A \otimes \mathcal{H}_D$ implements a quantum database if $\forall x \in \{0, 1, \cdots, 2^n - 1\}$ is fulfilled $U_{\text{qDB}}\left(|x\rangle \otimes |0\rangle^{\otimes m}\right) = |x\rangle \otimes |D_x\rangle$.

Remark 7.6.1.1 The quantum database reads the index $|x\rangle$, and writes in the information data register $|D_x\rangle$.

Proposition 7.6.1.1 Given a U_{qDB} a linear unitary operator for any superposition $\sum_{x=0}^{2^n-1} \alpha_x |x\rangle$ is fulfilled $U_{\text{qDB}}\left(\sum_{x=0}^{2^n-1} \alpha_x |x\rangle \otimes |0\rangle^{\otimes m}\right) = \sum_{x=0}^{2^n-1} \alpha_x |x\rangle \otimes |D_x\rangle$.

Theorem 7.6.1.1 Being U_{qDB} a unitary operator, therefore exists $U_{\text{qDB}}^\dagger$ unitary as $U_{\text{qDB}}^\dagger\left(|x\rangle \otimes |D_x\rangle\right) = |x\rangle \otimes |0\rangle^{\otimes m}$. For any state $\sum_{x=0}^{2^n-1} \alpha_x |x\rangle \otimes |D_x\rangle$,

$$U_{\text{qDB}}^\dagger = \left(\sum_{x=0}^{2^n-1} \alpha_x |x\rangle \otimes |D_x\rangle\right) = \sum_{x=0}^{2^n-1} \alpha_x |x\rangle \otimes |0\rangle^{\otimes m}$$

Corollary 7.6.1.1 Considering the Definition 7.6.1.1, the access is time constant in respect to the superposition $|x\rangle$. Therefore, it is optimal to apply well-known search algorithms such as Grover.

Consider that in a quantum EIT multi-level ensemble, the $|x\rangle \otimes |0\rangle^{\otimes m} \mapsto |x\rangle \otimes |D_x\rangle$ is carried out by applying a pulse ℓ_x simultaneously. The light mode ℓ_x and the atomic ensemble $\mathcal{E}$ are described by a unitary operator U_{EIT}. Thus, the $\sum_{x=0}^{2^n-1} \alpha_x |x\rangle \mapsto \sum_{x=0}^{2^n-1} \alpha_x |x\rangle |D_x\rangle$ is coherent

and reversible.

Similarly, in a DLCZ scheme, each index $|x\rangle$ containing the address x is generated in one of the collective excitation modes in the atomic assembly. The reversibility between the photon and the collective mode ensures the reading/writing of the information $|D_x\rangle$.

As an example, a simulation has been prepared in Qiskit's QASM simulator with a use case in data science. Refer to Figure A.10 to review the quantum circuit with high-level gates, and review the Appendix D for full implementation details, as well as a review of Grover and QFT. A dataset is proposed with salaries segregated by sex and department in which they work. The problem is raised of detecting which department complies with equal pay. In the code, the data is randomly generated, and a department is forced to have equal pay. The problem is solved by classical means, and the generated data is reused to pass it through the proposed quantum circuit. It is composed of the definition of U_{qDB} as a block called `QuantumDatabase`. The information $|D_x\rangle$ in the data qubits is passed to the `DataProcessor` gate. In it, a Quantum Fourier Transform (QFT) is defined that acts as an adder. Later, an oracle U_f is implemented that marks whether the equal pay is met and has been named the `DataValidator` gate. In Grover's theory, the previous gate applies the characteristic function $f(x)$ that equals 1 when equal pay is met. Finally, the operations are undone with the inverses of the operations and the diffusion operator $D = (H^{\otimes n})(2\,|0\rangle\langle 0| - I)(H^{\otimes n})$ is applied, amplifying the state in the sequence $G = D \cdot U^{\dagger}_{\text{qDB}} U_f U_{\text{qDB}}$. At the end of the circuit, a measurement is made on the address qubits that have marked the department that meets the condition.

The advantage is in using quantum superposition of the addresses $|x\rangle$, in this case, of the departments. With parallel access to the salary information $|D_x\rangle$. In summary,

$$|x\rangle\,|0\rangle^{\otimes m} \xrightarrow{\overbrace{\text{Write}}^{U_{\text{qDB}}}} |x\rangle\,|D_x\rangle \xrightarrow{\overbrace{\text{Operate}}^{U_f}} |x\rangle\,(\pm\,|D_x\rangle) \xrightarrow{\overbrace{\text{Read}}^{U^{\dagger}_{\text{qDB}}}} |x\rangle\,|0\rangle^{\otimes m}$$

$$\underbrace{U^{\dagger}_{\text{qDB}} U_f U_{\text{qDB}}}_{\text{Write—Operate—Read}} \;:\; |x\rangle\,|0\rangle^{\otimes m} \mapsto |x\rangle\,|0\rangle^{\otimes m} \tag{7.1}$$

7.6.2 Role of Quantum Data Scientist

A quantum database scheme has been proposed both at the hardware level to demonstrate the technical feasibility of production. A way of encoding a database using address requests and value encoding has also been developed, applying it to a specific use case of a database in data science. It has been pointed out how the data scientist can participate in the tasks of producing algorithms for error correction, as well as in the use of the database itself. IBM (IBM Quantum, 2024), marks the beginning of the data scientist in its development roadmap in the participation of tasks in the platform as a code assistant for Qiskit, Qiskit functions service, mapping collections, specific libraries, general purpose QC libraries. The author of this thesis proposes to add a complementary path in which data science techniques can be useful when collaborating multidisciplinary in the production of real quantum computing. Not only from the point of view of a fault-tolerant quantum computer, but through the QKD connection and a quantum database to complete the real use of quantum technology.

It is recommended to read an article published by the author in IEEE Computer Society (Raigada García, 2024e), where the need for the Quantum Data Scientist versus the Quantum Machine Learning Engineer (QMLE) is expressed. In general terms, the QMLE is concerned with translating ML algorithms into their quantum form. While the Data Scientist is interested in making the quantum form usable from a business and social perspective.

Chapter 8

Conclusion

At the beginning of the work, the aim was to provide a way to use data safely —both in transit (QKD) and in storage. As well as to solve the problems in Big Data management through new technologies.

The work concludes with a complete definition in the hardware field where, through atomic multi-assemblies and management of the dynamics of quantum systems, the feasibility of a physical implementation has been exposed. In addition, an even more powerful DLCZ architecture has been pointed out, definitively forming a framework for high-fidelity data encoding based on the security of quantum mechanics —the behaviour of nature.

An extensive framework has been formed in terms of initiation to quantum mechanics applied to quantum computing systems focused on data scientists. It has been carried out in concise and precise definitions although not exhaustive in all the literature, since the extension would be too ambitious. For this reason, an essential selection of definitions and theorems has been made where the author has formulated very technical concepts in a simple way. In addition, a roadmap has been outlined for more ambitious readers, recommending the readings that follow this work.

With all this, a self-contained introductory manual to quantum data science has been achieved. At the same time, a clear definition has been made that tries to solve the fundamental problems in data science: Big Data and its fast, reliable and rapid management, while offering a social solution to the problems related to data security.

Appendix A

Appendix of images

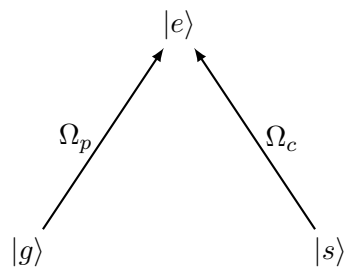

Figure A.1: Schema of a system with three levels of energy

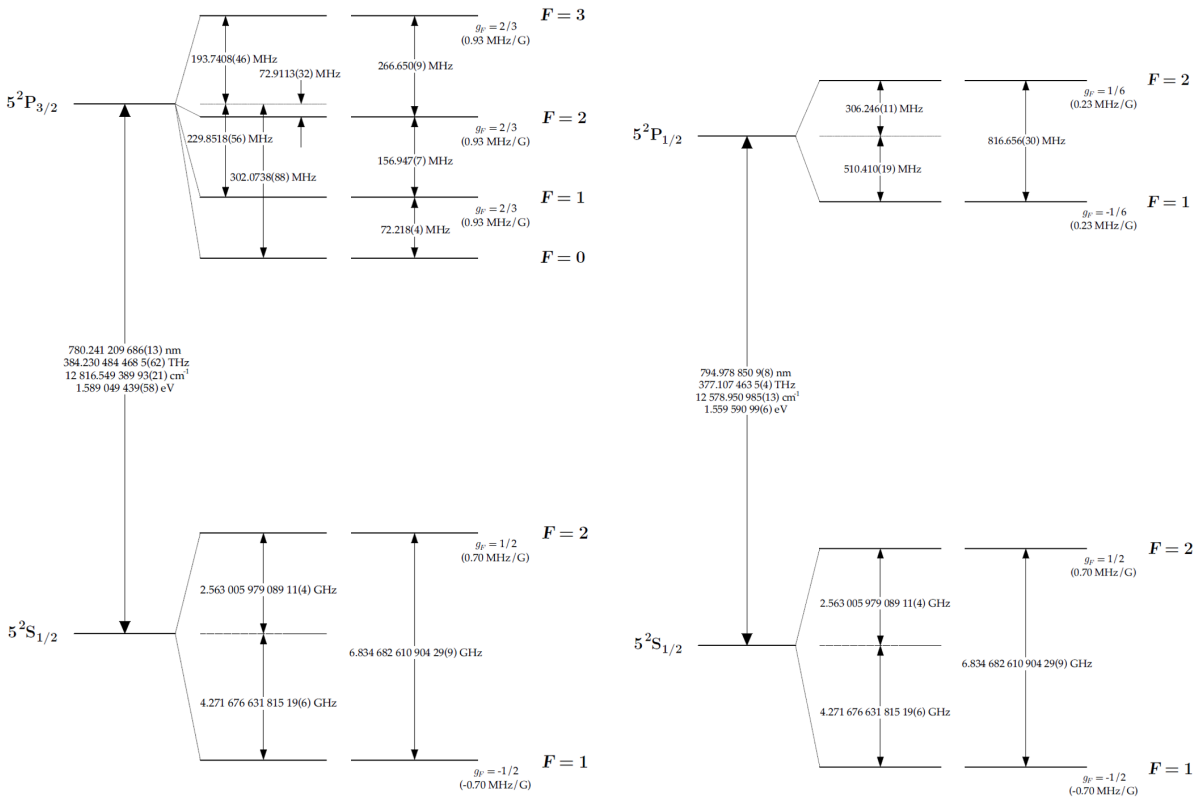

Figure A.2: **a)** Transition diagram of the hyperfine structure D_2 **b)** Transition diagram of the hyperfine structure D_1 (Steck, 2001)

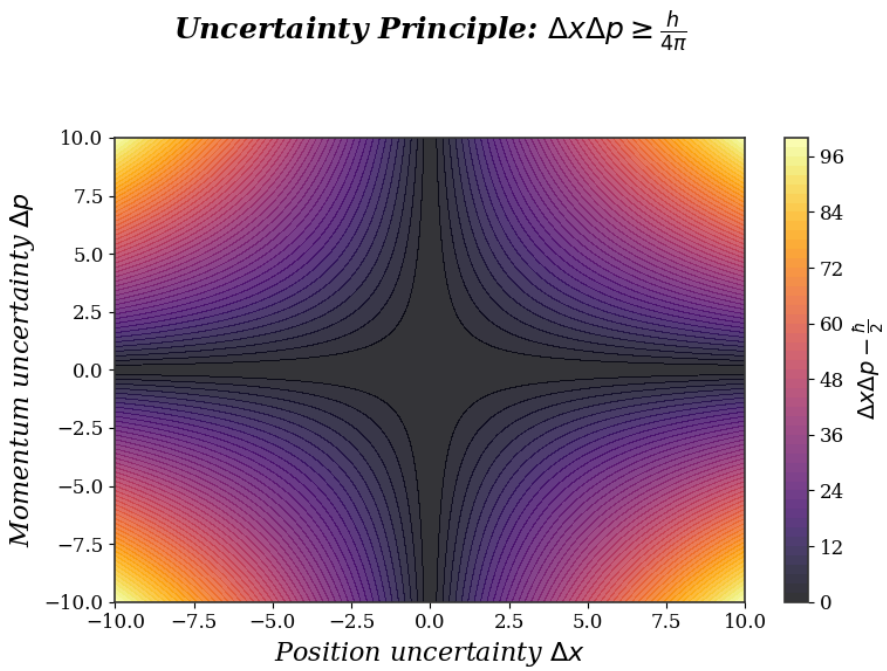

Figure A.3: Heisenberg uncertainty principle, illustrating the relationship between the uncertainties of position (Δx) and momentum (Δp). $\Delta x \Delta p = \frac{h}{4\pi}$ represents the quantum limit beyond which the uncertainty product is physically impossible (in quantum terms and not in classical physics). The colour gradient reflects different values of $\Delta x \Delta p - \frac{h}{4\pi}$. Own image generated with Python code.

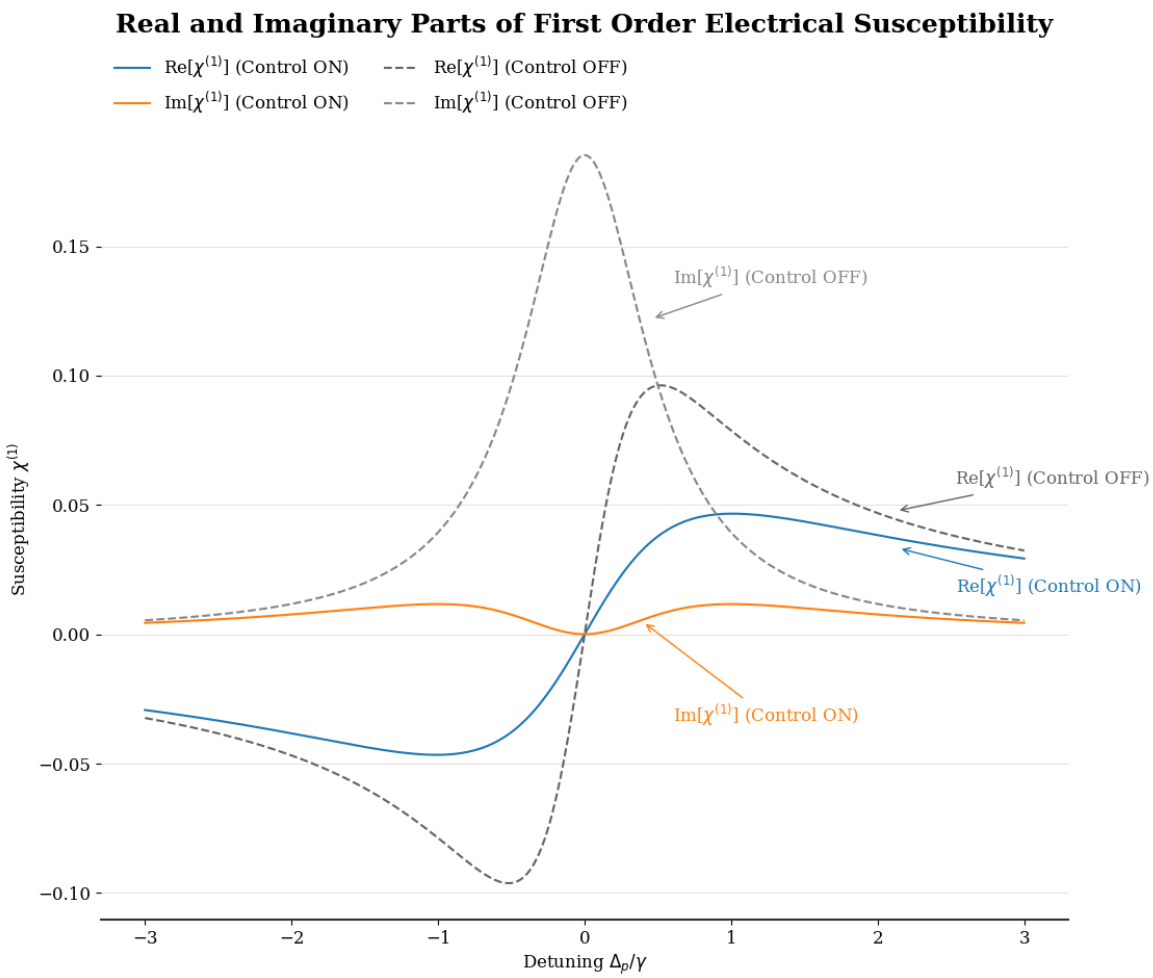

Figure A.4: Graph showing the real and imaginary parts of the first-order electrical susceptibility for the ON and OFF laser control states. Solid lines represent the ON state (Control ON). Dashed lines represent the OFF state (Control OFF).

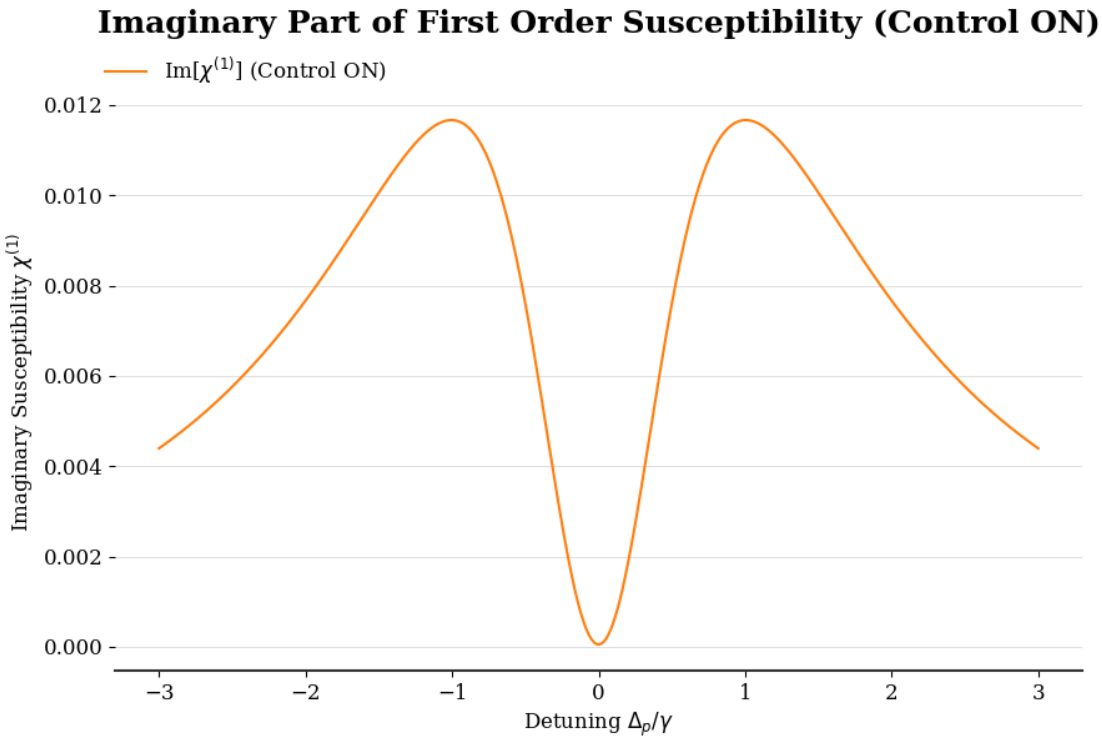

Figure A.5: Graph showing the imaginary part of the first order electrical susceptibility with the control laser in the active state (Control ON).

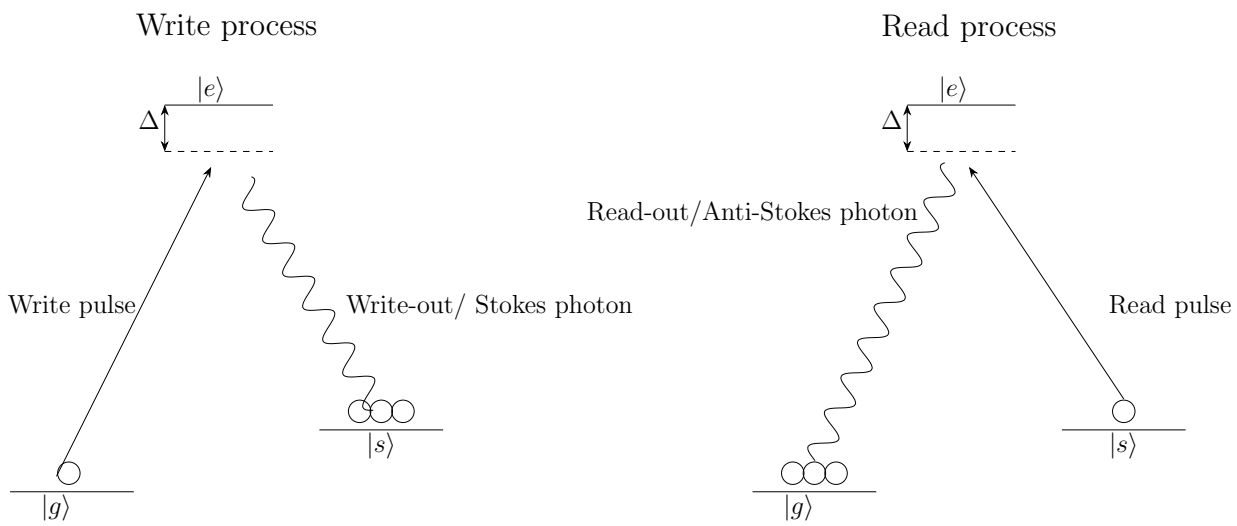

Figure A.6: Schema illustrating the DLCZ memory with the Write and Read processes for the creation of collective atomic excitations in an atomic ensemble.

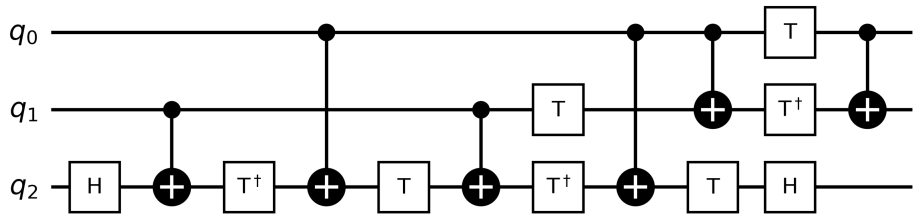

Figure A.7: Toffoli matrix decomposition circuit into universal quantum gates.

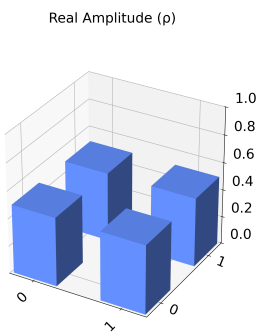

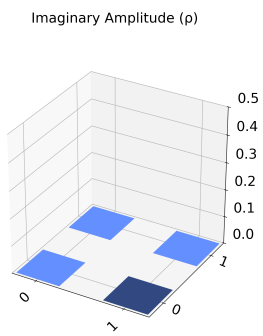

(a) Density matrix of the pure state

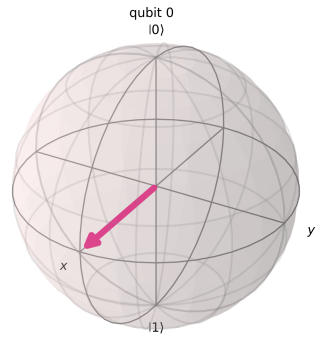

(b) Bloch Sphere of the pure state

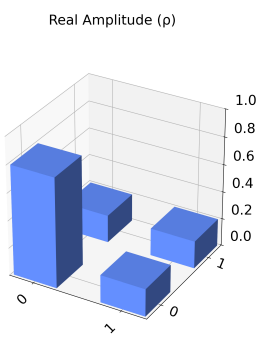

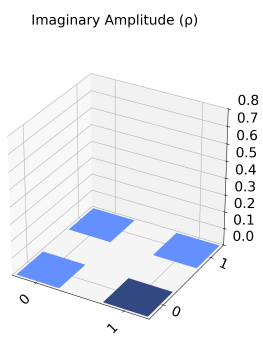

(c) Density matrix of the mixed state

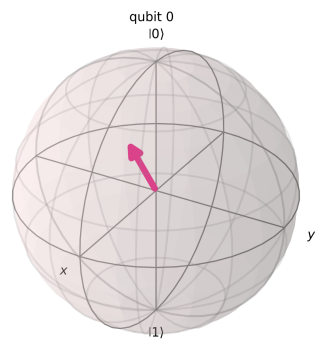

(d) Bloch Sphere of the mixed state

Figure A.8: Image (a) shows the density matrix of the pure state $|+\rangle$, uniform superposition on the states $|0\rangle$ and $|1\rangle$. Image (b) shows the representation on the Bloch sphere. Density matrix (c) shows the mixed state resulting from a probabilistic mixture (or superposition) of the states $|0\rangle$ and $|+\rangle$, with probability of 40 % and 60 % respectively. Representation (d) reflects the mixed state on the Bloch sphere.

[§]Image generated with Qiskit Software in Python.

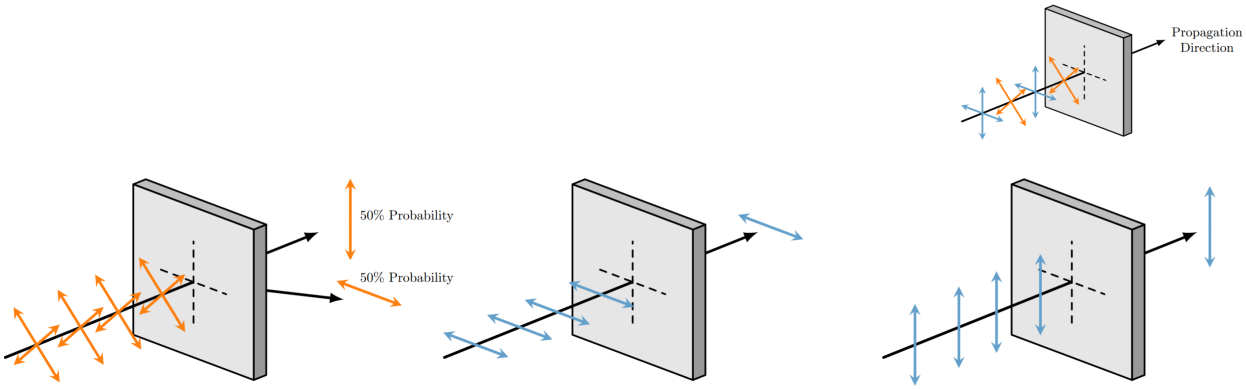

Figure A.9: Representation of polarizing filters. Note that if a photon is polarized on the diagonal basis, passing through a rectilinear polarizing filter, it is deflected to the left 50% of the time and 50% of the time to the right.

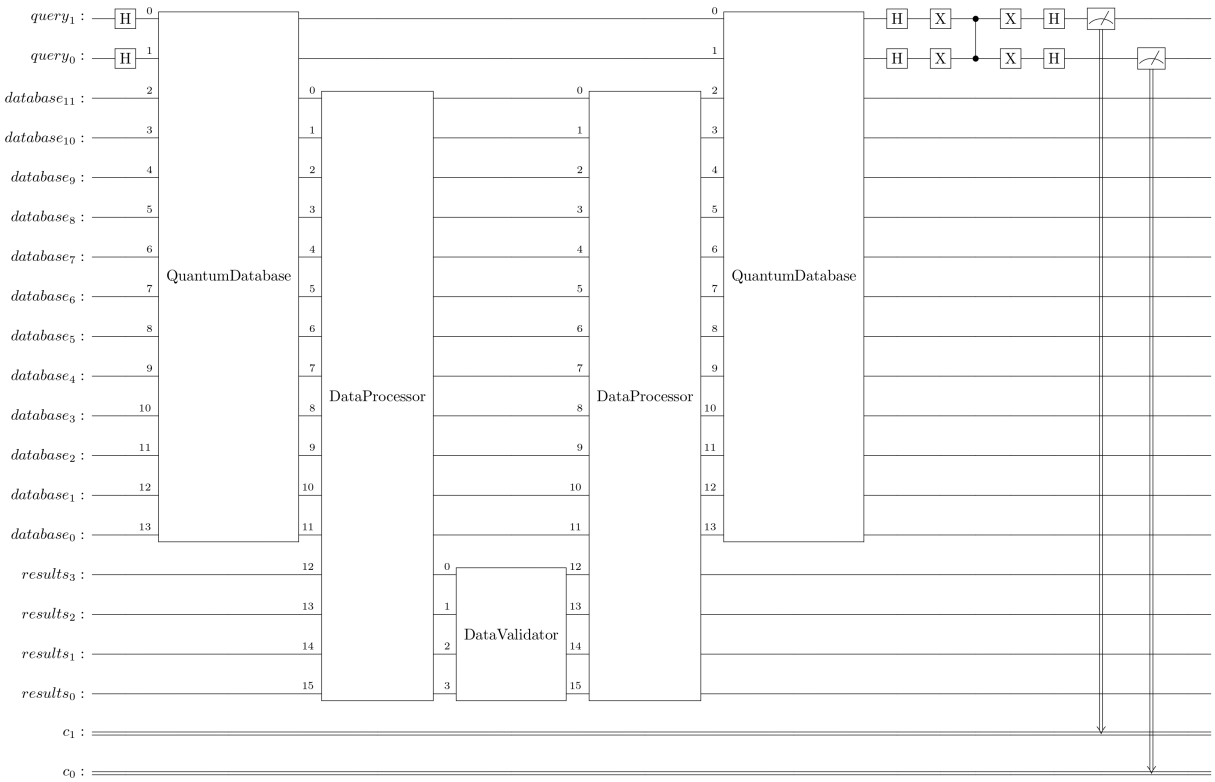

Figure A.10: Quantum Circuit of the Quantum Database.

§ *Licensed under a Creative Commons Attribution-ShareAlike 4.0 International License.*
© Copyright 2021 – TikZ.net. Adapted by Ricard Santiago Raigada García in 2024.

Appendix B

Tables

It was considered that the tables belonging to appendices with specific topics such as probability or quantum computing should be placed in the same appendix in order to maintain a focus on each specialized appendix. Therefore, only the tables from the main thesis body appear in this section.

Table B.1: Values of K, $E_{F=x}$, E_{EQ} y E_{MD} for different values of F

F	K	$E_{F=x}$	E_{EQ}	E_{MD}
3	$K_3 = 4.5$	$E_{F=3} = 193.7407$	$E_{EQ,3} = 6.24825$	$E_{MD,3} = 190.6166$
2	$K_2 = -1.5$	$E_{F=2} = -72.9113$	$E_{EQ,2} = -18.74475$	$E_{MD,2} = -63.5389$
1	$K_1 = -5.5$	$E_{F=1} = -229.8523$	$E_{EQ,1} = 6.24825$	$E_{MD,1} = -232.9764$
0	$K_0 = -7.5$	$E_{F=0} = -302.0738$	$E_{EQ,0} = 31.24125$	$E_{MD,0} = -317.6944$

Table B.2: Properties of a Complex Vector Space

Property	**Expression**
Commutativity	$\vec{u} + \vec{v} = \vec{v} + \vec{u}$
Associativity	$(\vec{u} + \vec{v}) + \vec{w} = \vec{u} + (\vec{v} + \vec{w})$
Zero Vector	$\exists\, \vec{0} \in V : \vec{v} + \vec{0} = \vec{v}$
Additive Inverse	$\exists\, (-\vec{v}) \in V : \vec{v} + (-\vec{v}) = \vec{0}$
Distributivity Over Addition	$a \cdot (\vec{u} + \vec{v}) = (a \cdot \vec{u}) + (a \cdot \vec{v})$
Distributivity Over Scalars	$(a + b) \cdot \vec{v} = (a \cdot \vec{v}) + (b \cdot \vec{v})$
Scalar Associativity	$a \cdot (b \cdot \vec{v}) = (ab) \cdot \vec{v}$
Scalar Identity	$1 \cdot \vec{v} = \vec{v}$

Table B.3: Example of BB84 Protocol Transmission of 8 Bits

Bit #	**Alice's Bit b_i**	**Alice's Basis**	**Alice's Sent State**	**Bob's Basis**	**Bob's Measurement Outcome**	**Public Discussion**	**Final Key Contribution**
1	0	Z (Comp.)	$\|0\rangle = \updownarrow$	Z (Comp.)	$\|0\rangle = \updownarrow$	Bases match (Z/Z)	Keep bit = 0
2	1	X (Diag.)	$\|-\rangle = \nwarrow\!\!\searrow$	Z (Comp.)	$\|1\rangle = \leftrightarrow$ or error	Bases differ (X/Z)	Discard
3	0	X (Diag.)	$\|+\rangle = \nearrow\!\!\swarrow$	X (Diag.)	$\|+\rangle = \nearrow\!\!\swarrow$	Bases match (X/X)	Keep bit = 0
4	1	Z (Comp.)	$\|1\rangle = \leftrightarrow$	Z (Comp.)	$\|1\rangle = \leftrightarrow$	Bases match (Z/Z)	Keep bit = 1
5	0	X (Diag.)	$\|+\rangle = \nearrow\!\!\swarrow$	Z (Comp.)	$\|0\rangle = \updownarrow$ or $\|1\rangle$ equally likely	Bases differ (X/Z)	Discard
6	1	X (Diag.)	$\|-\rangle = \nwarrow\!\!\searrow$	X (Diag.)	$\|-\rangle = \nwarrow\!\!\searrow$	Bases match (X/X)	Keep bit = 1
7	1	Z (Comp.)	$\|1\rangle = \leftrightarrow$	X (Diag.)	$\|+\rangle = \nearrow\!\!\swarrow$ or $\|-\rangle$ random	Bases differ (Z/X)	Discard
8	0	Z (Comp.)	$\|0\rangle = \updownarrow$	Z (Comp.)	$\|0\rangle = \updownarrow$	Bases match (Z/Z)	Keep bit = 0

Table B.4: Department Pay Distribution

Man	**Female**	**Department**
4174	1330	1
4507	4507	2
1860	3135	3
2294	4444	4
2130	4171	1
2095	2095	2
4772	4735	3
4092	1130	4
2638	2685	1
3169	3169	2
1466	1769	3
2238	3391	4

Appendix C

Proofs of Chapter 7

Proof of the Definition 7.1.1.1 Let two representations:

$$|\psi\rangle = \sum_{i=1}^{n} \psi_i \, |e_i\rangle = \sum_{i=1}^{n} \phi_i \, |e_i\rangle$$

$$0 = |\psi\rangle - |\psi\rangle = \sum_{i=1}^{n} (\psi_i - \phi_i) \, |e_i\rangle$$

The lineality implies for $\{|e_i\rangle\}$ is linearly independent, then if $\sum_{i=1}^{n}(\psi_i - \phi_i) \, |e_i\rangle$, it is given $\psi_i - \phi_i = 0 \quad \forall i$.

Proof of the Definition 7.1.1.1.1 For all vector $|\psi\rangle \in \mathcal{V}$,

$$\| \, |\psi\rangle \, \| = \sqrt{\langle\psi|\psi\rangle}$$

Given $\langle\psi|\psi\rangle \geq 0$ then, $\| \, |\psi\rangle \, \| =\geq 0$. If $|\psi\rangle = 0$, then $\| \, |\psi\rangle \, \| = 0 \implies \langle\psi|\psi\rangle = 0$.

Proof of the Definition 7.1.1.1.2 Given a $\langle e_i|e_j\rangle = \delta_{ij}$ space, and the quantum state $|\psi\rangle = \frac{1}{\sqrt{2}} \, |e_1\rangle + \frac{1}{\sqrt{2}} \, |e_2\rangle$, then

$$\langle\psi|\psi\rangle = \frac{1}{2} + \frac{1}{2} = 1$$

Hence $\| \, |\psi\rangle \, \| = 1$,concluding that it is a unit vector.

Proof of the Definition 7.1.1.1.3 Given $|\psi\rangle = \alpha \, |0\rangle + \beta \, |1\rangle = \alpha^{'} \, |0\rangle + \beta^{'} \, |1\rangle$:

$$0 = (\alpha - \alpha^{'}) \, |0\rangle + (\beta - \beta^{'}) \, |1\rangle$$

Due to $\{|0\rangle, |1\rangle\}$ are an orthonormal base, then:

$$\alpha - \alpha^{'} = 0, \quad \beta - \beta^{'} = 0$$

$$\langle\psi|\psi\rangle = |\alpha|^2 + |\beta|^2 = 1$$

Proof of the Definition 7.1.1.1.4 If $\| |\phi\rangle \| = 1$, $\| |\psi\rangle \| = 1$; and $\langle\phi|\psi\rangle = 0$, then $\{|\phi\rangle, |\psi\rangle\}$ is linearly independent and orthonormal.

Proof of the Definition 7.1.1.1.5 Consider the vector $|\chi\rangle = |\psi\rangle - \frac{\langle\phi|\psi\rangle}{\langle\phi|\phi\rangle}|\phi\rangle$, the norm is computed as:

$$\langle\chi|\chi\rangle = \langle\psi|\psi\rangle - \frac{|\langle\phi|\psi\rangle|^2}{\langle\phi|\phi\rangle}|\phi\rangle$$

If $\langle\chi|\chi\rangle \geq 0$, then $\langle\psi|\psi\rangle\langle\phi|\phi\rangle \geq |\langle\phi|\psi\rangle|^2$, the square root of both sides conduce to the Cauchy-Schwarz inequality.

Proof of the Definition 7.1.1.1.6 A normed vector in $\mathcal{H}$ only makes sense if $\langle\psi|\psi\rangle \geq 0$ —or $\langle\psi|\psi\rangle = 0$ if and only if $\psi = 0$. An inner product $\langle\cdot|\cdot\rangle$ in $\mathcal{H}$ must comply with conjugate linearity, conjugate symmetry and the positivity defined above:

$$\langle a\psi_1 + b\psi_2|\phi\rangle = a^*\langle\psi_1|\phi\rangle + b^*\langle\psi_2|\phi\rangle$$
$$\langle\psi|\phi\rangle = \langle\phi|\psi\rangle^*$$

For any $\alpha \in \mathbb{C}$ and $\psi \in \mathcal{H}$:

$$\|\alpha\psi\| = \sqrt{\langle\alpha\psi|\alpha\psi\rangle} = \sqrt{|\alpha|^2\langle\psi|\psi\rangle} = |\alpha|\sqrt{\langle\psi|\psi\rangle} = |\alpha|\|\psi\|$$

By Cauchy-Schwarz for the inner product, one concludes:

$$|\langle\psi + \phi|\psi + \phi\rangle| \leq \|\psi\|^2 + 2|\langle\psi|\phi\rangle| + \|\phi\|^2,$$
$$\|\psi + \phi\| \leq \|\psi\| + \|\phi\|$$

Thus:

$$\|\psi\| \geq 0, \quad \|\psi\| = 0 \iff \psi = 0$$

$$\|\alpha\psi\| = |\alpha|\|\psi\| \quad \forall \alpha \in \mathbb{C}$$

$$\|\psi + \phi\| \leq \|\psi\| + \|\phi\|$$

$\|\psi\|$ is a norm of $\mathcal{H}$.

Proof of the Definition 7.1.1.1.7 If $\sum_i c_i |e_i\rangle = 0 \implies c_i = 0 \quad \forall i$. There is no alternative expansion that does not contradict uniqueness.

Proof of the Definition 7.1.1.1.8 If $\{|\psi_n\rangle\}$ is a Cauchy sequence in the complex space $\mathcal{H}$, then $\exists |\psi\rangle \in \mathcal{H}$ s.t. $\| |\psi_n\rangle - |\psi\rangle \| \implies 0$. Completeness is a required property of $\mathcal{H}$ space, therefore every Cauchy sequence converges in $\mathcal{H}$ space.

Proof of Remark 7.1.1.1.1 A qubit with $|\psi\rangle = \frac{1}{\sqrt{2}}|0\rangle + \frac{1}{\sqrt{2}}|1\rangle$, then the norm is:

$$\| |\psi\rangle \|^2 = \frac{1}{2} + \frac{1}{2} = 1$$

Hence $\| |\psi\rangle \| = 1$, concluding that it is a valid qubit.

Proof of the Definition 7.1.1.1.9 Let $\dim(\mathcal{H}_A \otimes \mathcal{H}_B) = \dim(\mathcal{H}_A) \cdot \dim(\mathcal{H}_B)$, and $(|\psi\rangle, |\phi\rangle) \mapsto |\psi\rangle \otimes |\phi\rangle$. If $\left\{|e_i\rangle^A\right\}_{i=1}^m$ and $\left\{|f_j\rangle^B\right\}_{j=1}^n$ are the orthonormal basis of $\mathcal{H}_A$ and $\mathcal{H}_B$ respectively; then $\left\{|e_i\rangle^A \otimes |f_j\rangle^B\right\}_{i,j}$ is base of $\mathcal{H}_A \otimes \mathcal{H}_B$ with $m \times n$ elements. By definition of tensor product, bilinearity is direct $(|\psi_1\rangle + |\psi_2\rangle) \otimes |\phi\rangle = |\psi_1\rangle \otimes |\phi\rangle + |\psi_2\rangle \otimes |\phi\rangle$.

Proof of the Definition 7.1.1.2.1 Any normal operator A in a finite-dimensional $\mathcal{H}$ space can be diagonalized using a unitary transformation. By the spectral theorem it is known that an orthonormal base of eigenvectors diagonalizes, then $\exists \{|e_i\rangle\}$ s.t. $A|e_i\rangle = \lambda_i |e_i\rangle, \quad \forall i$. In consequence, one can express A as:

$$A = \sum_{i=1}^{n} \lambda_i |e_i\rangle \langle e_i|$$

Proof of the Definition 7.1.1.2.2 Assume $|\psi\rangle$ is an eigenvector of H:

$$H|\psi\rangle = \lambda |\psi\rangle$$

The inner product of the state $|\psi\rangle$ is $\langle\psi|H|\psi\rangle = \lambda\langle\psi|\psi\rangle$. Considering H is hermitian,

$$\langle\psi|H|\psi\rangle = \langle H\psi|\psi\rangle = \overline{\langle\psi|H|\psi\rangle}$$

Then, $\lambda\langle\psi|\psi\rangle$ is real as $\langle\psi|\psi\rangle > 0$.

Proof of the Theorem 7.1.1.2.1 The operator H is hermitian, the eigenvalues λ_i are real, and by the spectral theorem $\exists\{|e_i\rangle\}$ of $\mathcal{H}$:

$$H\,|e_i\rangle = \lambda_i\,|e_i\rangle\,, \quad \forall i$$
$$H = \sum_{i=1}^{n} \lambda_i\,|e_i\rangle\,\langle e_i|$$

Proof of the Definition 7.1.1.2.3 Let the following Hamiltonian $H \in \mathbb{C}^2$:

$$H = \begin{pmatrix} 2 & 0 \\ 0 & 3 \end{pmatrix}$$

The eigenvectors are:

$$|e_1\rangle = \begin{pmatrix} 1 \\ 0 \end{pmatrix}, \quad |e_2\rangle = \begin{pmatrix} 0 \\ 1 \end{pmatrix}$$

The eigenvalues are:

$$\lambda_1 = 2, \quad \lambda_2 = 3$$

Therefore, H can be written as:

$$H = 2\,|e_1\rangle\,\langle e_1| + 3\,|e_2\rangle\,\langle e_2|$$

The eigenvalues λ_i being the eigenenergies of the system.

Proof of the Definition 7.1.1.2.4 If U is unitary, thus $U^\dagger U = I$, and $U^\dagger = U^{-1}$:

$$\langle U\phi|U\psi\rangle = \langle\phi|U^\dagger U|\psi\rangle = \langle\phi|I|\psi\rangle = \langle\phi|\psi\rangle$$

Preserve the inner product.

Proof of the Definition 7.1.1.2.5 Given an orthonormal base $\{|e_i\rangle\}$ of $\mathcal{H}$:

$$\begin{aligned}\mathrm{Tr}(AB) &= \sum_i \langle e_i|AB|e_i\rangle = \sum_i \sum_j \langle e_i|A|e_j\rangle\langle e_j|B|e_i\rangle \\ &= \sum_j \sum_i \langle e_j|B|e_i\rangle\langle e_i|A|e_j\rangle = \sum_j \langle e_j|BA|e_j\rangle = \mathrm{Tr}(BA)\end{aligned}$$

Proof of the Definition 7.1.1.2.6 Consider A, B are Hermitian. The adjoint of the commutator is computed as:

$$[A,\, B]^\dagger = (AB - BA)^\dagger = B^\dagger A^\dagger - A^\dagger B^\dagger = BA - AB = -[A,\, B]$$

Thus, $[A,\, B]^\dagger = -[A,\, B] \implies [A,\, B]$ is anti-Hermitian.

Proof of the Definition 7.1.1.2.7 For an antisymmetric tensor T^{ij}, it is given $T^{ii} = 0 \quad \forall i$.

$$T^{ii} = -T^{ii} \mid i = j, \quad 2T^{ii} = 0 \implies T^{ii} = 0$$

The diagonal elements of an antisymmetric tensor being zero.

Proof of the Definition 7.1.1.2.8 Any coefficient $\mathbb{R}$ that multiplies any linear combination of $I,\, \sigma_x,\, \sigma_y,\, \sigma_z$ will also be Hermitian. This $\{I,\, \sigma_x,\, \sigma_y,\, \sigma_z\}$ forms a basis for the Hermitian operators in $\mathbb{C}^2$.

Proof of the Definition 7.1.1.3.1 Let H Hermitian, then $e^{-iHt/\hbar}$ is unitary. Based on $H = H^\dagger \implies (e^{-iHt/\hbar})^\dagger = e^{-iHt/\hbar}$. By power series, and hermiticity:

$$e^{-iHt/\hbar}e^{-iHt/\hbar} = e^{-iHt/\hbar + iHt/\hbar} = e^0 = I$$

Then, $e^{-iHt/\hbar}$ is unitary.

Proof of Postulate 7.1.2.1.1 Let ρ Hermitian, semi-defined positive, and $\mathrm{Tr}(\rho) = 1$, it is proved by:

$$\rho^\dagger = \left(\sum_j p_j \left|\psi_j\right\rangle \left\langle\psi_j\right|\right)^\dagger = \sum_j p_j \left|\psi_j\right\rangle \left\langle\psi_j\right| = \rho$$

$$\langle\phi|\,\rho\,|\phi\rangle = \sum_j p_j\,|\langle\psi_j|\phi\rangle|^2 \geq 0$$

$$\mathrm{Tr}(\rho) = \sum_j p_j \mathrm{Tr}\left(|\psi_j\rangle\,\langle\psi_j|\right) = \sum_j p_j = 1$$

Proof of Postulate 7.1.2.1.2 The outcome probability of ρ is given by $p(i) = \mathrm{Tr}(P_i\rho)$. After a measurement, the outcome is:

$$p_i = \frac{P_i\rho P_i}{p(i)}$$

It is positive, and has a trace 1, therefore is a valid density operator. The wave function may be in superposition, but after a measurement it collapses into $|0\rangle, |1\rangle$ providing no information about its complex phase. Repeated measurements on the state will always equal the collapsed classical state.

Proof of Postulate 7.1.2.1.3 Considering a $U(t)$ unitary evolution:

$$\mathrm{Tr}(\rho(t)) = \mathrm{Tr}(U(t)\rho(0)U^\dagger(t)) = \mathrm{Tr}(\rho(0)) = 1$$

Positivity is preserved under unitary transformations:

$$\langle\phi|\,\rho(t)\,|\phi\rangle = \langle\phi|\,U(t)\rho(0)U^\dagger(t)\,|\phi\rangle = \left\langle U^\dagger(t)\phi\right|\rho(0)\left|U^\dagger(t)\phi\right\rangle \geq 0$$

Proof of Postulate 7.1.2.2.1 Think that the quantum states are no orthogonal. A measurement of $\langle\rho|E_1|\rho\rangle = 1$ and $\langle\sigma|E_2|\sigma\rangle = 1$. Recall the completeness condition. The decomposition of $|\sigma\rangle$ it is $|\psi\rangle = \alpha\,|\rho\rangle + \beta\,|\varphi\rangle$. Assuming $|\varphi\rangle$ is orthogonal to $|\rho\rangle$, the complex probability amplitude would be equal to one, and $|\beta| < 1$. It is contradictory due to $\langle\sigma|E_2|\sigma\rangle = |\beta|^2\langle\varphi|E_2|\varphi\rangle < 1$. Therefore, an indistinguishable superposition state is assumed. Only orthogonal states can satisfy that both measurements are 100 % reliable.

Proof of Theorem 7.1.2.2.1 Consider the same two quantum states and prior probabilities showed in the Theorem. One has to measure with outcome in $\{0, 1\}$ to guess the ρ state. Consider the POVM measurement $\{E_0, E_1\}$ with $E_0 + E_1 = I, \quad E_0, E_1 \geq 0$. The probability error is:

$$P = p_0\mathrm{Tr}(E_1\rho_0) + p_1\mathrm{Tr}(E_0\rho_1)$$

Define $\Delta := p_0\rho_0 - p_1\rho_1$ to minimize the probability error over POVMs:

$$P = \frac{1}{2}\left[p_0 \mathrm{Tr}(E_1\rho_0) + p_1 \mathrm{Tr}(E_0\rho_1)\right] \cdot 2$$

Considering the above identity one gets:

$$P = p_0 \mathrm{Tr}(E_1\rho_0) + p_1 \mathrm{Tr}(E_0\rho_1) = p_0 \mathrm{Tr}(E_1\rho_0) + p_1 \mathrm{Tr}((I - E_1)\rho_1)$$
$$P = p_1 + \mathrm{Tr}(E_1(p_0\rho_0 - p_1\rho_1)) = p_1 + \mathrm{Tr}(E_1\Delta)$$

Δ can be defined as a spectral decomposition:

$$\Delta = \sum_i d_i \left|d_i\right\rangle \left\langle d_i\right|$$

Therefore, it leads to a difference of two real-scale densities since Δ is Hermitian and $d_i \in \mathbb{R}$. Take E_0 as the projector onto the subspace associated with non-positive eigenvalues and E_1 onto the positive eigenvalues:

$$E_1 = \sum_{d_i > 0} \left|d_i\right\rangle \left\langle d_i\right|, \quad E_0 = I - E_1 = \sum_{d_i \leq 0} \left|d_i\right\rangle \left\langle d_i\right|$$

Leading to:

$$\mathrm{Tr}(E_1\Delta) = \sum_{d_i > 0} d_i$$

The trace norm is given by the absolute magnitudes of the eigenvalues $\|\Delta\|_1 = \sum_i |d_i|$.The two spectra are separated by the positive and negative subspaces:

$$\sum_{d_i > 0} d_i = \frac{1}{2}\left(\|\Delta\|_1 + \mathrm{Tr}(\Delta)\right),$$
$$\sum_{d_i < 0} d_i = \frac{1}{2}\left(\mathrm{Tr}(\Delta) - \|\Delta\|_1\right)$$

The trace of the state with its associated probability leads to the probability, it is achieved by defining $\mathrm{Tr}(\Delta) = p_0 - p_1$. The hypothesis of $p_0 - \rho_0$ is posed as $|0\rangle$ and $p_1 - \rho_1$ as $|1\rangle$. The optimal choice is made from the following calculation using the identity and distinguishing the positive and

negative parts of the spectrum of Δ:

$$P = p_1 + \mathrm{Tr}(E_1\Delta) = p_1 + \sum_{d_i>0} d_i$$

$$\sum_{d_i>0} d_i = \frac{1}{2}\left(\|\Delta\|_1 + (p_0 - p_1)\right)$$

$$P = p_1 + \frac{1}{2}\left(\|\Delta\|_1 + p_0 - p_1\right) = \frac{p_0 + p_1}{2} + \frac{\|\Delta\|_1}{2}$$

$$P_{\mathrm{err}} = \frac{1}{2} + \frac{\|\Delta\|_1}{2}$$

The key is to check the signs that minimize the term $\sum_{d_i>0} d_i$. Specifically, the minimum error is obtained with the POVM that guesses $|0\rangle$ if $\Delta > 0$ and $|1\rangle$ if $\Delta < 0$. The success probability is given by:

$$P_{\mathrm{succ}} = \frac{1}{2}\left(1 + \|p_0\rho_0 - p_1\rho_1\|_1\right)$$

Consequently, it is shown that the minimum probability of error is given by:

$$P_{\mathrm{err}} = \frac{1}{2}\left(1 - \|p_0\rho_0 - p_1\rho_1\|_1\right)$$

Proof of the Definition 7.1.2.3.1 Let $\{P_i\}$ an orthogonal projector set, can be defined $M = \sum_i \lambda_i P_i, \quad \lambda_i \in \mathbb{R}$. Since P_i is orthogonal and Hermitian, M is an observable whose eigenprojectors are $\{P_i\}$.

Proof of the Definition 7.1.2.4 Consider:

$$\mathrm{POVM} = \{E_1,\, E_2\} : \quad E_1 = \frac{1}{2}\begin{pmatrix} 1 & 1 \\ 1 & 1 \end{pmatrix},\, E_2 = I - E_1$$

Note that $E_1 + E_2 = I$ and that $\langle\psi|E_i|\psi\rangle \geq 0$, but are not orthogonal. Finally, the probabilities associated with the POVM elements of a state ρ are given by:

$$p(i) = \mathrm{Tr}(E_i\rho), \quad i = 1, 2$$

Proof of the Definition 7.1.2.5.1 For a global phase $e^{i\theta}$, take into account:

$$\langle (e^{i\theta}\psi)|M|(e^{i\theta}\psi)\rangle = e^{-i\theta}e^{i\theta}\langle\psi|M|\psi\rangle = \langle\psi|M|\psi\rangle.$$

It is invariant. For a relative phase $|\psi\rangle = \alpha\,|0\rangle + \beta\,|1\rangle$. If $\alpha e^{i\phi}$ with $\phi \neq 0$, then, it may be variant if M is not diagonal in $\{|0\rangle, |1\rangle\}$ due to the fact that the crossed elements $\alpha\overline{\beta}$ change their phase.

Proof of the Definition 7.1.2.5.2 Let a $H = \lambda_1\,|e_1\rangle\,\langle e_1| + \lambda_2\,|e_2\rangle\,\langle e_2| \in \mathbb{C}^2$ with initial state:

$$|\psi(t)\rangle = \alpha e^{-i\lambda_1 t/\hbar}\,|e_1\rangle + \beta e^{-i\lambda_2 t/\hbar}\,|e_2\rangle$$

The $(\lambda_1 - \lambda_2)t/\hbar$ determines the relative phase, thus the interference patron.

Proof of the Definition 7.1.2.6.1 Let $|\psi\rangle_{AB} = |\phi\rangle_A \otimes |\chi\rangle_B \quad \forall M_A \otimes N_B$:

$$\langle\psi_{AB}|M_A \otimes N_B|\psi_{AB}\rangle = \langle\phi|M_A|\phi\rangle\,\langle\chi|N_B|\chi\rangle.$$

Entanglement is shown by being impossible to decompose into a product of independent expectations, thus indicating the absence of non-trivial quantum correlations.

Proof of the Definition 7.1.2.6.2 Given the spectral decomposition of ρ, the semi-positive define, and $\sum_i \lambda_i = 1$; it is an ensemble. The ensemble representation is non-unique, since there are other unitary combinations within the subspace with degenerate eigenvalues.

Proof of the Definition 7.1.2.6.3 Given $\{E_k\}$, exists a Stinespring dilatation:

$$U : |\psi\rangle \otimes |0\rangle_E \mapsto \sum_k E_k|\psi\rangle \otimes |k\rangle_E$$

The trace over E gives $\mathcal{E}(\rho)$, U is isometric and expands to a unitary operator in $\mathcal{H} \otimes \mathcal{H}_E$. A complementary definition can be found in the definitions of the quantum entropy section (Section 7.2.1).

Proof of the Definition 7.1.4.1 Consider $\rho_A = \mathrm{Tr}_B(|\psi\rangle\,\langle\psi|)$. ρ_A is a density operator in $\mathcal{H}_A$, therefore it is diagonalizable. In the arbitrary base $\{|w_i\rangle\} \in \mathcal{H}_B$, define $\left|\tilde{\psi}\right\rangle = \sum_i \sqrt{\lambda_i}\,|u_i\rangle \otimes |w_i\rangle$:

$$V\colon \mathcal{H}_B \implies \mathcal{H}_B, \quad V\colon\ |w_i\rangle \mapsto |v_i\rangle$$

The base $\{|v_i\rangle\}$ diagonalize $\rho_B = \mathrm{Tr}_A(|\psi\rangle\langle\psi|)$. If $(I_A \otimes V)$ acts on $\left|\tilde{\psi}\right\rangle$, then:

$$|\psi\rangle = \sum_i \sqrt{\lambda_i}\,|u_i\rangle \otimes |v_i\rangle$$

Proof of the Definition 7.1.5.1 Consider the mixed state of the case, Figure A.8. The spectral decomposition was computed. Now, define $\{|f_1\rangle, |f_2\rangle\} \in \mathcal{H}_B$ and $|\Psi\rangle = \sqrt{\lambda_1}\,|v_1\rangle \otimes |f_1\rangle + \sqrt{\lambda_2}\,|v_2\rangle \otimes |f_2\rangle$, then:

$$\mathrm{Tr}_B = (|\psi\rangle\langle\psi|) = \lambda_1\,|v_1\rangle\langle v_1| + \lambda_2\,|v_2\rangle\langle v_2| = \rho$$

Proof of the Definition 7.1.6.1 An unitary operator preserves inner product. For $\langle\psi|\phi\rangle = \langle\psi|\phi\rangle^2$, $\{0, 1\}$ are the unique possible values for the two states. If $\langle\psi|\phi\rangle = 1$, $|\psi\rangle = |\phi\rangle$; or orthogonal for zero value of inner product. This leads to a contradiction for any state non-equal or orthogonal. Plus, intuitively, one cannot clone an unknown state, and if someone measured it, it would collapse the state.

Proof of the Definition 7.2.1 For $p_i \log p_i \leq 0$ implicitly from $0 \leq p_i \leq 1$, then $-p_i \log p_i \geq 0$. Summing over i preserves positivity.

Proof of the Definition 7.2.2 Consider a binary distribution with $p = \frac{1}{2}$, then $H_2(\frac{1}{2}) = 1$. The greater uncertainty for a binary entropy function.

Proof of the Definition 7.2.3 Consider $\varphi(x) = x \log x$ the second derivative is $1/x > 0 \forall x > 0$, therefore, convex. Span The Kullback-Leibler Divergence:

$$D(p\|q) = \sum_i p_i\,(\log p_i - \log q_i)$$

Based on the convexity:

$$D(p\|q) = \sum_i p_i \log p_i - \sum_i p_i \log q_i$$

$$|D(p\|q)| = \left(\sum_i p_i \log p_i - \sum_i q_i \log q_i\right) - \left(\sum_i p_i \log q_i - \sum_i q_i \log q_i\right)$$

Using the definition of $\varphi(x)$ and Gibbs inequality:

$$\sum_i p_i \log p_i - \sum_i q_i \log q_i \geq \sum_i p_i \log q_i - \sum_i q_i \log q_i = 0$$

Applying Gibbs inequality:

$$\sum_i p_i \log p_i - \sum_i p_i \log q_i \geq \sum_i p_i \log p_i - \sum_i p_i \log p_i = 0$$

$$D(p \parallel q) = \sum_i p_i \log \frac{p_i}{q_i} \geq 0$$

The Kullback-Leibler divergence ensures a non-negative solution due to $D(p \parallel q) = 0 \implies \log \frac{p_i}{q_i} = \alpha \quad \forall p_i > 0$, where α is a constant. The summation of p_i and q_i are 1 therefore the unique solution is $p_i = q_i \quad \forall i$.

Proof of the Definition 7.2.4 If $\exists x\colon \quad p(y|x) \quad$ s.t. $p(y|x) = \delta_{y=y_0}$ is deterministic, and $H(p/y|x)) = 0$. Considering the deterministic

$$\forall x, \quad p(y|x) \implies H(Y|X) = 0$$

Proof of the Definition 7.2.5 Know that $I(X\colon Y) = 0$ if and only if X and Y are independent, by probability theory, $p(x, y) = p(x)p(y)$, then:

$$H(X, Y) = H(X)H(Y) \Rightarrow I(X\colon Y) = 0$$

Proof of the Definition 7.2.7 The Markov chain implies $p(x,\, y,\, z) = p(x)\, p(y|x)\, p(z|y)$. One can write the mutual information as:

$$I(X\colon Z) = H(Z) - H(Z|X)$$

$$I(X\colon Y) = H(Y) - H(Y|X)$$

By Markov chain $p(z|x,\, y))\, p(z|y) \implies H(Z|X) = H(Z|X,\, Y)$. Z is dependent on X via Y.

$$I(X\colon Z|Y) = 0$$

It is said that X, Z are conditional independent of Y. By the mutual condition rule:

$$I(X\colon Z) = I(X\colon Z|Y) + I(X\colon Y) - I(Z\colon Y|X)$$

Considering $I(X\colon Z|Y) = 0$:

$$I(X\colon Z) = I(X\colon Y) - [I(Z\colon Y|X) - I(Z\colon Y|X)]$$

$$I(X : Z) = H(Z) - H(Z|X) = H(Z) - H(Z|X,\, Y,\, X)$$

$$I(X : Y) - I(X : Z) = H(Y) + H(X) - H(X,\, Y) - [H(Z) + H(X) - H(X,\, Z)]$$

$$= H(Y) - H(Z) - H(X,\, Y) + H(X,\, Z)$$

Given $X \to Y \to Z$, it is shown that $H(X,\, Z) + H(Y) \leq H(X,\, Y) + H(Z)$ since $I(X\colon Z) \leq I(X\colon Y)$.

Appendix D

Quantum Database Example Use

This appendix presents an example of the use of the Quantum Database (qDB) in detail. This thesis has been aligned with the university's objectives regarding gender perspective. Therefore, a particular use case in data science has been selected that would be applicable both in sample balancing searches in datasets and in the particular detection of departments or organizations that have gender-segmented pay equality. Definitely, the objective that is raised once the quantum data is encoded and stored is to operate with them to solve: the detection of departments that comply with pay equality. To achieve this, the use of the qDB will be exemplified, as well as the quantum parallelization and superposition that can help optimize searches in large vector spaces or Hilbert spaces $\mathcal{H}$ in datasets will be illustrated.

The qDB as well as the quantum algorithms used to perform an operation, such as in this case, the Grover algorithm, are based on the structure of Hilbert spaces $\mathcal{H}$. When one talks about large vector spaces, they are also part of a larger space called the Hilbert space $\mathcal{H}$. As we have seen, these have inner product and complete vector spaces and are ideal for the representation of quantum states.

The quantum algorithms that can be applied make use of the Hilbert space $\mathcal{H}$ and generally take advantage of superposition and quantum entanglement to explore multiple possibilities simultaneously, such as Grover's algorithm. For this reason, the use of a qDB in the field of complexity makes it favourable compared to the classical way, since a classical algorithm, as the size of the vector space grows, does so exponentially because the complexity of classical algorithms increases linearly or polynomially.

The use of Hilbert spaces allows defining unitary operators such as U_{qDB}, which is essential for

encoding and operating with data in the qDB. Therefore, linearity and reversibility are obtained in the unitary operators in the Hilbert space $\mathcal{H}$. This is an important difference from classical usage, since a classical logic circuit does not have reversibility in operations. However, in the quantum format there is reversibility of states that are essential for the coherence of quantum calculations.

The qDB is not limited to large vector spaces or, in general, to Hilbert spaces of fixed dimension. The design is flexible and can admit other configurations as long as the properties that make the quantum states and properties viable are maintained. In essence, more dimensions can be defined as long as the Hilbert space that houses the necessary quantum properties is preserved.

In general terms, one could consider generating different Hilbert spaces $\mathcal{H}$ with encoded data similar to the classical partitioning of a classical database and, through the use of addressing, operate in all spaces in parallel with multiple objectives or the same objective in a multi-space partitioning. It is clear that the decisions of the data structures on the qDB make evident the design work of a data scientist, for example, to partition by features, which allow a better use of the quantum algorithms implemented in the qDB.

D.1 Problem Description

Consider a company that wants to analyse salary equity between various departments. The database contains salary information segregated by sex and department of the employees. The objective is to find which department meets the condition of salary equality between women and men.

In the table B.4 you can check the structure and specific simulated data of the database. It contains three columns:

- Man: with salary information per individual.
- Female: with salary information per individual.
- Department: numerical reference within the range $1 - 4$ corresponding to the department number.

Departments can be generalized to be numbered between 0 and $N - 1$, where N is the total number of departments. However, it is a mere notation that can be adapted to each particular use case.

D.2 Implementation of the Quantum Database (qDB)

The Quantum Database (qDB) is implemented using a query register and a database register, where each address is associated with a set of corresponding characteristics, therefore to data.

The quantum circuit A.10 has three main parts:

- Query register $\mathcal{H}_A$: the n-qubit register stores the queries or indexes of the departments.
- Database register $\mathcal{H}_D$: corresponds to the m-qubit register that stores the particular characteristics associated with each department, specifically, salary information.
- Auxiliary register: these are additional qubits used to implement operations and facilitate phase inversion for Grover's algorithm.

In general terms, the code implements the quantum and classical registers, for the example case:

- Quantum registers:
  - 2 qubits for queries `query_n`. There are only two since applying superposition we obtain $|00\rangle, |01\rangle, |10\rangle, |11\rangle$.
  - 12 qubits for Database register `database_n`. The database register stores the scaled salary characteristics of each department. Since each department has 6 people working, 3 women and 3 men, 6 qubits are associated with it; totaling 12 qubits for the 4 departments.
- Classical registers `c_n`: the states are collapsed and the measurements of the query qubits are stored in a pair of bits.

At the beginning of the quantum circuit, two Hadamard gates are applied to the query qubits to generate a uniform superposition of all possible addresses for each department. Then, the high-level quantum gate `QuantumDatabase` is used, which maps each query to its corresponding salary characteristics stored in the `database` register. The next step of the circuit is to apply the data processing gate `DataProcessor` that uses QFT to transform the stored data and prepare the `results` qubits for validation. Finally, the `DataValidator` gate is applied, which corresponds to

an oracle that in this particular case is Grover's algorithm that marks the solutions that meet the salary equality condition.

In the previous circuit, the inversion of the `DataProcessor` and `QuantumDatabase` gates must be performed to reverse the previous operations and prepare the circuit for amplitude amplification. Which leads to the last phase which is to apply the Grover diffusion operator that amplifies the amplitude of the marked solutions increasing the probability of measuring the correct address at the end of the circuit where a measurement of the `query` qubits is performed and stored in the `c_n` qubits.

D.3 Simulation

The simulation has been implemented on the Qiskit QASM backend with 1000 shots, which generates a probability distribution. As an example, the code in the classical part where the data is generated is forced to make the department with equal pay be department 3 which has an address 10. If the simulator is run, the distribution is obtained:

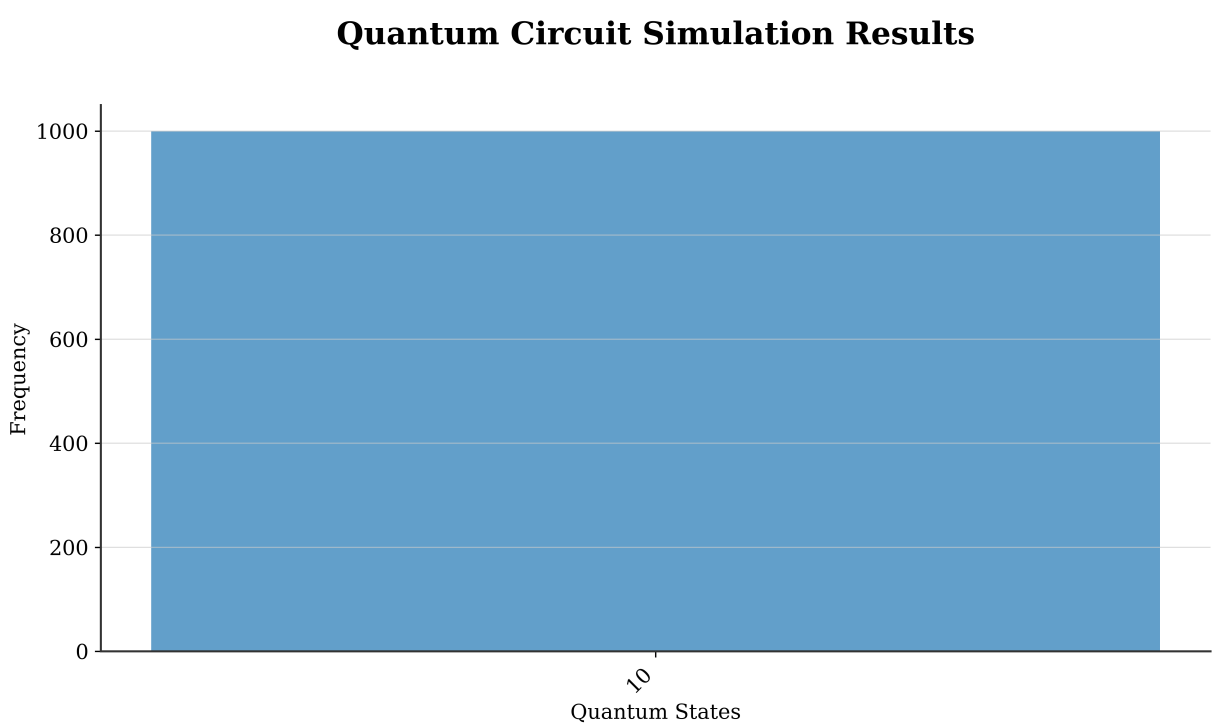

Figure D.1: Probability distribution where the correct solution is department 3 with coded address 10, and 1000 shots.

In the project, the flags `--equal_department` can be executed, which specifies the department

in which salary equality is forced in the composition of the classic dataset to validate the solution. Also the flags `--save` and `--no-save` can be used to indicate whether the image of the histogram is to be saved.

D.4 Breve Overview of Grover's Search

An overview of the operation of Grover's search algorithm is provided, which is a continuation of Shor's proposed algorithm. Although a light review of the algorithm has been carried out, several texts have been consulted that can help the reader to understand the algorithm in depth as well as a more formal and general approach. Refer to the text Vasconcelos, 2020, for a pedagogical approach; refer to Nielsen and Chuang, 2010, pp. 248–275, for a systematic review; and Grover, 1996, for the original paper.

Consider a space of $N = 2^n$ states $|x\rangle, \quad x \in \{0, \cdots, N-1\}$, where one wants to find the marked state $|x_s\rangle$ with a reduced number of queries to an oracle in $\mathcal{O}(\sqrt{N})$ steps.

The initial state is defined as a uniform superposition of all indices:

$$|\psi_0\rangle = H^{\otimes n} = \frac{1}{\sqrt{N}} \sum_{x=0}^{N-1} |x\rangle \tag{D.1}$$

The oracle is a black box which marks the target states if the desired condition is met. In particular, it adds a -1 phase to the marked states and leaves the rest unchanged:

$$\begin{cases} -|x\rangle, & x \in \{\text{solutions}\} \\ |x\rangle, & \text{else} \end{cases} \tag{D.2}$$

The diffusion operator $\mathcal{D}$ inverts the amplitudes with respect to their average. This means that it amplifies the amplitudes of the marked states while decreasing the amplitudes of the unmarked states. The diffusion operator is defined as $\mathcal{D} = 2|\psi_0\rangle\langle\psi_0| - I$.

The sequence $\mathcal{O}+\mathcal{D}$ above is repeated $\sim \frac{\pi}{4}\sqrt{N}$. The process is usually interpreted geometrically from a 2-dimensional subsphere generated by the uniform initial state $|\psi_0\rangle$ and a space representing the solution $|x_s\rangle$. It is understood that $|s\rangle$ corresponds to the marked state or the projection of the solution space and $\left|s^{\perp}\right\rangle$ the orthogonal submanifold to $|s\rangle$.

To illustrate, a single marked state is considered for simplicity, then $|\psi_0\rangle$ is decomposed as:

$$|\psi_0\rangle = \alpha\,|s\rangle + \beta\left|s^{\perp}\right\rangle, \quad \|\,|\psi_0\rangle\,\| = 1 \tag{D.3}$$

Typically, coefficients like $\alpha = \frac{1}{\sqrt{N}}$ and $\beta = \sqrt{\frac{N-1}{N}}$ are found in most texts. In the plane $\{|s\rangle, \left|s^{\perp}\right\rangle\}$, $\mathcal{O}$ reflects the component in $|s\rangle$ — sign change. Geometrically, it is a reflection of the amplitude of $\alpha, \alpha\,|s\rangle \implies -\alpha\,|s\rangle$.

The diffusion operator $\mathcal{D} = 2\,|\psi_0\rangle\,\langle\psi_0| - I$ reflects the current vector relative to the initial vector $|\psi_0\rangle$. This leads to an effective rotation in the plane $\{|s\rangle, \left|s^{\perp}\right\rangle\}$. That is, the oracle reflection rotates the current state by a certain angle around $\left|s^{\perp}\right\rangle$. The diffusion completes the rotation such that each iteration there is an angular increase of 2θ on the plane.

Note that the amplification for each of the iterations additionally rotates θ or 2θ bringing the state vector closer to $|s\rangle$. Note that $\sin\theta \approx \alpha = \frac{1}{\sqrt{N}}$ so that $\theta = \frac{1}{\sqrt{N}}$. If we consider k iterations, then we obtain that $k \approx \frac{\pi}{4\theta} \approx \frac{\pi}{4}\sqrt{N}$, consequently the probability of success is defined as $P_{\text{success}}(k) = \sin^2((2k+1)\frac{\theta}{2})$. With a maximum ~ 1 when $(2k+1)\frac{\theta}{2} \approx \frac{\pi}{2}$.

D.5 Breve Overview of Quantum Fourier Transformation

Again, this text has a special approach and is adapted to the particular case, so it would be advisable for the reader interested in understanding QFT in a rigorous manner to refer to the texts on which the author of the thesis has based himself. Consider consulting Nielsen and Chuang, 2010, pp. 216–234; for some early use case discoveries, see Deutsch, 1985; Peter Shor, 1994.

Quantum Fourier Transformation (QFT) is the quantum version of Discrete Fourier Transformation (DFT). QFT can be used for various purposes, such as in Shor's algorithm to detect periodicities and to take advantage of factorization properties. QFT transforms a state encoding amplitudes in the domain of $|x\rangle$ to the domain of frequencies $|k\rangle$.

Let $|x\rangle$ be a ground state with $x \in \{0, 1, \cdots, N-1\}$, and $N = 2^n$. QFT_N acts as:

$$\text{QFT}_N\,|x\rangle = \frac{1}{\sqrt{N}} \sum_{k=0}^{N-1} e^{2\pi i \frac{xk}{N}}\,|k\rangle\,, \tag{D.4}$$

where x, k are represented via $\log_2 N = n$-qubits.

Geometrically, QFT performs a redistribution of amplitudes and assigns complex phases that encode information about periodicities. To do this, it is based on a state $|x\rangle$ that represents a

position and is mapped to a superposition whose phases depend linearly on xk. In reality, QFT performs a global rotation in $\mathcal{H}$ by reorganizing the canonical basis $\{|0\rangle, \cdots, |N-1\rangle\}$ to the basis $\{|k\rangle\}$. The QFT phase allows the use of constructive and destructive interference on the complex plane. In the case of the proposed example, QFT acts as an adder that allows knowing when it is 0 that there is wage equality.

DFT requires $\mathcal{O}(N \log N)$ classical operations, while QFT is implemented in $\mathcal{O}((\log_2 N)^2) \equiv \mathcal{O}(n^2)$.

Appendix E

Fundamentals of Probability

This appendix provides a refresher on the fundamental concepts of probability theory, as they are important for understanding the probabilistic nature of quantum mechanics. For example, to understand the probability amplitude of a wave function or the Copenhagen interpretation proposed by Max Born, in the famous and relevant publication *Zur Quantenmechanik der Stoßvorgänge*, (Born, 1926).

The reader should expect a quick and concise review. For a detailed discussion of probability and statistics, the book *All of Statistics* (Wasserman, 2013) is recommended. For a focus on mechanical statistics, the book *Statistical Mechanics*, (Sethna, 2021) is recommended.

E.1 Basics

E.1.1 Sample Space

The set of all possible outcomes, $\Omega = \{\omega_1, \cdots, \omega_n\}$ of a random experiment is known as the sample space, Ω. Each individual element is called an elementary event.

E.1.2 Probability of an event

The probability of an event A is a number between 0 and 1. Determines the probability that the event occurs. The well-known Kolmogorov Axioms are:

Table E.1: Axioms of Probability, (Wasserman, 2013)

Axiom	**Expression**
Axiom 1	$\mathbb{P}(\Omega) = 1$
Axiom 2	$\mathbb{P}(A) \geq 0 \quad \forall A \subseteq \Omega$
Additivity	If A_n are mutually exclusive events, then $\mathbb{P}\left(\bigcup_{i=1}^{n} A_i\right) = \sum_{i=1}^{n} \mathbb{P}(A_i)$

E.2 Random Variables

A random variable (r.v.) is a function that maps $X\colon \Omega \to \mathbb{R}$ a real value to each outcome ω, (Wasserman, 2013). They are classified into r.v. discrete and continuous. Discrete r.v. takes a finite set of values, $X \in \{x_1, \cdots, x_n\}$. While continuous r.v. takes any value under an interval of real numbers, $X \in \mathbb{R}$.

E.2.1 Probability Function

For the discrete probability function, a probability is assigned to each possible value of X.

$$\mathbb{P}(X = x_i) = p_i, \quad \sum_i p_i = 1 \tag{E.1}$$

For a continuous probability function, it is described with a probability density function $f_x(x)$:

$$\mathbb{P}(a \leq X \leq b) = \int_a^b f_x(x)dx, \quad \int_{-\infty}^{\infty} f_x(x)dx = 1 \tag{E.2}$$

E.3 Cumulative Distribution Function (CDF)

The CDF of a r.v. X is:

$$F_X(x) = \mathbb{P}(X \leq x) \tag{E.3}$$

Recall that $F_X(-\infty) = 0$, $F_X(\infty) = 1$, and $F_X(x)$ it is an increasing function.

E.4 Expected Value

The expected value of a r.v. X is a measure of central tendency distribution:

$$\mathbb{E}[X] = \begin{cases} \sum_i x_i \mathbb{P}(X = x_i) & \text{if } X \text{ is discrete} \\ \int_{-\infty}^{\infty} x f_x(x) dx & \text{if } X \text{ is continuous} \end{cases} \tag{E.4}$$

E.4.1 Variance and Standard Deviation

The variance is the measure of dispersion of the values of X regarding their expectation:

$$\text{Var}(X) = \mathbb{E}[X^2] - (\mathbb{E}[X])^2 \tag{E.5}$$

The standard deviation is the square root of the variance:

$$\sigma_X = \sqrt{Var(X)} \tag{E.6}$$

E.4.2 Covariance and Correlation

The covariance is the measure of the lineal relation between two r.v. X, Y:

$$\text{Cov}(X, Y) = \mathbb{E}[(X - \mathbb{E}[X])(Y - \mathbb{E}[Y])] \tag{E.7}$$

The correlation coefficient is the normalized covariance over the range $\{-1, 1\}$:

$$\rho_{X,Y} = \frac{\text{Cov}(X, Y)}{\sigma_X \sigma_Y} \tag{E.8}$$

E.5 Independent Events

Let A and B be independent events if $\mathbb{P}(A \cap B) = \mathbb{P}(A)\mathbb{P}(B)$. Let X and Y independent r.v. if for all x and y: $\mathbb{P}(X \leq x, Y \leq y) = \mathbb{P}(X \leq x)\mathbb{P}(Y \leq y)$.

E.6 Common Probability Distributions

E.7 Moment Generating Function

The moment generating function of a r.v. X is (Ramachandran & Tsokos, 2015):

Table E.2: Common Probability Distributions

Distribution	**Formula**
Binomial	$\mathbb{P}(X = k) = \binom{n}{k} p^k (1-p)^{n-k}, \quad k = 0, 1, \ldots, n$
Normal (Gaussian)	$f_X(x) = \frac{1}{\sigma\sqrt{2\pi}} e^{-\frac{(x-\mu)^2}{2\sigma^2}}$
Poisson	$\mathbb{P}(X = k) = \frac{\lambda^k e^{-\lambda}}{k!}, \quad k = 0, 1, 2, \ldots$
Exponential	$f_X(x) = \lambda e^{-\lambda x}, \quad x \geq 0$

$$M_X(t) = \mathbb{E}[e^{tX}] = \int_{-\infty}^{+\infty} e^{tx} f_X(x)\, dx \quad \text{(continuous)} \tag{E.9}$$

$$M_X(t) = \mathbb{E}[e^{tX}] = \sum_k e^{tk} P(X = k) \quad \text{(discrete)} \tag{E.10}$$

E.8 Fourier Transform of the Wave Function

Based on the momentum distribution, the Fourier transform of $\Psi(x)$ is presented.

$$\Phi(p) = \frac{1}{\sqrt{2\pi\hbar}} \int_{-\infty}^{+\infty} e^{-ipx/\hbar} \Psi(x)\, dx \tag{E.11}$$

To compute the position probability density is used $|\Psi(x)|^2$, similarly to compute the momentum probability density is used $|\Phi(x)|^2$.

Appendix F

Formalisms of Quantum Mechanics

This appendix is intended to recall certain formalities of the framework of quantum mechanics. The purpose is to provide the non-specialist reader with a concise and summarized introduction to the fundamental concepts. Consequently, detailed derivations of formulae or rigorous axiomatics are beyond the scope of this section. For a book recommendation based on focus and target audience, the reader is referred to the section I.

F.1 Dirac notation

In Dirac or Bra-Ket notation, quantum states and operators are described in terms of: dual vector $\langle\phi|$, state vector $|\psi\rangle$, inner product $\langle\phi|\psi\rangle$ and operators $\hat{A}\,|\psi\rangle = |A\psi\rangle$. If $\psi \equiv |\psi\rangle$ then $\psi^* \equiv \langle\psi|$.

F.2 Axioms of quantum mechanics

In quantum mechanics, there are four main axioms: states, observables, time evolution, and measurement (Tong, 2021).

F.2.1 States

A pure state is denoted by $|\Psi\rangle$ and a mixed state is denoted by density matrices. The state vectors in the Hilbert space, $\mathcal{H}$, constitute a state.

F.2.2 Observables

It represents the measurable physical quantity and is represented by Hermitian operators in the space $\mathcal{H}$. An observable contains eigenvalues, a_n, and eigenvectors, $|a_n\rangle$, such that:

$$\hat{A}\,|a_n\rangle = a_n\,|a_n\rangle \tag{F.1}$$

F.2.3 Time Evolution

Time evolution in a quantum system is described by the Schrödinger equation, for a time-independent system:

$$i\hbar\frac{\partial}{\partial t}\,|\psi(t)\rangle = \hat{H}\,|\psi(t)\rangle \tag{F.2}$$

$\hat{H}$ is the Hamiltonian of the system.

F.2.4 Measurement

Performing a measurement in a state $|\psi\rangle$ produces an eigenvalue, a_n, and collapses the wave function into the state $|a_n\rangle$ with probability:

$$P(a_n) = |\langle a_n|\psi\rangle|^2 \tag{F.3}$$

F.3 Classical Mechanics vs. Quantum Mechanics

In classical mechanics, to know the position of a particle at a given time, $x(t)$, Newton's second law must be applied:

$$m\frac{d^2x}{dt^2} = -\frac{\partial V}{\partial x} \tag{F.4}$$

Due to the particularity of the wave-particle duality phenomenon in quantum mechanics, the wave function $\Psi(x,t)$ is used. The total energy Hamiltonian of a system is defined as the sum of the kinetic energy operators $\hat{T}$ and potential energy operators $\hat{V}$. Considering the momentum operator described as $\hat{p} = -i\hbar\nabla$ it is obtained:

$$\hat{H} = \frac{\hat{p}^2}{2m} + \hat{V}(x) = -\frac{\hbar^2}{2m}\nabla^2 + \hat{V}(x) \tag{F.5}$$

Therefore, the time-independent Schrödinger equation is obtained as:

$$\hat{H}\Psi(x) \equiv -\frac{\hbar^2}{2m}\nabla^2\Psi(x) + \hat{V}(x)\Psi(x) = E\Psi(x) \tag{F.6}$$

The possible wave functions that satisfy the equation F.6 is called eigenfunctions of the Hamiltonian:

$$\hat{H}\psi_n(x) = E_n\psi_n(x) \tag{F.7}$$

E_n is the nth energy level of the system.

F.4 Hermitian Operators

Any operator $\hat{A}$ is Hermitian if:

$$\hat{A}^\dagger = \hat{A} \tag{F.8}$$

F.5 Normalization of the Wave Function

The wave function is normalized to interpret $|\psi(x)|^2$ as a probability density. Therefore:

$$\int_{-\infty}^{+\infty} |\psi(x)|^2 dx = 1 \tag{F.9}$$

F.6 Orthonormality

Two functions are orthogonal if the inner product is zero:

$$\langle\psi_m|\psi_n\rangle = \int_{-\infty}^{+\infty} \psi_m^*\psi_n(x)dx = 0 \tag{F.10}$$

If $\langle\psi_n|\psi_n\rangle = 1$, then it is normalized. This is known as the Kronecker delta function:

$$\begin{aligned} \delta_{nm} &= 1 \quad \text{if n=m,} \\ &= 0 \quad \text{if n}\neq \text{ m.} \end{aligned} \tag{F.11}$$

F.7 States in Superposition

A quantum state can be a linear superposition of more states. Assume $|\phi\rangle$ and $|\chi\rangle$ are any two states, so it is described as:

$$|\psi\rangle = c_1 |\phi\rangle + c_2 |\chi\rangle \tag{F.12}$$

Note that the complex coefficients c_1 and c_2 are the probability amplitudes of the states and that by the above properties, performing the square module $|c_1|^2 + |c_2|^2 = 1$ gives the probability equal to one. The probability of any state with coefficient c_n will be the probability of performing a measurement and the wave function collapsing into the associated state.

F.8 Commutators

A commutator is defined as:

$$[\hat{A},\, \hat{B}] = \hat{A}\hat{B} - \hat{B}\hat{A} \tag{F.13}$$

Commutators are essential to understand the compatibility of observables. The reader will notice that they are essential in quantum mechanics and in particular in this thesis in relation to the Heisenberg principle, the relations to determine a good quantum number or in symmetries.

F.9 Angular Momentum

The angular momentum, $\hat{L}$, is composed of the orbital angular momentum and the spin angular momentum.

The orbital angular momentum is the motion of the particle around the origin with $x = (x, y, z)$(Tong, 2021):

$$\hat{L}_x = -i\hbar\left(y\frac{\partial}{\partial z} - z\frac{\partial}{\partial y}\right), \quad \hat{L}_y \quad = -i\hbar\left(z\frac{\partial}{\partial x} - x\frac{\partial}{\partial z}\right), \quad \hat{L}_z = -i\hbar\left(x\frac{\partial}{\partial y} - y\frac{\partial}{\partial x}\right) \tag{F.14}$$

Spin is the intrinsic degree of freedom of particles, with components:

$$\hat{S}_x, \quad \hat{S}_y, \quad \hat{S}_z \tag{F.15}$$

Table F.1: Quantum numbers and their allowed values

Quantum numbers	**Allowed values**
Orbital, l	$l = 0, 1, 2, \ldots$
Magnetic, m_l	$m_l = -l, -l+1, \ldots, l$
Spin, s	$s = \frac{1}{2}, 1, \ldots$
Magnetic spin, m_s	$m_s = -s, -s+1, \ldots, s$

The functions $Y_{lm}(\theta,\, \phi)$ are the spherical harmonics describing the angular distributions of the orbital angular momentum states (Fox, 2006).

The total angular momentum $\mathbf{J}$ quantized in quantum mechanics, important both for quantum mechanics and for direct application to quantum optical systems. The total angular momentum $\mathbf{J}$ considers both orbital and spin contributions.

Commutation relation using the Levi-Civita ϵ_{ijk}:

$$[J_i,\, J_j] = i\hbar\epsilon_{ijk}J_k, \qquad \Leftrightarrow \quad \mathbf{J}\times\mathbf{J} = i\hbar\mathbf{J}, \tag{F.16}$$

$$[J^2,\, J_i] = 0 \tag{F.17}$$

Ladder operator properties:

$$J_\pm = J_x \pm iJ_y, \quad (J_\pm)^\dagger = J_\mp, \tag{F.18}$$

$$[J_z,\, J_\pm] = \pm\hbar J_\pm, \tag{F.19}$$

$$[J_+,\, J_-] = 2\hbar J_z. \tag{F.20}$$

Expressing for $J^2 = J_x^2 + J_y^2 + J_z^2$ with ladder operator:

$$J^2 = J_+ J_- + J_z^2 - \hbar J_z, \tag{F.21}$$

$$J^2 = J_- J_+ + J_z^2 + \hbar J_z. \tag{F.22}$$

Eigenvalue of J^2 and J^z for a $|jm\rangle$ state:

$$J^2|jm\rangle = \hbar^2 j(j+1)|jm\rangle, \tag{F.23}$$

$$J_z|jm\rangle = \hbar m|jm\rangle, \quad m = -j, \ldots, j. \tag{F.24}$$

Ladder operator action:

$$J_\pm|jm\rangle = \hbar\sqrt{j(j+1) - m(m \pm 1)}|j, m \pm 1\rangle. \tag{F.25}$$

F.10 Eigenfunctions and Eigenvalues

The eigenvalues of physical observables are real, since the observable operators are hermitian. An eigenfunction $\psi_n(x)$ of an operator $\hat{A}$ satisfies:

$$\hat{A}\psi_n(x) = a_n\psi_n(x) \tag{F.26}$$

Rewriting in $N \times N$ matrix format, the eigenvalues can be found by solving the following equation, where up to N λ numbers can be obtained:

$$A\vec{u} = \lambda\vec{u} \tag{F.27}$$

The vector $\vec{u}$ is called an eigenvector. Similarly, it can be solved for an operator $\hat{O}$ for some function $\psi(x)$ (Tong, 2021).

F.11 Expected Value

The expected value of $\langle x \rangle$ is the mean value measured (Tipler, 2000) on an ensemble of identically prepared systems. It can be calculated as:

$$\int_{-\infty}^{+\infty} = x\,|\psi(x,t)|^2\,dx \tag{F.28}$$

In time-dependent format, it is rewritten as $\frac{d\langle x\rangle}{dt}$.

Appendix G

Fundamentals of Quantum Computing

Table G.1: Quantum Universal Gates

Gate	**Matrix Representation**
$-\boxed{H}-$	$H = \frac{1}{\sqrt{2}}\begin{pmatrix} 1 & 1 \\ 1 & -1 \end{pmatrix}$
$-\boxed{T}-$	$T = \begin{pmatrix} 1 & 0 \\ 0 & e^{i\pi/4} \end{pmatrix}$
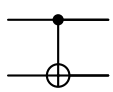	$CNOT = \begin{pmatrix} 1 & 0 & 0 & 0 \\ 0 & 1 & 0 & 0 \\ 0 & 0 & 0 & 1 \\ 0 & 0 & 1 & 0 \end{pmatrix}$

Table G.2: Quantum Gates and Matrix Representations

Gates	**Matrix Representation**
$-\boxed{X}-$	$X = \begin{pmatrix} 0 & 1 \\ 1 & 0 \end{pmatrix}$
$-\boxed{Y}-$	$Y = \begin{pmatrix} 0 & -i \\ i & 0 \end{pmatrix}$
$-\boxed{Z}-$	$Z = \begin{pmatrix} 1 & 0 \\ 0 & -1 \end{pmatrix}$

Continued on next page

Table G.2 – continued from previous page

Gates	**Matrix Representation**
$R_x(\theta)$	$R_x(\theta) = \begin{pmatrix} \cos\left(\frac{\theta}{2}\right) & -i\sin\left(\frac{\theta}{2}\right) \\ -i\sin\left(\frac{\theta}{2}\right) & \cos\left(\frac{\theta}{2}\right) \end{pmatrix}$
$R_y(\theta)$	$R_y(\theta) = \begin{pmatrix} \cos\left(\frac{\theta}{2}\right) & -\sin\left(\frac{\theta}{2}\right) \\ -\sin\left(\frac{\theta}{2}\right) & \cos\left(\frac{\theta}{2}\right) \end{pmatrix}$
R_φ	$R_\varphi = \begin{pmatrix} 1 & 0 \\ 0 & -e^{i\varphi} \end{pmatrix}$
S	$S = \begin{pmatrix} 1 & 0 \\ 0 & i \end{pmatrix}$
T	$T = \begin{pmatrix} 1 & 0 \\ 0 & e^{i\pi/4} \end{pmatrix}$
	$\text{SWAP} = \begin{pmatrix} 1 & 0 & 0 & 0 \\ 0 & 0 & 1 & 0 \\ 0 & 1 & 0 & 0 \\ 0 & 0 & 0 & 1 \end{pmatrix}$
H	$\text{Bell State} = \frac{1}{\sqrt{2}} \begin{pmatrix} 1 & 0 & 1 & 0 \\ 0 & 1 & 0 & 1 \\ 0 & 1 & 0 & -1 \\ 1 & 0 & -1 & 0 \end{pmatrix}$

Continued on next page

Table G.2 – continued from previous page

Gates	**Matrix Representation**
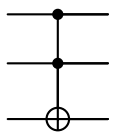	$\text{Toffoli} = \begin{pmatrix} 1 & 0 & 0 & 0 & 0 & 0 & 0 & 0 \\ 0 & 1 & 0 & 0 & 0 & 0 & 0 & 0 \\ 0 & 0 & 1 & 0 & 0 & 0 & 0 & 0 \\ 0 & 0 & 0 & 1 & 0 & 0 & 0 & 0 \\ 0 & 0 & 0 & 0 & 1 & 0 & 0 & 0 \\ 0 & 0 & 0 & 0 & 0 & 1 & 0 & 0 \\ 0 & 0 & 0 & 0 & 0 & 0 & 0 & 1 \\ 0 & 0 & 0 & 0 & 0 & 0 & 1 & 0 \end{pmatrix}$
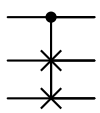	$\text{Fredkin} = \begin{pmatrix} 1 & 0 & 0 & 0 & 0 & 0 & 0 & 0 \\ 0 & 1 & 0 & 0 & 0 & 0 & 0 & 0 \\ 0 & 0 & 1 & 0 & 0 & 0 & 0 & 0 \\ 0 & 0 & 0 & 1 & 0 & 0 & 0 & 0 \\ 0 & 0 & 0 & 0 & 1 & 0 & 0 & 0 \\ 0 & 0 & 0 & 0 & 0 & 0 & 1 & 0 \\ 0 & 0 & 0 & 0 & 0 & 1 & 0 & 0 \\ 0 & 0 & 0 & 0 & 0 & 0 & 0 & 1 \end{pmatrix}$

Table G.3: Non-exhaustive Circuit Equivalences Precomputed

Circuit	**Equivalence**
HXH	Z
HZH	X
HYH	$-Y$
$H^\dagger$	$H^\dagger H = H^-1$
$X^2 = Y^2 = Z^2$	I
H	$(X+Z)/\sqrt{Z}$
H^2	I
$SWAP_{12}$	$C_{12}C_{21}C_{12}$

Appendix H

Fundamentals of Quantum Optics

This appendix is intended to recall formalities of quantum optics. The purpose is to provide the non-specialist reader with a concise and summarized introduction to the fundamental concepts.

Physics usually uses harmonic oscillators to describe a system. In the classic version, the restoring force is proportional to the displacement x as $F = -kx$. The motion follows Hooke's law (Griffiths & Schroeter, 2019, p. 39) By using the derivative of x, and considering the Newton's second law, one obtains the motion equation:

$$m\frac{d^2x}{dt^2} = -kx \tag{H.1}$$

It can be expressed in the form of a differential equation and use the angular frequency as:

$$\frac{d^2x}{dt^2} + \omega^2 x = 0, \quad \omega = \sqrt{\frac{k}{m}} \tag{H.2}$$

Consider A as the amplitude and ϕ as the initial phase; the general solution is:

$$x(t) = A\cos(\omega t + \phi) \tag{H.3}$$

The energy of the system can be computed as:

$$E = \frac{1}{2}mv^2 + \frac{1}{2}kx^2 = \frac{1}{2}m\omega^2 A^2 \tag{H.4}$$

The term $\frac{1}{2}mv^2$ is the kinetic energy, and the second term $\frac{1}{2}kx^2$ is the potential energy $V(x)$.

Energy is usually rewritten as:

$$E = \frac{p^2}{2m} + \frac{1}{2}m\omega^2 x^2 \tag{H.5}$$

To determine the quantum harmonic oscillator, the canonical commutation relation $[x, \hat{p}] = i\hbar$ is used to define the Hamiltonian by replacing the classical variables x and p:

$$\hat{H} = \frac{\hat{p}^2}{2m} + \frac{1}{2}m\omega^2 \hat{x}^2 \tag{H.6}$$

The harmonic oscillator potential is:

$$V(x) = \frac{1}{2}m\omega^2 x^2 \tag{H.7}$$

The Hamiltonian can be rewritten using the ladder operators[§]:

$$\hat{H} = \hbar\omega \left(\hat{a}^\dagger \hat{a} + \frac{1}{2}\right) \tag{H.8}$$

Energy can be written as:

$$E_n = \hbar\omega \left(n + \frac{1}{2}\right), \quad n = 1, 2, \cdots \tag{H.9}$$

Some important relations are:

$$\hat{x} = \sqrt{\frac{\hbar}{2m\omega}}(\hat{a} + \hat{a}^\dagger) = \frac{d(\hat{a} + \hat{a}^\dagger)}{\sqrt{2}}$$

Furthermore, ladder operators obey the canonical commutation relation:

$$[\hat{a}_{\mathbf{k},\lambda}, \hat{a}^\dagger_{\mathbf{k}',\lambda'}] = \delta_{\mathbf{k},\mathbf{k}'}\delta_{\lambda,\lambda'},$$

$$[\hat{a}_{\mathbf{k},\lambda}, \hat{a}_{\mathbf{k}',\lambda'}] = [\hat{a}^\dagger_{\mathbf{k},\lambda}, \hat{a}^\dagger_{\mathbf{k}',\lambda'}] = 0.$$

The state $|0\rangle$ is defined as:

$$\hat{a}_{\mathbf{k},\lambda}|0\rangle = 0$$

To represent n photons in the $(\mathbf{k}, \lambda)$ mode, one uses:

[§] $\hat{a}^\dagger = \sqrt{\frac{m\omega}{2\hbar}}\left(\hat{x} - i\frac{\hat{p}}{m\omega}\right)$: creation operator; $\hat{a} = \sqrt{\frac{m\omega}{2\hbar}}\left(\hat{x} + i\frac{\hat{p}}{m\omega}\right)$: annihilation operator. Recall $[\hat{a}, \hat{a}^\dagger] = 1$.

$$\hat{a}^{\dagger}_{\mathbf{k},\lambda}|n\rangle = \sqrt{n+1}|n+1\rangle$$

$$\hat{a}_{\mathbf{k},\lambda}|n\rangle = \sqrt{n}|n-1\rangle$$

Using the definition of the quantum harmonic oscillator, the electromagnetic field can be quantized based on the mode of the field. The electric field in the quantization field V can be written as:

$$\mathbf{E}(\mathbf{r},t) = \sum_{k,\lambda} \mathbf{E}_{\mathbf{k},\lambda} e^{i(\mathbf{k}\cdot\mathbf{r}-\omega_k t)} + c.c. \tag{H.10}$$

The term $\mathbf{E}_{\mathbf{k},\lambda}$ is the complex amplitude, the wave vector is represented by $\mathbf{k}$ defining the direction and the angular frequency associated to the mode $\mathbf{k}$ as $\omega_k = c|\mathbf{k}|$. A magnetic field, $\mathbf{B}$ it is related to $\mathbf{E}$ trough $\mathbf{B} = \nabla \times \mathbf{A}$, where $\mathbf{A}$ is the vector potential.

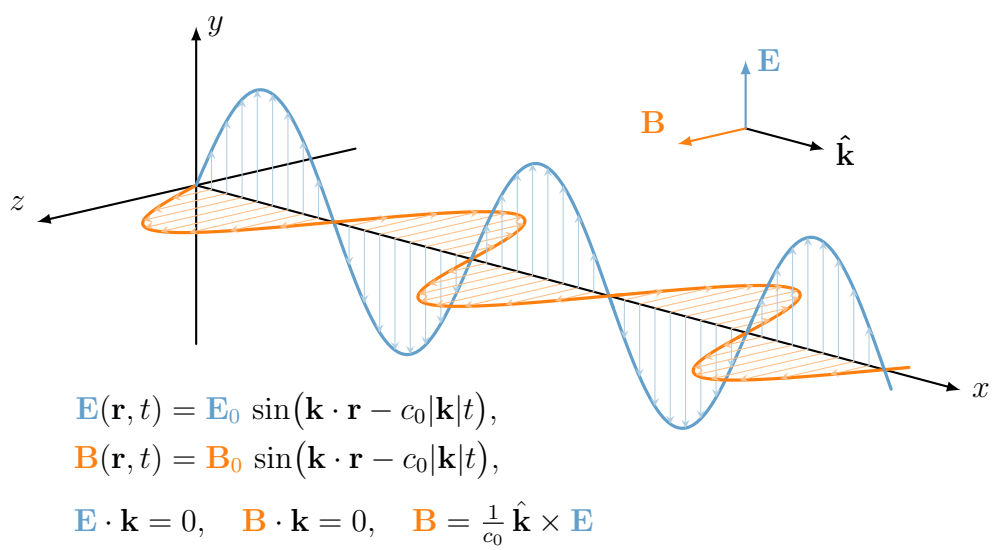

Figure H.1: Graphical representation of electromagnetic wave.

The quantum representation of the electric field can be written as:

$$\hat{\mathbf{E}}(\mathbf{r},t) = i\sum_{\mathbf{k},\lambda} \sqrt{\frac{\hbar\omega_k}{2\epsilon_0 V}} \left(\hat{a}_{\mathbf{k},\lambda}\mathbf{e}_{\mathbf{k},\lambda} e^{i(\mathbf{k}\cdot\mathbf{r}-\omega_k t)} - \hat{a}^{\dagger}_{\mathbf{k},\lambda}\mathbf{e}^{*}_{\mathbf{k},\lambda} e^{-i(\mathbf{k}\cdot\mathbf{r}-\omega_k t)}\right).$$

$\omega_k = c|\mathbf{k}|$ depends on $\mathbf{k}$ to determine the wavelength of the mode, and the modulus of $\mathbf{k}$ in a discrete mode in cavity is $|\mathbf{k}| = \frac{2\pi}{\mathbf{L}}$, where $\mathbf{L}$ is the dimension of the cavity. The angular frequency

§ *Licensed under a Creative Commons Attribution-ShareAlike 4.0 International License.*
© Copyright 2021 – TikZ.net. Adapted by Ricard Santiago Raigada García in 2024.

ω_k is related to the energy by $E_k = \hbar\omega_k$.

The dynamics of the electromagnetic field is described by Maxwell's equations (Fox, 2006, p. 10):

$$\nabla \cdot \mathbf{E} = \frac{\rho}{\epsilon_0}, \quad \nabla \cdot \mathbf{B} = 0,$$

$$\nabla \times \mathbf{E} = -\frac{\partial \mathbf{B}}{\partial t}, \quad \nabla \times \mathbf{B} = \mu_0 \mathbf{J} + \mu_0 \epsilon_0 \frac{\partial \mathbf{E}}{\partial t}.$$

The induced polarization in the quantum medium is quantized as $\hat{\mathbf{P}} = \epsilon_0 \chi^{(1)} \hat{\mathbf{E}}$, where $\chi^{(1)}$ is the linear electrical susceptibility of the first order. In non-linear mediums, includes terms that are non-linearly dependent on the field:

$$\mathbf{P} = \epsilon_0 \left(\chi^{(1)} \mathbf{E} + \chi^{(2)} \mathbf{E}^2 + \chi^{(3)} \mathbf{E}^3 + \dots \right) \tag{H.11}$$

The second harmonic generator is $\nabla^2 \mathbf{E}^{(2)} - \mu_0 \epsilon_0 \frac{\partial^2 \mathbf{E}^{(2)}}{\partial t^2} = -\mu_0 \frac{\partial^2 \mathbf{P}^{(2)}}{\partial t^2}$.

Appendix I

Recommended Readings

For those who want a more comprehensive approach, the following reading recommendation is made. As a starter text with a focus on quantum computing, Hidary, 2019 is recommended. It is a text that covers several important concepts in quantum mechanics such as superposition, entanglement, and reversibility. It introduces the formalisms of quantum computing in a simple way with a language accessible to data scientists or computer scientists. In the third part, you can find a compendium of mathematical tools with a focus on quantum computing.

For more advanced readers, *Quantum Computing and Quantum Information* is recommended (Nielsen & Chuang, 2010). This is the most important book and a pillar in advanced quantum computing courses. The reader can expect more technical language and much more specialized chapters; however, it is a fantastic text that covers all areas of interest in information and quantum computing. The language tends to have a focus on quantum computing, so it is still suitable for someone who has not taken formal courses in quantum mechanics.

For an audience coming from a formal education in physics and taking the first courses in quantum mechanics, *Física Cuántica* it is recommended (Del Río Carlos, 2017) —there is no international version. The reader will find an introduction to quantum phenomena and elementary quantum mechanics. In the third part of the book, applications to atoms and molecules are found. It is a long but highly didactic book. Normally used in the initial courses of quantum mechanics in physics faculties.

As an intermediate difficulty book, *Introduction to Quantum Mechanics* by Griffiths and Schroeter, 2019 is recommended. It is a book focused on quantum mechanics. It contains many exercises that can help the reader to validate his or her understanding. It is recommended to alternate the reading

with the following recommendation.

For those seeking a book to get to an advanced level in quantum physics and that contains applications that allow understanding much of the physics included in the theoretical part of this thesis, the great book *Mastering Quantum Mechanics* by Professor Barton Zwiebach of MIT is recommended (Zwiebach, 2022). It is a book that requires the reader to have a background in physics to be able to understand it. The reader will need to have knowledge of complex analysis. For those who need a completely specialized course from the beginning to the PhD level, *Complex Analysis* is recommended (Gamelin, 2003).

Appendix J

Glossary

A

Angular Frequency 32
Angular Momentum 17

B

Binomial Theorem 37
Borh's Magneton 22
Bose-Einstein Condensation 16

C

Coherence 25, 36
Collective Excited State 36
Collective Operators 40
Collective Spin-Wave State 44
Complexity theory 3
PSPACE 3
Coupling Spin-orbit Constant 19

D

Dark State 14, 35, 36
general 37, 38
simple 36
Data
Big Data 4, 6
data analysts 4
data science 6
data scientists 4
data security 6
de Broglie 30
Decoherence 25, 26, 28
rates 29
Definitions
π-pulse sequence 65
adjoint 50
amplitude damping quantum channel 60
anticommutator 50
antisymmetric 50
average fidelity of a gate 63
Bekenstein's Entropy Bound 59
binary entropy 56
Cauchy-Schwarz inequality 49
Choi-Jamiołkowski isomorphism 58
coded space 65
commutator 50
complex vector space 48
conditional entropy 56
data compression 57
data processing inequality 57
decoy state 61
density operator 53
depolarizing quantum channel 60
dimension 48
distinguishable 51
eavesdropping 61
eigenenergies 50
eigenvector 50
ensemble 52
entangled 52
entropic uncertainty relation 59
evolution 51
Fannes'inequality 57
fault tolerance threshold 64
fidelity 63
fidelity of a gate 63
first order error 65

gates 53
global phase 52
Helstrom Bound Theorem 51
Hermitian 50
Hilbert space 49
Holevo Bound 58
Holevo-Schumacher-Westmoreland 58
inner product space 49
joint entropy 57
Klein's inequality 57
Kullback-Leibler divergence 56
linear transformation 48
Maassen–Uffink entropic uncertainty 59
measurement 51
mixed state 53
multi-qubit tomography 64
norm 49
normalized 49
orthonormal basis 49
Pauli matrices 50
phase shift channel 60
PNS attack 61
Positive Operator-Valued Measure 52
projective measurement 51
pure state 53
pure states 49
purification 54
quantum channel 52
quantum database 66
quantum relative entropy 57
quantum state 51
quantum state tomography 63
qubit 49
randomized benchmarking 63
Schmidt decomposition 54
Shannon entropy 56
stabilizer code 65
strong subadditivity 57
surface code 64
syndrome 65
trace 50
transverse quantum gate 64
unit vector 49
unitary 50
unitary operator 52
vector 48
von Neumann entropy 57
Wiener-Khinchine 60
Definitionscompletely positive trace-preserving CPTP 52
Degeneracy 21
Detuning 33
Dipolar Magnetic Interaction Constant 19
Dipolar Momentum Operator 39
Dipole Moment 15
Dirac Equation 17
Dirac Notation 15
Dissipation 28
Doppler Cooling 17
Duan-Lukin-Cirac-Zoller memories 44

E

Electric Quadrupolar Interaction 20
Electric Quadrupole Interaction 20
Electromagnetic Field 33
Electromagnetically Induced Transparency 14, 26, 35
Electron Magnetic Moment 19, 22
Energy Correction 22
Error Correction 25
Excited State 15
External Magnetic Field 21

F

Fast Oscillations 33, 39
Fine Structure 18, 22
Fock States 61

G

Ground State 15

H

Hessian matrix 44

I

Internal Magnetic Field 21

K

Kinetic Evolution 39

L

L-BFGS-B 44
Ladder Operators 31, 37
Landé Factor 21
Lindblad Equation 28
Luminous States 35

M

Machine Learning 4
quantum machine learning 5
Magnetic Angular Momentum 19
Magnetic Dipole Interaction 20
Maxwell-Bloch Equaqtion 46
Mixing Angles 35, 37
lambda 38

N

NISQ 3
Quantum hybrid approach 3

O

Open Quantum System 26, 28

P

Perturbation Theory 21
Perturbed Hamiltonian 33
Polariton 42
Polarization Vector 32, 33
Potential 18, 19

Q

Quantization Volume 32
Quantum Channels 59
Quantum Defect Theory 18
Quantum Key Distribution 1, 55
amplified spontaneous emission (ASE) 4
optical amplifier 4
optical fiber 4
passive eavesdropping 4
satellite-based QKD 3
Shor's algorithm 4
Quantum Mechanics
quantum communication 25
Quantum mechanics 1
quantum communication 6
quantum computing 1
Quantum database 4
quantum entanglement 2
quantum supremacy 2
superposition 2
Quantum Memory
quantum database 42
Quantum memory 1
quantum database 1
Quantum Numbers 17
Quantum state 2
Quantum System 24
QuTIP 44

R

Rabi Frequencies 15, 35
Rabi Frequency 29, 38
vacuum 38
Radioactive Decay 35
Refractive Index 15
Rotating Wave Approximation 27, 29, 33, 34, 39
Rubidium 16
Rydberg Blockade 46

S

Schrödinger Equation 34
Slow Envelope Operator 39
Spin-orbit Coupling 17
Spontaneous Raman Scattering 45
Symmetric Collective State 44

T

Total Angular Momentum 19, 21
Total Magnetic Moment 21

U

Unperturbed Hamiltonian 33

W

Writing Beam 45

Z

Zeeman Effect 21
strong 22
weak 21

Bibliography

Acharya, R., Aghababaie-Beni, L., Aleiner, I., Andersen, T. I., Ansmann, M., Arute, F., Arya, K., Asfaw, A., Astrakhantsev, N., Atalaya, J., Babbush, R., Bacon, D., Ballard, B., Bardin, J. C., Bausch, J., Bengtsson, A., Bilmes, A., Blackwell, S., Boixo, S., … Zobrist, N. (2024). Quantum error correction below the surface code threshold. https://arxiv.org/abs/2408.13687v1

Aharonov, D., & Ben-Or, M. (1999). Fault-Tolerant Quantum Computation With Constant Error Rate. *SIAM Journal on Computing*, *38*(4), 1207–1282. https://doi.org/10.1137/S0097539799359385

Alexander Semenovich, H. (1979). *On Capacity of a Quantum Communications Channel* (tech. rep.). Problems of Inf. Transm.

Anderson, M. H., Ensher, J. R., Matthews, M. R., Wieman, C. E., & Cornell, E. A. (1995). Observation of Bose-Einstein condensation in a dilute atomic vapor. *Science*, *269*(5221), 198–201. https://doi.org/10.1126/SCIENCE.269.5221.198

Bekenstein, J. D. (1981). Universal upper bound on the entropy-to-energy ratio for bounded systems. *Physical Review D*, *23*(2), 287–298. https://doi.org/10.1103/PhysRevD.23.287

Bennett, C. H., & Brassard, G. (2014). Quantum cryptography: Public key distribution and coin tossing. *Theoretical Computer Science*, *560*, 7–11. https://doi.org/10.1016/j.tcs.2014.05.025

Berta, M., Christandl, M., Colbeck, R., Renes, J. M., & Renner, R. (2009). The Uncertainty Principle in the Presence of Quantum Memory. *Nature Physics*, *6*(9), 659–662. https://doi.org/10.1038/nphys1734

Biercuk, M. J., Doherty, A. C., & Uys, H. (2010). Dynamical decoupling sequence construction as a filter-design problem. *Journal of Physics B: Atomic, Molecular and Optical Physics*, *44*(15). https://doi.org/10.1088/0953-4075/44/15/154002

Bloch, F. (1946). Nuclear Induction. *Physical Review*, *70*(7-8), 460–474. https://doi.org/10.1103/PhysRev.70.460

Boller, K. J., Imamolu, A., & Harris, S. E. (1991). Observation of electromagnetically induced transparency. *Physical Review Letters*, *66*(20), 2593. https://doi.org/10.1103/PhysRevLett.66.2593

Born, M. (1926). Zur Quantenmechanik der Stoßvorgänge. *Zeitschrift für Physik*, *37*(12), 863–867. https://doi.org/10.1007/BF01397477/METRICS

Brown, G., Carlyle, M., Salmerón, J., & Wood, R. (2006). Defending Critical Infrastructure. *Interfaces*, *36*, 530–544. https://doi.org/10.1287/inte.1060.0252

Brown University. (2010, October). *Hyperfine Structure of Rubidium* (tech. rep.). https://advlabs.aapt.org/wiki/File%3A2370

Brunton, S. L., & Kutz, J. N. (2022). Data-driven science and engineering : machine learning, dynamical systems, and control, 590. https://books.google.com/books/about/Data_Driven_Science_and_Engineering.html?hl=es&id=rxNkEAAAQBAJ

Campbell, L., & Garnett, G. (1882). *The life of James Clerk Maxwell* (2nd ed.). Macmillan; Co.

Charles Galton, D. (1927, July). *The Electron as a Vector Wave* (Vol. 116). Proceedings of the Royal Society of London. Series A, Containing Papers of a Mathematical; Physical Character. https://royalsocietypublishing.org/doi/pdf/10.1098/rspa.1927.0134

Chrapkiewicz, R., Wasilewski, W., & Radzewicz, C. (2014). How to measure diffusional decoherence in multimode rubidium vapor memories? *Optics Communications*, *317*, 1–6. https://doi.org/10.1016/J.OPTCOM.2013.12.020

Chuang, I. L., & Nielsen, M. A. (1996). Prescription for experimental determination of the dynamics of a quantum black box. *Journal of Modern Optics*, *44-11*(12), 2455–2467. https://doi.org/10.1080/09500349708231894

Del Río Carlos, S. (2017, April). *Física cuántica*. Comercial Grupo ANAYA, S.A.

Deutsch, D. (1985). Quantum theory, the Church–Turing principle and the universal quantum computer. *Proceedings of the Royal Society of London. A. Mathematical and Physical Sciences*, *400*(1818), 97–117. https://doi.org/10.1098/RSPA.1985.0070

Deutsch, D. (1983). Uncertainty in Quantum Measurements. *Physical Review Letters*, *50*(9), 631–633. https://doi.org/10.1103/PhysRevLett.50.631

Ding, Y., & Chong, F. T. (2020a). *Quantum Computer Systems*. Springer International Publishing. https://doi.org/10.1007/978-3-031-01765-0

Ding, Y., & Chong, F. T. (2020b). Quantum Computer Systems: Research for Noisy Intermediate-Scale Quantum Computers. *Synthesis Lectures on Computer Architecture*, *15*(2), 1–227. https://doi.org/10.2200/s01014ed1v01y202005cac051

Dirac, P. A. M., & Fowler, R. H. (1928). The quantum theory of the electron. *Proceedings of the Royal Society of London. Series A, Containing Papers of a Mathematical and Physical Character*, *117*(778), 610–624. https://doi.org/10.1098/rspa.1928.0023

Duan, L.-M., Lukin, M., Cirac, I., & Zoller, P. (2001). Long-distance quantum communication with atomic ensembles and linear optics. *Nature*, *414*(6862), 413–418. https://doi.org/10.1038/35106500

Einstein, A. (2011). *The ultimate quotable Einstein* (A. Calaprice, Ed.). Princeton University Press. https://doi.org/doi.org/10.1515/9781400835966

Fannes, M. (1973). A continuity property of the entropy density for spin lattice systems. *Communications in Mathematical Physics*, *31*(4), 291–294. https://doi.org/10.1007/BF01646490/METRICS

Fleischhauer, M., & Lukin, M. D. (2000). Dark-State Polaritons in Electromagnetically Induced Transparency. *Physical Review Letters*, *84*(22), 5094–5097. https://doi.org/10.1103/PhysRevLett.84.5094

Fleischhauer, M., & Lukin, M. D. (2002). Quantum memory for photons: Dark-state polaritons. *Physical Review A*, *65*(2), 022314. https://doi.org/10.1103/PhysRevA.65.022314

Fleischhauer, M., Imamoglu, A., & Marangos, P. J. (2005). Electromagnetically induced transparency. *Reviews of Modern Physics*, *77*(2), 633–673. https://doi.org/https://doi.org/10.1103/RevModPhys.77.633

Fox, M. (2006, October). *Quantum Optics: An Introduction*.

Fuchs, C. A. (1997). Nonorthogonal Quantum States Maximize Classical Information Capacity. *Physical Review Letters*, *79*(6),

1162–1165. https://doi.org/10.1103/PhysRevLett.79.1162

Gamelin, T. (2003, November). *Complex analysis*. Springer Science & Business Media.

Glisic, S. G., & Lorenzo, B. (2022, April). *Artificial Intelligence and Quantum Computing for Advanced Wireless Networks*. John Wiley & Sons.

Gottesman, D. (1997a). A Theory of Fault-Tolerant Quantum Computation. *Physical Review A - Atomic, Molecular, and Optical Physics*, *57*(1), 127–137. https://doi.org/10.1103/PhysRevA.57.127

Gottesman, D. (1997b). Stabilizer Codes and Quantum Error Correction. https://arxiv.org/abs/quant-ph/9705052v1

Griffiths, D. J., & Schroeter, D. F. (2019, November). *Introduction to Quantum Mechanics*. Cambridge University Press.

Grover, L. K. (1996). A fast quantum mechanical algorithm for database search. *Proceedings of the Annual ACM Symposium on Theory of Computing*, *Part F129452*, 212–219. https://doi.org/10.1145/237814.237866

Haapasalo, E. (2021). The Choi–Jamiołkowski isomorphism and covariant quantum channels. *Quantum Studies: Mathematics and Foundations*, *8*(3), 351–373. https://doi.org/10.1007/S40509-021-00249-7/METRICS

Hammerer, K., Sørensen, A. S., & Polzik, E. S. (2010). Quantum interface between light and atomic ensembles. *Reviews of Modern Physics*, *82*(2), 1041–1093. https://doi.org/10.1103/REVMODPHYS.82.1041/FIGURES/21/MEDIUM

Harris, S. E. (1989). Lasers without inversion: Interference of lifetime-broadened resonances. *Physical Review Letters*, *62*(9), 1033. https://doi.org/10.1103/PhysRevLett.62.1033

Hausladen, P., Jozsa, R., Schumacher, B., Westmoreland, M., & Wootters, W. K. (1996). Classical information capacity of a quantum channel. *Physical Review A*, *54*(3), 1869–1876. https://doi.org/10.1103/PhysRevA.54.1869

Hidary, J. D. (2019). *Quantum Computing: An Applied Approach* (2nd ed.). Springer International Publishing. https://doi.org/10.1007/978-3-030-23922-0

Holevo, A. S. (1973). Statistical problems in quantum physics, 104–119. https://doi.org/10.1007/BFB0061483

Holevo, A. S. (1998). The capacity of the quantum channel with general signal states. *IEEE Transactions on Information Theory*, *44*(1), 269–273. https://doi.org/10.1109/18.651037

Holloway, C. L., Simons, M. T., & Gordon, J. A. (2016). Simultaneous Use of Cs and Rb Rydberg Atoms for Dipole Moment Assessment and RF Electric Field Measurements via Electromagnetically Induced Transparency. https://doi.org/10.1063/1.4963106

IBM Quantum. (2024). *Development & Innovation Roadmap* (tech. rep.). https://ibm.com/quantum/assets/IBM_Quantum_Developmen_ & _Innovation_Roadmap_Explainer_2024-Update.pdf

James P, G. (1964). Noise at optical frequencies; information theory. *Quantum Electronics and Coherent Light, Proceedings of the International School of Physics 'Enrico Fermi' XXXI, Academic Press, New York*.

Jaynes, E. T., & Cummings, F. W. (1962). Comparison of quantum and semiclassical radiation theories with application to the beam maser. *Proceedings of the IEEE*,

51(1), 89–109. https://doi.org/10.1109/PROC.1963.1664

Jiang, M., Luo, S., & Fu, S. (2013). Channel-state duality. *Physical Review A*, *87*(2). https://doi.org/10.1103/PhysRevA.87.022310

Jozsa, R. (1994). Fidelity for Mixed Quantum States. *Journal of Modern Optics*, *41*(12), 2315–2323. https://doi.org/10.1080/09500349414552171

Kaku, M. (2024, April). *Quantum supremacy*. Vintage.

King, C., & Ruskai, M. B. (1999). Minimal Entropy of States Emerging from Noisy Quantum Channels. *IEEE Transactions on Information Theory*, *47*(1), 192–209. https://doi.org/10.1109/18.904522

Kitaev, A. Y. (1997). Fault-tolerant quantum computation by anyons. *Annals of Physics*, *303*(1), 2–30. https://doi.org/10.1016/S0003-4916(02)00018-0

Knill, E., Leibfried, D., Reichle, R., Britton, J., Blakestad, R. B., Jost, J. D., Langer, C., Ozeri, R., Seidelin, S., & Wineland, D. J. (2007). Randomized Benchmarking of Quantum Gates. *Physical Review A - Atomic, Molecular, and Optical Physics*, *77*(1). https://doi.org/10.1103/PhysRevA.77.012307

Kraus, K. (1987). Complementary observables and uncertainty relations. *Physical Review D*, *35*(10), 3070–3075. https://doi.org/10.1103/PhysRevD.35.3070

Kullback, S., & Leibler, R. A. (1951). On Information and Sufficiency. *The Annals of Mathematical Statistics*, *22*(1), 79–86. https://doi.org/10.1214/aoms/1177729694

Kunczik, L. (2022, April). *Reinforcement Learning with Hybrid Quantum Approximation in the NISQ Context*. Springer Nature.

Lambropoulos, P., & Petrosyan, D. (2007). *Fundamentals of quantum optics and quantum information*. Springer Berlin Heidelberg. https://doi.org/10.1007/978-3-540-34572-5

Legendre, P. (1993). Spatial Autocorrelation: Trouble or New Paradigm? *Ecology*, *74*(6), 1659–1673. https://doi.org/10.2307/1939924

Li, C., Zhu, X., Zhao, J., Zhang, L., Jia, S., & Feng, Z. (2009). High sensitivity spectroscopy of cesium Rydberg atoms using electromagnetically induced transparency. *Optics Express, Vol. 17, Issue 18, pp. 15821-15826*, *17*(18), 15821–15826. https://doi.org/10.1364/OE.17.015821

Lieb, E. H. (1973). Convex trace functions and the Wigner-Yanase-Dyson conjecture. *Advances in Mathematics*, *11*(3), 267–288. https://doi.org/10.1016/0001-8708(73)90011-X

Lieb, E. H., & Ruskai, M. B. (1973). A Fundamental Property of Quantum-Mechanical Entropy. *Physical Review Letters*, *30*(10), 434–436. https://doi.org/10.1103/PhysRevLett.30.434

Lieb, E. H., & Ruskai, M. B. (2002). Proof of the strong subadditivity of quantum-mechanical entropy. *Inequalities*, 63–66. https://doi.org/10.1007/978-3-642-55925-9{_}6

Likharev, O. K. (2024). *Essential Graduate Physics-Quantum Mechanics* (tech. rep.). https://LibreTexts.org

Lindblad, G. (1975). Completely positive maps and entropy inequalities. *Communications in Mathematical Physics*, *40*(2), 147–151. https://doi.org/10.1007/BF01609396/METRICS

Lloyd, S. (2011, April). *Programming the universe*. Random House.

Lo, H.-K., Ma, X., & Chen, K. (2004). Decoy State Quantum Key Distribution. *Physical Review Letters*, *94*(23). https://doi.org/10.1103/PhysRevLett.94.230504

Lukin, M. D., Yelin, S. F., & Fleischhauer, M. (2000). Entanglement of Atomic Ensembles by Trapping Correlated Photon States. *Physical Review Letters*, *84*(18), 4232. https://doi.org/10.1103/PhysRevLett.84.4232

Lütkenhaus, N., & Jahma, M. (2002). Quantum key distribution with realistic states:photon-number statistics in the photon-number splitting attack. *New Journal of Physics*, *4*(1), 44. https://doi.org/10.1088/1367-2630/4/1/344

Maassen, H., & Uffink, J. B. (1988). Generalized entropic uncertainty relations. *Physical Review Letters*, *60*(12), 1103–1106. https://doi.org/10.1103/PhysRevLett.60.1103

Manchaiah, D., Kumar, R., & Easwaran, R. K. (2022). A theoretical analysis on quantum memory parameters in ultracold 87 Rb and 133 Cs alkali species using EIT protocol in the presence of structured light. *Quantum Information Processing*, *21*(3), 1–19. https://doi.org/10.1007/S11128-022-03449-1/METRICS

Massachusetts Institute of Technology. (2024a). Practical Realities of Quantum Computation and Quantum Communication. https://xpro.mit.edu/programs/program-v1:xPRO+QCR/

Massachusetts Institute of Technology. (2024b). Requirements for Large-Scale Universal Quantum Computation. https://xpro.mit.edu/programs/program-v1:xPRO+QCR/

Nielsen, M. A., & Chuang, I. L. (2010, April). *Quantum Computation and Quantum Information*. Cambridge University Press.

Pauli, W. (1927). Zur Quantenmechanik des magnetischen Elektrons. *Zeitschrift für Physik*, *43*(9-10), 601–623. https://doi.org/10.1007/BF01397326/METRICS

Peter Shor. (1994). Algorithms for Quantum Computation: Discrete Log and Factoring. *Proc. 35th Annual Symposium on Foundations of Computer Science*. https://doi.org/DOI:10.1109/sfcs.1994.3657004,69,121

Preskill, J. (2022). Quantum Information Chapter 10. Quantum Shannon Theory. Course Information for Physics 219/Computer Science 219 Quantum Computation Instituto Tecnológico de California. http://www.theory.caltech.edu/people/preskill/ph219/

Puri, R. R. (2001). Atom-Field Interaction Hamiltonians, 137–153. https://doi.org/10.1007/978-3-540-44953-9{_}7

Raigada García, R. S. (2024a). Optimizing quantum circuits for efficient execution on superconducting hardware: a case study of the Cuccaro adder. https://openaccess.uoc.edu/handle/10609/150164

Raigada García, R. S. (2024b). Explaining the paper: quantum error correction below the surface code threshold. https://openaccess.uoc.edu/handle/10609/151207

Raigada García, R. S. (2024c). Perturbative Corrections for the Anharmonic Oscillator. https://openaccess.uoc.edu/handle/10609/151513

Raigada García, R. S. (2024d). Time-independent perturbation theory applied to a spin-1/2 particle. https://openaccess.uoc.edu/handle/10609/151512

Raigada García, R. S. (2024e, December). Quantum Data Scientist: The New Role of the 21st Century. https://www.computer.

org / publications / tech - news / trends / quantum-data-scientist/

Ramachandran, K. M., & Tsokos, C. P. (2015). Basic Concepts from Probability Theory. *Mathematical Statistics with Applications in R*, 53–109. https://doi.org/10.1016/B978-0-12-417113-8.00002-3

S. Malinovsky, V., & R. Berman, P. (2011). *Principles of Laser Spectroscopy and Quantum Optics*. Princeton University Press. https://doi.org/10.1515/9781400837045-007

Saksida, P. (2005). *Maxwell-Bloch equations, C. Neumann system, and Kaluza-Klein theory* (tech. rep.).

Salgado, D., Sánchez-Gómez, J. L., & Ferrero, M. (2004). A simple proof of the Jamiolkowski criterion for complete positivity of linear maps. *Open Systems and Information Dynamics*, *12*(1), 55–64. https://doi.org/10.1007/s11080-005-0486-2

Sangouard, N., Simon, C., De Riedmatten, H., & Gisin, N. (2009). Quantum repeaters based on atomic ensembles and linear optics. *Reviews of Modern Physics*, *83*(1), 33–80. https://doi.org/10.1103/RevModPhys.83.33

Sazonov, S. V. (2017). On the approximations of slowly varying envelope and slowly varying profile in nonlinear optics. *Journal of Physics: Conference Series*, *859*(1), 012015. https://doi.org/10.1088/1742-6596/859/1/012015

Schumacher, B., Westmoreland, M., & Wootters, W. K. (1996). Limitation on the Amount of Accessible Information in a Quantum Channel. *Physical Review Letters*, *76*(18), 3452–3455. https://doi.org/10.1103/PhysRevLett.76.3452

Schumacher, B., & Westmoreland, M. D. (1997). Sending classical information via noisy quantum channels. *Physical Review A*, *56*(1), 131–138. https://doi.org/10.1103/PhysRevA.56.131

Scully, M. O., & Zubairy, M. S. (1997, November). *Quantum Optics*. Cambridge University Press.

Sethna, J. P. (2021, November). *Statistical Mechanics: Entropy, Order Parameters, and Complexity*. Oxford University Press, USA.

Shannon, C. E. (1948, October). *A Mathematical Theory of Communication* (tech. rep.).

Shor, P. W. (1997). Polynomial-Time Algorithms for Prime Factorization and Discrete Logarithms on a Quantum Computer. *SIAM Journal on Computing*, *26*(5), 1484–1509. https://doi.org/10.1137/s0097539795293172

Silver, D., Huang, A., Maddison, C. J., Guez, A., Sifre, L., van den Driessche, G., Schrittwieser, J., Antonoglou, I., Panneershelvam, V., Lanctot, M., Dieleman, S., Grewe, D., Nham, J., Kalchbrenner, N., Sutskever, I., Lillicrap, T., Leach, M., Kavukcuoglu, K., Graepel, T., & Hassabis, D. (2016). Mastering the game of Go with deep neural networks and tree search. *Nature*, *529*(7587), 484–489. https://doi.org/10.1038/nature16961

Silver, D., Schrittwieser, J., Simonyan, K., Antonoglou, I., Huang, A., Guez, A., Hubert, T., Baker, L., Lai, M., Bolton, A., Chen, Y., Lillicrap, T., Hui, F., Sifre, L., van den Driessche, G., Graepel, T., & Hassabis, D. (2017). Mastering the game of Go without human knowledge. *Nature*, *550*(7676), 354–359. https://doi.org/10.1038/nature24270

Steck, D. A. (2001). *Rubidium 87 D Line Data* (tech. rep.). http://steck.us/alkalidata,

Stone, J. (2015, April). *Information theory*. Sebtel Press.

Tipler, P. (2000, April). *Física Moderna (6a. ed.)*.

Tong, D. (2021). Quantum Mechanics: The Formalism of Quantum Mechanics. https://www.damtp.cam.ac.uk/user/tong/qm/qmhtml/S3.html

Trabesinger, A. (2012). Quantum simulation. *Nature Physics*, *8*(4), 263. https://doi.org/10.1038/nphys2258

UChicago. (2024). Professional Certificate in Quantum Computer Systems Design. https://www.edx.org/certificates/professional-certificate/uchicagox-quantum-computer-systems-design

Umegaki, H. (1962). Conditional expectation in an operator algebra. IV. Entropy and information. *Kodai Mathematical Seminar Reports*, *14*(2), 59–85. https://doi.org/10.2996/kmj/1138844604

Vahala, K. (2004, November). *Optical microcavities*. World Scientific.

Valencia, A. M. (2024). Michio Kaku: "Pensamos que la inteligencia es saber cosas, pero la esencia de la inteligencia es ver el futuro". https://www.bbc.com/mundo/articles/c4njwdqelzwo

Vasconcelos, F. (2020). *Introduction to Quantum Computing Lecture 6: Shor's and Grover's Algorithms* (tech. rep.). https://stellar.mit.edu/S/course/6/ia20/6.S089/materials.html

Viola, L., & Lloyd, S. (1998). Dynamical suppression of decoherence in two-state quantum systems. *Physical Review A - Atomic, Molecular, and Optical Physics*, *58*(4), 2733–2744. https://doi.org/10.1103/PhysRevA.58.2733

Warwick, A. (2003, December). *Masters of Theory*. University of Chicago Press.

Wasserman, L. (2013, November). *All of Statistics*. Springer Science & Business Media.

Wehrl, A. (1978). General properties of entropy. *Reviews of Modern Physics*, *50*(2), 221–260. https://doi.org/10.1103/RevModPhys.50.221

Wiener, N. (1930). Generalized harmonic analysis. *https://doi.org/10.1007/BF02546511*, *55*(none), 117–258. https://doi.org/10.1007/BF02546511

Wittek, P. (2014, August). *Quantum Machine Learning: What Quantum Computing Means to Data Mining*. Elsevier. https://doi.org/10.1016/C2013-0-19170-2

Wootters, W. K., & Zurek, W. H. (1982). A single quantum cannot be cloned. *Nature 1982 299:5886*, *299*(5886), 802–803. https://doi.org/10.1038/299802a0

Xue, Y., Jiao, Y., Jiao, Y., Hao, L., Zhao, J., & Zhao, J. (2021). Microwave two-photon spectroscopy of cesium Rydberg atoms. *Optics Express, Vol. 29, Issue 26, pp. 43827-43835*, *29*(26), 43827–43835. https://doi.org/10.1364/OE.442703

Ye, J., Swartz, S., Jungner, P., & Hall, J. L. (1996). *Hyperfine structure and absolute frequency of the 87 Rb 5P 3 2 state* (tech. rep. No. 16).

Yuen, H. P., & Ozawa, M. (1993). Ultimate information carrying limit of quantum systems. *Physical Review Letters*, *70*(4), 363–366. https://doi.org/10.1103/PhysRevLett.70.363

Zhang, Z., Chen, C., Zhuang, Q., Wong, F. N. C., & Shapiro, J. H. (2018). Experimental quantum key distribution at 1.3 gigabit-per-second secret-key rate over a 10 dB loss channel. *Quantum Science and Technology*, *3*(2), 25007. https://doi.org/10.1088/2058-9565/aab623